PREVENTING AND REVERSING BLINDESS: COMP-ANG1 AND ENDOTHELIAL PROGENITOR CELLS AS A NOVEL THERAPEUTIC APPROACH IN DIABETIC RETINOPATHY

by

Judd Michael Cahoon

A dissertation submitted to the faculty of
The University of Utah
in partial fulfillment of the requirements for the degree of

Doctor of Philosophy

Department of Neuroscience

The University of Utah

August 2015

The University of Utah Graduate School

STATEMENT OF DISSERTATION APPROVAL

The dissertation of **Judd Michael Cahoon**

has been approved by the following supervisory committee members:

Balamurali Ambati	, Chair	**27 June 2014** Date Approved
Karen Wilcox	, Co-chair	**27 June 2014** Date Approved
Monica Vetter	, Member	**27 June 2014** Date Approved
David Krizaj	, Member	**27 June 2014** Date Approved
Wolfgang Baehr	, Member	**27 June 2014** Date Approved

and by **Richard Dorsky**, Chair/Dean of

the Department/College/School of **Neuroscience**

and by David B. Kieda, Dean of The Graduate School.

ABSTRACT

Diabetes affects 25.8 million people in the United States and its prevalence is expected to triple in the next 20 years. Diabetic retinopathy (DR) affects nearly 30% of people with diabetes and is the leading cause of blindness in the working-age population. Current treatments for DR improve vision in only a minority of patients, and carry significant risks. This work advances a new approach that works by reversing retinal vascular damage and restoring normal perfusion to improve vision in this condition.

Chapter 1 reviews the epidemiology, pathophysiology, and current standards of therapy for diabetic retinopathy. The roles of vascular maturation factor Angiopoietin-1 (Ang1) and its receptor Tie2 are introduced.

Chapter 2 describes the development of an improved method for visualization of leukocytes in the diabetic mouse retina, which was critical for studies in this dissertation and broadly applicable to fields studying leukocyte endothelial interaction and inflammation.

Chapter 3 focuses on the studies describing prevention of neurovascular dysfunction in diabetic retinopathy achieved by treating diabetic mice with gene therapy expressing COMP-Ang1. This chapter further details the studies performed to reverse diabetic retinopathy with a combination therapy consisting of endothelial colony-forming cells (ECFCs) and COMP-Ang1. We demonstrated that COMP-Ang1 enhanced the

vasculogenic capabilities of ECFCs leading to increased integration into the diabetic retina and preservation of visual function in mice with advanced diabetic retinopathy.

Chapter 4 represents my contributions toward the understanding of how targeting alternative VEGF receptor 2 splicing can suppress hemangiogenesis and lymphangiogenesis in the retina and choroid. This work was published in the FASEB journal in 2013.

Chapter 5 describes my work published in PLoS ONE describing suppression of both tumor and ocular neovascularization, wherein we used morpholinos to increased soluble VEGF receptor 1.

Chapter 6 concludes this work by recapping how the work accomplished in this dissertation built off of previous discoveries.

The Appendix describes studies initiated to test the effects of COMP-Ang1 in an acute model of retinal ischemia, central retinal artery occlusion.

I wish to dedicate this work to Lindsay, Maggie, and Bennett for sticking with me. Secondly, I wish to dedicate this work to an outstanding mentor who has done more to inspire me and shape my outlook than anyone else. Thank you, Bala, for your encouragement, guidance, and mentorship.

“Nulla tenaci inviva est via,” Spyker 1914

TABLE OF CONTENTS

LIST OF TABLES

LIST OF FIGURES

ACKNOWLEDGEMENTS

I must acknowledge the longsuffering and patience of my family for enduring my extended absences as I sometimes lost myself in lab. Importantly, I must express my extreme gratitude to my mentor, Dr. Bala Ambati. Bala encompasses all aspects of a mentor, academically, clinically, and in his humanitarian efforts. He has singularly shaped my view of health care, the current research environment, and what it takes to be a person who happens to be a physician, instead of the other way around. In total, he has inspired me to chase the dream and become a physician-scientist. This dissertation will serve as only the first step in my progress.

I would also like to recognize the programs that have supported me along the way. The Interdepartmental Program In Neuroscience has supported me since I joined in 2010, especially Tracy Marble, who keeps me in track. The MD-PhD program at the University of Utah has been an exceptional place to grow as a person, build lasting friendships, and commiserate with colleagues as we develop. I would especially like to thank Janet Bassett for her encouragement and kindness.

CHAPTER 1

AN INTRODUCTION TO DIABETIC RETINOPATHY AND COMP-ANG1

This chapter will introduce the concepts behind the pathogenesis of diabetic retinopathy and the angiopoietin-Tie2 signaling pathway. The concepts of endothelial progenitor cells and vector gene therapy will be introduced. Finally, the hypothesis that gene therapy with COMP-Ang1 plus endothelial progenitor cells can prevent and reverse the damage caused by diabetic retinopathy will also be introduced.

1.1 Clinical features of diabetic retinopathy

Diabetic retinopathy (DR) is a neurovascular disease affecting patients with long standing diabetes (e.g., elevated blood glucose levels) and is the leading cause of blindness in the working-age population in the US (Frank, 2004; R. Klein, Knudtson, Lee, Gangnon, & Klein, 2008). For the first 10 – 15 years of diabetes, no clinically apparent signs of DR manifest in the retina, making it an insidious and chronic disease.

Physicians classify DR based on the severity of symptoms presented during a fundus exam (Wilkinson et al., 2003). Mild DR presents with micro-aneurysms that can appear and disappear over time; however, patients can still maintain 20/20 visual acuity, delaying them from seeking treatment. Moderate DR presents with more red blood cell leakage (hemorrhage), plasma leakage (edema), and lipid leakage (exudate) (see Figure 1.1). Clinically significant macular edema (CSME) can also occur if retinal thickening occurs within 500 μm of macula (Sander, Hamann, & Larsen, 2008). Diabetics with mild to moderate retinopathy are followed with annual eye exams to monitor the progression of the disease (Aiello et al., 2010).

Patients are diagnosed with severe DR if there is either retinal hemorrhage in four quadrants, venous bleeding in two quadrants, or intraretinal microvascular abnormalities

Figure 1.1: A healthy retina (fundus photo, left) is compared to a retina with mild diabetic retinopathy (middle) and proliferative diabetic retinopathy (right). Areas of vascular leak and hemorrhage are evident as small red spots and yellow exudate in the mild diabetic retinopathy fundus exam (middle) and pre-retinal hemorrhage is evident in the proliferative diabetic retinopathy fundus exam (right). All photos used with permission and courtesy of Dr. Bala Ambati.

in one quadrant—the so-called 4:2:1 rule (R. Klein, Klein, & Moss, 1992). These patients require eye exams every four months. Proliferative DR is characterized by blood vessel growth into the vitreous and requires immediate treatment, as this is a sight-threatening condition.

Risk factors DR progression include duration of poor glucose control, poor lipid levels, and poor blood pressure control (Yau et al., 2012). After 20 years of poor glycemic control, 100% of patients initially diagnosed under the age of 30 will develop DR, with half of those patients developing the serious complications related to proliferative DR (R. Klein, Klein, Moss, Davis, & DeMets, 1984; Sjølie & Green, 1987). As such, this disease has a higher prevalence in patients with type 1 diabetes because these patients are typically diagnosed at a younger age (R. Klein, Knudtson, Lee, Gangnon, & Klein, 2009).

Observation of patients with DR is accomplished with a fundus exam, fluorescein angiography, and optical coherence tomography (OCT). OCT is used for fast, non-

invasive visualization of the retina to assess traction and neuronal changes and identify any diabetic macular edema (DME). Functional examinations of the diabetic retina include electro-retinal grams (ERGs) and visual acuity (VA) testing. Changes in oscillatory potentials (found with ERGs) and contrast sensitivity (determined by VA testing) are some of the earliest indications of DR (Bresnick & Palta, 1987; Bresnick, Korth, Groo, & Palta, 1984).

1.2 Epidemiology

Diabetes currently affects more than 371 million people worldwide—a number that is projected to increase to over 500 million by 2030 (J. E. Shaw, Sicree, & Zimmet, 2010). DR affects 35% of all diabetic patients with 7% experiencing proliferative DR and another 7% with diabetic macular edema (DME) (Yau et al., 2012). Currently, over 130 million people are at risk of losing their vision due to diabetic complications (Ko et al., 2012).

Global risk factors are largely similar (O. S. Huang et al., 2010). Diabetes duration—measured by glycosylated hemoglobin (HbA1c)—and high blood pressure are consistently elevated in most studies of DR (Yau et al., 2012). The Diabetic Complications Control Trial showed that hyperglycemia is responsible for many diabetic pathologies and tight glucose control (defined as HbA1c < 7%) leads to a 76% reduction in DR ("The effect of intensive treatment of diabetes on the development and progression of long-term complications in insulin-dependent diabetes mellitus. The Diabetes Control and Complications Trial Research Group," 1993). Reducing HbA1c by 1% lessened the rate of progression of DR by 40%. Tight glycemic control even resulted in a 10-year

"memory effect," where after a one-year period of tight glucose control patients were allowed to return to higher HbA1c levels and still experienced beneficial effects from glycemic control ten years afterwards (White et al., 2008). This metabolic memory phenomenon could be from the effects of glycemic status on gene expression or advanced glycation end-product (AGE) formation. However, tight glucose control is only achieved by a small number of patients and glycemic control itself is not without drawbacks. It should be noted that tight blood glucose control (6% HbA1c) leads to an increase in all-cause mortality (A. T. C. C. R. I. D. S. Group et al., 2008).

Control of other risk factors has been met with only modest success. (A. S. Group, Cushman, et al., 2010a; B. E. Klein, Klein, Moss, & Palta, 1995; Wong et al., 2009). For example, patients with high cholesterol had more macular lipid deposits and treatment with fenofibrates and statins helped reduce retinopathy endpoints, but not to same degree as glycemic control (Chew et al., 1996). Blood pressure control exerts only a modest effect on the progression of DR (A. S. Group, Ginsberg, et al., 2010b; A. S. Group, Group, et al., 2010c; Stratton et al., 2001).

Finally, DR awareness is very low; up to 80% of people with DR are unaware they have the disease (Bressler et al., 2014; O. S. Huang et al., 2009). In light of the difficulties patients face in controlling their blood sugar, further treatments for DR are required. Development of new treatments requires an understanding of the pathophysiology behind DR.

1.3 Cellular mechanisms for diabetic retinopathy

Hemodynamic, metabolic, and genetic alterations occur in diabetes. Early stages can be divided into three pathologic components: 1) capillary degeneration and non-perfusion, 2) vascular permeability and edema, and 3) neuroglial dysfunction and degeneration (Forbes & Cooper, 2013). Targeted therapies exist or have been investigated to stymie capillary degeneration. Similarly, many therapies have been developed (experimentally) to reduce vascular permeability and capillary degeneration. Far fewer potential therapeutics target neuroglial dysfunction.

The cellular contribution to DR can be divided between factors within and without the retina. Within the retina, the vascular component, glial cells, microglia, and neural cells (especially photoreceptors) may contribute to pathology (Li et al., 2012). Most of the reactive oxygen species (ROS) in the retina originate within photoreceptors (PR), mainly in the outer segments (Du, Veenstra, Palczewski, & Kern, 2013). Diabetes alters the metabolic phenotype of PRs, resulting in ischemia that mediates pro-inflammatory changes in the vasculature. Capillary nonperfusion, due to platelet aggregation, leukocyte adhesion, and intercellular adhesion molecule (ICAM) expression can lead to hypoxia and vascular endothelial growth factor (VEGF) release (Adamis, Joussen, et al., 2001a). The same processes that lead to neovascularization (e.g., VEGF) also lead to leaky vessels, which can gain traction on the vitreous and cause retinal detachment. In severe cases of DR neovascularization of the iris can occur, which is very painful for the patient (Fernández-Vigo, Castro, & Macarro, 1997).

Vascular disruptions are indications of pericyte loss. Pericytes are vascular support cells found abundantly in the retina at a 1:1 ratio with the endothelial cells

(Mizutani, Kern, & Lorenzi, 1996). Pericytes provide structural and trophic support to the underlying endothelium (Romeo, Liu, Asnaghi, Kern, & Lorenzi, 2002) and dropout has been associated with increased formation of microaneurysms.

Outside the retina, leukocytes are the predominate pathological drivers of DR (Joussen et al., 2004). Elimination of inflammatory proteins in bone marrow derived cells results in retinal sparing from diabetic-induced damage. Leukocytes from diabetic patients are cytotoxic to retinal endothelial cells *in vitro* (Li et al., 2012). Vascular endothelial cells of the retina respond to diabetes by increasing intercellular adhesion molecules (ICAM) expression, inducing leukocyte adhesion to the vascular wall. These leukocytes can occlude capillaries resulting in retinal hypoxia. Diminishing endothelial-leukocyte interaction is an attractive therapeutic approach.

1.4 Molecular mechanisms in diabetic retinopathy

Hyperglycemia results in repeated acute changes in cellular metabolism and cumulative long-term changes in stable macromolecules. These changes have reciprocal effects.

Some of the key biochemical changes sustained from diabetes include formation of advanced glycation end products (AGES), increased flux through the polyol pathway, activation of the PKC pathway (which increases VEGF), an accelerated inflammatory response with increased inflammatory cytokine production, and enhanced reactive oxygen species (ROS) (Forbes & Cooper, 2013). These biochemical features lead to functional changes such as decreased blood flow, loss of tight junctions, and permeability changes. Finally, structural changes occur: pericyte, endothelial, and ganglion cell loss,

with accompanying growth factor alteration, vessel occlusion, and ultimately neovascular DR as a result of these biochemical changes.

Aldose reductase, found in pericytes, can reduce glucose to sorbitol. However, the high levels of glucose in the diabetic retina result in accumulation of sorbitol in the pericytes causing osmotic pressure, swelling, and eventually death of pericytes. This is referred to as increased flux through the polyol pathway.

Oxidative stress—defined as an imbalance between ROS and the antioxidant species in a system—is a major underlying problem in DR. It can damage DNA, fatty acids, and enzymes (Xie et al., 2008). Lipid peroxidation, a consequence of oxidative stress, damages the cellular membrane leading to cellular injury. Enzymes can be inappropriately activated or inactivated through thiol oxidation and carbonyl formation. Hyperglycemia eventually leads to decreased superoxide dismutase (SOD), a key enzyme responsible for combatting ROS. Finally, ROS can increase caspase numbers, leading to apoptosis of retinal cells including pericytes, endothelial cells, and ganglion cells. Furthermore, glucose reacts with H_2O_2 in the presence of iron and copper to form radicals, which can impair mitochondrial electron transport.

Inflammatory cytokines (like TNF-α and IL1-β) are up regulated in diabetes, while anti-inflammatory cytokines are down regulated. Inflammation can damage the mitochondria and exacerbate ROS production. Elevated levels of activated leukocytes have been noted after one week of diabetes (Joussen et al., 2004). In diabetics, leukocytes have increased CD11b, CD18, and ICAM-1 circulating in the serum, which increases their reactivity (Fasching et al., 1996; Limb, Webster, Soomro, Janikoun, & Shilling, 1999; Muni et al., 2013). Leukostasis is associated with capillary occlusion and

ROS-mediated cell death, which further amplifies the local inflammatory response. Experimentally, reduced leukocyte entrapment often leads to reduced progression of DR. Pro-inflammatory cytokines are associated with progression of DR and up-regulated factors include Ang2, MMP, TNF-α, CCl2, and the Kallikrein-kinin system. Activation of microglia also plays a role in the pathogenesis of DR as microglia increase nitric oxide (NO) and other inflammatory cytokines.

AGEs occur due to the overwhelming amount of a substrate, i.e., glucose, non-enzymatically binding to proteins. In fact, the nonenzymatic glycosylation of hemoglobin (HbA1c) is the basis for measuring the severity of diabetes. AGEs are found in the diabetic microenvironment and alter the normal homeostasis of the cell (Goldin, Beckman, Schmidt, & Creager, 2006; Singh, Barden, Mori, & Beilin, 2001).

The pathophysiology of DR is often described as vascular in nature. Pericytes are particularly sensitive to increased flux through the polyol pathway in addition to damage from AGEs. Loss of pericytes results in diminished structural and trophic support to the endothelium. Endothelial cells ultimately become weaker, resulting in microaneurysms and endothelial apoptosis. Lack of endothelial cells decreases delivery of oxygen and essential nutrients to the retina resulting in ischemia-driven VEGF secretion. Excessive VEGF secretion results in increased vascular permeability, immature neovascularization, and increased inflammation. Preventing vascular disturbances could have beneficial side effects for the entire retina. Thus far the lynchpin for therapy in DR has been directed at VEGF.

1.5 Pharmacotherapies for diabetic retinopathy

With the understanding that the foundation of treatment for diabetic eye disease is systemic glucose control, pharmacotherapeutic strategies still must be pursued because many patients are not able to achieve targeted systemic control. Current first-line clinical therapies for DR include pan-retinal laser photocoagulation (PRP) and VEGF inhibition (Diabetic Retinopathy Clinical Research Network et al., 2012). The rationale behind both of these treatments is to reduce VEGF levels in the retina.

Multiple VEGF inhibitors are used in the treatment of DR but only one, ranibizumab, is FDA approved for DME. Because the half-life of anti-VEGF agents is only 8-9 days in the eye, treatments consist of monthly intraocular injections and are accompanied by PRP to treat proliferative DR. While treatment intervals can be reduced after one year, regular intravitreal injections are still required. PRP improves tight junctions in the retina, as the grid laser stimulates retinal pigmented epithelial (RPE) cells to phagocytose hard exudates. Laser treatment is considered the gold standard of proliferative DR and is used as an adjunct to anti-VEGF therapies in other forms of DR, including macular edema.

VEGF is up regulated in DME and numerous trials have shown anti-VEGF is beneficial; however, despite treatments that reduce intraocular VEGF levels the retinal vasculature does not always return to normal (Brown et al., 2013; Nguyen et al., 2012; 2010). Anti-VEGF drugs are more efficacious in proliferative DR, but response of DME to anti-VEGF agents is variable (Mitchell, Wong, Diabetic Macular Edema Treatment Guideline Working Group, 2014). Once anti-VEGF therapy is stopped, the edema resurfaces. Thus, the effects of anti-VEGF therapy on DME are transient at best,

especially since 50% of patients still have DME after a year of treatment. Furthermore, overuse of anti-VEGF medications could be toxic to the eye as it has been shown that VEGF is good for retinal health (Quaggin, 2012; Sivaskandarajah et al., 2012).

Switching to intravitreal steroid as a way to reduce inflammation is a second line of therapy, but visual acuity worsens after a year of treatment, due to increased cataract formation (Elman et al., 2011; Campochiaro et al., 2012, 2011). Currently, intraocular implants do exist for long-acting steroids (Ciulla, Harris, McIntyre, & Jonescu-Cuypers, 2014).

PRP is the current standard treatment for proliferative DR (Bressler, Beck, & Ferris, 2011). PRP reduces DR by increasing O_2 availability and decreasing VEGF production. However, some patients treated with PRP still have persistent neovascularization. Although a more invasive and riskier surgery, early vitrectomy has proven beneficial for advanced active proliferative DR in young patients with long standing DR.

PRP is a brutal effort to reduce VEGF by eliminating parts of the retina that respond to hypoxia by secreting VEGF. This results in diminished night vision and poor peripheral vision in an attempt to salvage central vision. Current antibody injection therapies against VEGF are potent, selective, and administered at high doses, with all trials showing similar responses. However, the fact that only 50% of treated eyes respond to anti-VEGF therapy indicates that there are most likely VEGF-independent pathways responsible for some pathogenesis in DR. Targeting a new pathway in the diabetic retina is necessary to overcome the current treatment plateau.

1.6 The angiopoietin-1 Tie2 system

During physiologic homeostasis, vasculature stabilization is mediated, in part, through angiopoietin-1 (Ang1) (Thurston et al., 2000). Ang1 helps maintain blood vessel quiescence by binding the endothelial tyrosine kinase with Ig and epidermal growth factor homology domain receptor 2 (Tie2) (Asahara et al., 1998; Partanen et al., 1992). Both Ang1 and Tie2 are necessary for fetal development (Suri et al., 1996; Takakura et al., 1998). The effects of Tie2 phosphorylation/activation include decreased leakage, leukocyte adhesion, and apoptosis (Adamis, Joussen, et al., 2001a; Joussen et al., 2004; Thurston et al., 2000).

Tie2 activates mDia to sequester Src, which mediates VEGF-induced internalization of vascular endothelial cadherin (VE-cadherin) (Gavard, Patel, & Gutkind, 2008). VE-cadherin is a calcium-dependent transmembrane protein in the adherens junction between endothelial cells that promotes vascular integrity and decreases vascular permeability (Carmeliet et al., 1999). By preventing Src from phosphorylating VE-cadherin, Tie2 results in greater junctional integrity between endothelial cells and decreased leakage (see Figure 1.2).

Tie2 also increases PI3K/Akt signaling, leading to inhibition of caspase 9 and other apoptotic factors, thus promoting endothelial cell survival (Papapetropoulos et al., 2000). Ang1 exhibits its anti-inflammatory effects through Tie2 by blocking nuclear factor kappa b (NFkB) through ABIN2. Inhibition of NFkB prevents ICAM and integrin signaling used in leukocyte recruitment (Hughes, Marron, & Brindle, 2003; Jeon et al., 2003; Tadros, Hughes, Dunmore, & Brindle, 2003). Patients with DR have decreased vitreous levels of Ang1 (J. I. Patel, Hykin, Gregor, Boulton, & Cree, 2005). Restoration

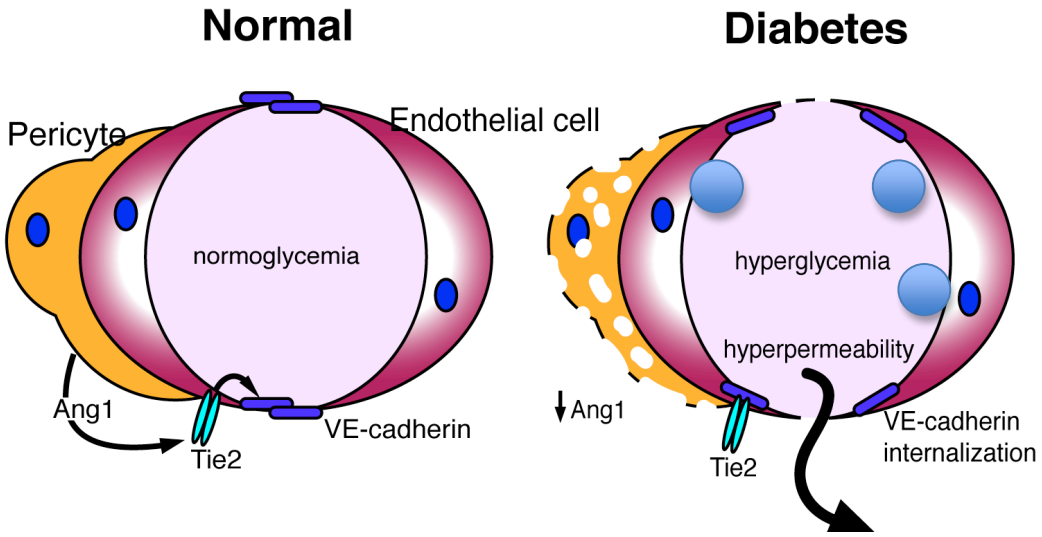

Figure 1.2: A schematic depicting damage caused by hyperglycemia to the retinal vasculature. Shown on the left is a normal retinal capillary composed of two endothelial cells and a supporting pericyte. Pericytes secrete Ang1, which supports endothelial health and VE-cadherin stabilization. During diabetes, pericytes and Ang1 are lost, resulting in VE-cadherin internalization and degradation, increased vascular hyperpermeability, and increased leukocyte adhesion (inflammation).

of Ang1 signaling could serve as a complimentary strategy to VEGF inhibition in the treatment of DR.

1.7 Development of COMP-Ang1

Ang1 structure contains three basic parts: a short N-terminal domain which superclusters the protein into variably sized multimers, a central coiled-coil domain responsible for oligimerizing the individual proteins, and a C-terminal fibrinogen-like domain responsible for binding the receptor (S. Davis et al., 2003; Procopio, Pelavin, Lee, & Yeilding, 1999). However, the coiled-coil domain and the N-terminal superclustering region result in protein aggregation and insolubility, making it difficult to

work with in a pharmacological setting (Maisonpierre et al., 1997). Cartilage oligo matrix protein (COMP) Ang1 was developed to overcome these limitations. By replacing the superclustering region of the N-terminus and the coiled-coil domain with COMP, researchers were able to generate a soluble yet stable and potent version of the native Ang1 protein (Cho et al., 2004). COMP-Ang1 has been shown to reduce neurovascular deficits in ischemic stroke, diabetic nephropathy, and wound healing, but has yet to be tested in DR (Cho et al., 2006; S. Lee et al., 2007; Shin et al., 2010).

1.8 Stem cell therapy of the diabetic retina

Stem cell therapy for DR has recently gained traction (Bhatwadekar, Shaw, & Grant, 2010). There are currently almost 2,000 clinical trials involving bone marrow stem cells for the treatment of DR and age-related macular degeneration. Endothelial progenitor cells (EPCs), which are found circulating in the serum, can inhibit damage and stimulate repair in the diabetic retina (Busik et al., 2009; "Circulating mononuclear progenitor cells: differential roles for subpopulations in repair of retinal vascular injury," 2013).

The term EPC encapsulates a diverse group of CD34+ cell-types with myeloid, haematopoietic or endothelial characteristics (Afzal et al., 2007; O'Neill et al., 2012; Stitt et al., 2011). Adipocyte-derived EPCs have been able to generate pericytes or endothelial cells, depending on the mode of delivery (Traktuev et al., 2008). EPC delivery has reduced leakage and improved ERG in animal models of ischemic retinopathy (Ritter et al., 2006). However, bone marrow-derived EPCs are impacted by the biochemical alterations of diabetes, which could play a role in faulty repair of the retinal vasculature

(Yellowlees Douglas et al., 2012). Serum levels of EPCs respond to, and have been used as biomarkers of, various diseases including diabetes, hypertension, coronary artery disease, smoking, and aging (Brunner et al., 2011). Following the levels of EPCs in the systemic circulation has even proved a useful predictor of diabetic complications. Patients with DR have decreased levels of EPCs, that also demonstrate a reduced ability to differentiate and increased production of ROS. Diabetic EPCs do not respond to hypoxia and exhibit a decreased paracrine ability to induce vasodilatation in vessels (Jarajapu et al., 2014). Development of therapies that a) enhance endogenous EPC activity in diabetic patients or b) replace diabetic EPCs with nondiabetic, and therefore fully functioning, EPCs would be a great boon to DR therapy.

A unique EPC subtype, known as endothelial colony-forming cells (ECFCs, also known as outgrowth endothelial cells (OECs)), has been shown to encompass true endothelial progenitors that fully integrate into blood vessels and serve to regenerate damaged vasculature in the ischemic retina (Medina, O'Neill, Humphreys, Gardiner, & Stitt, 2010a), as well as other ischemic models (Alphonse et al., 2014; Critser & Yoder, 2010). Recently, ECFCs generated from cord blood have been able to generate both endothelial cells and pericytes (Medina, O'Neill, Humphreys, Gardiner, & Stitt, 2010a). These cells were pulled from the mononuclear layer and enriched by collagen adherence *in vitro*, and demonstrated the capability to form vasculature in a mouse. More importantly, they were even able to assimilate into a hypoxic retina (Medina, O'Neill, Sweeney, Guduric-Fuchs, Gardiner, Simpson, et al., 2010b). ECFCs represent a distinct subtype of endothelial progenitor cell with the potential to act as a cellular therapeutic in vascularizing the ischemic retina (Medina, O'Neill, O'Doherty, Wilson, & Stitt, 2012).

1.9 AAV2 mediated gene therapy

Due to the chronic nature of diabetes, repeated injections into the eye of pharmacotherapies are often required. The drawbacks to this delivery method are readily evident, but also include risks of infection, retinal damage, and uveitis (Jager, Aiello, Patel, & Cunningham, 2004). In order to gain long-term expression of any protein of interest, gene therapy is an attractive option. The concept behind gene therapy is to replace the deficient gene responsible for disease progression with a normally functioning gene. This can be accomplished by packaging a replication deficient and non-inflammatory viral construct with a plasmid encoding the gene of interest. Adeno-associated virus (AAV) has emerged as a leading candidate vector for gene therapy trials in patients with retinal pathologies (Maguire et al., 2008). Currently, most gene therapy approaches in the retina have focused on inherited genetic diseases like Lebers Congenital Amourosis (LCA) using AAV to replace the deficient copy of the *RPE65* gene (Maguire et al., 2008). As these clinical trials have progressed, it has become evident that AAV therapy in the eye is safe and effective at delivering gene products to the retina (Colella & Auricchio, 2012; Jacobson et al., 2012). A wide variety of AAV serotypes exist, each with its own tropism. AAV serotype 2 (AAV2) is trophic for post-mitotic cells and, when delivered as an intravitreal injection, remains in the inner retina (Yin et al., 2011). A single intravitreal injection of AAV2 has been shown to last in the retina for as long as two years and results in expression of product in the ganglion cell and inner plexiform layers. As patients with DR have chronically low levels of Ang1 due to pericyte loss, replacing Ang1 with gene therapy could serve as a way to mitigate the risks of regular intravitreal injections. This project aimed to promote constitutive

expression of COMP-Ang1 in a mouse model of diabetic retinopathy. As diabetic vascular damage is also located in the inner retina, AAV2 was the most appropriate choice of vector for COMP-Ang1.

1.10 Discussion

With this basic understanding of the enormity of the situation, the pathophysiology of diabetic retinopathy, and the potential for COMP-Ang1 to act as a therapeutic, this dissertation will focus on the effects of early AAV2-meditaed COMP-Ang1 administration to diabetic mice in an attempt to prevent neurovascular dysfunction and combination therapy of both COMP-Ang1 and ECFCs delivered to mice with advanced diabetic retinopathy in an attempt to rescue neurovascular dysfunction. (Figure 1.3) Chapter 2 is a published paper that demonstrates development of a necessary and

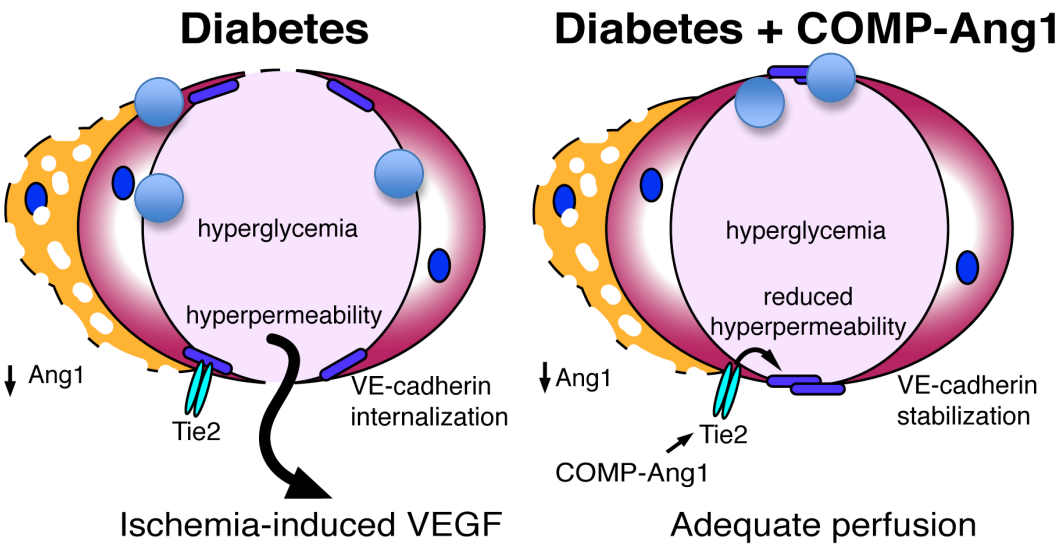

Figure 1.3: A schematized view of the potential for Tie2 modulation in the diabetic retina. COMP-Ang1 would serve to promote endothelial survival, decrease leukocyte-endothelial interactions, and promote vascular barrier integrity by increasing VE-cadherin stability.

novel technique to measure leukocyte flow in the diabetic retina.

1.11 References

Adamis, A. P., Joussen, A. M., Murata, T., Tsujikawa, A., Kirchhof, B., & Bursell, S. E. (2001a). Leukocyte-mediated endothelial cell injury and death in the diabetic retina. *The American Journal of Pathology*, *158*(1), 147–152. doi:10.1016/S0002-9440(10)63952-1

Adamis, A. P., Qaum, T., Xu, Q., Joussen, A. M., Clemens, M. W., Qin, W., et al. (2001b). VEGF-initiated blood-retinal barrier breakdown in early diabetes. *Investigative Ophthalmology & Visual Science*, *42*(10), 2408–2413.

Adamis, A. P., Xu, Q., & Qaum, T. (2001c). Sensitive blood-retinal barrier breakdown quantitation using Evans Blue. *Investigative Ophthalmology & Visual Science*, *42*(3), 789–794.

Afzal, A., Caballero, S., Sengupta, N., Chang, K.-H., Li Calzi, S., Guberski, D. L., et al. (2007). Ischemic vascular damage can be repaired by healthy, but not diabetic, endothelial progenitor cells. *Diabetes*, *56*(4), 960–967. doi:10.2337/db06-1254

Aiello, L. P., Avery, R. L., Arrigg, P. G., Keyt, B. A., Jampel, H. D., Shah, S. T., et al. (1994). Vascular endothelial growth factor in ocular fluid of patients with diabetic retinopathy and other retinal disorders. *The New England Journal of Medicine*, *331*(22), 1480–1487. doi:10.1056/NEJM199412013312203

Aiello, L. P., Edwards, A. R., Beck, R. W., Bressler, N. M., Davis, M. D., Ferris, F., et al. (2010). Factors associated with improvement and worsening of visual acuity 2 years after focal/grid photocoagulation for diabetic macular edema. *Ophthalmology*, *117*(5), 946–953. doi:10.1016/j.ophtha.2009.10.002

Akimov, N. P., & Rentería, R. C. (2012). Spatial frequency threshold and contrast sensitivity of an optomotor behavior are impaired in the Ins2Akita mouse model of diabetes. *Behavioural Brain Research*, *226*(2), 601–605. doi:10.1016/j.bbr.2011.09.030

Al-Saikhan, F. I. (2013). The gene therapy revolution in ophthalmology. *Saudi Journal of Ophthalmology : Official Journal of the Saudi Ophthalmological Society*, *27*(2), 107–111. doi:10.1016/j.sjopt.2013.02.001

Aldrich, T. H., Davis, S., Jones, P. F., Acheson, A., Compton, D. L., Jain, V., et al. (1996). Isolation of angiopoietin-1, a ligand for the TIE2 receptor, by secretion-trap expression cloning. *Cell*, *87*(7), 1161–1169.

Alphonse, R. S., Vadivel, A., Fung, M., Shelley, W. C., Critser, P. J., Ionescu, L., et al. (2014). Existence, functional impairment, and lung repair potential of endothelial colony-forming cells in oxygen-induced arrested alveolar growth. *Circulation*, *129*(21), 2144–2157. doi:10.1161/CIRCULATIONAHA.114.009124

Arevalo, J. F. (2013). Diabetic macular edema: Current management 2013. *World Journal of Diabetes*, *4*(6), 231–233. doi:10.4239/wjd.v4.i6.231

Asahara, T., Chen, D., Takahashi, T., Fujikawa, K., Kearney, M., Magner, M., et al. (1998). Tie2 receptor ligands, angiopoietin-1 and angiopoietin-2, modulate VEGF-induced postnatal neovascularization. *Circulation Research*, *83*(3), 233–240.

Augustin, H. G., Young Koh, G., Thurston, G., & Alitalo, K. (2009). Control of vascular morphogenesis and homeostasis through the angiopoietin–Tie system. *Nature Reviews Molecular Cell Biology*, *10*(3), 165–177. doi:10.1038/nrm2639

Barabas, P., Huang, W., Chen, H., Koehler, C. L., Howell, G., John, S. W. M., et al. (2011). Missing optomotor head-turning reflex in the DBA/2J mouse. *Investigative Ophthalmology & Visual Science*, *52*(9), 6766–6773. doi:10.1167/iovs.10-7147

Barber, A. J., Antonetti, D. A., Kern, T. S., Reiter, C. E. N., Soans, R. S., Krady, J. K., et al. (2005). The Ins2Akita mouse as a model of early retinal complications in diabetes. *Investigative Ophthalmology & Visual Science*, *46*(6), 2210–2218. doi:10.1167/iovs.04-1340

Bennett, J. (2004). Gene therapy for Leber congenital amaurosis. *Novartis Foundation Symposium*, *255*, 195–202– discussion 202–7.

Bennett, J., Ashtari, M., Wellman, J., Marshall, K. A., Cyckowski, L. L., Chung, D. C., et al. (2012). AAV2 gene therapy readministration in three adults with congenital blindness. *Science Translational Medicine*, *4*(120), 120ra15–120ra15. doi:10.1126/scitranslmed.3002865

Bhatwadekar, A. D., Shaw, L. C., & Grant, M. B. (2010). Promise of endothelial progenitor cell for treatment of diabetic retinopathy. *Expert Review of Endocrinology & Metabolism*, *5*(1), 29–37. doi:10.1586/eem.09.75

Bresnick, G. H., Korth, K., Groo, A., & Palta, M. (1984). Electroretinographic oscillatory potentials predict progression of diabetic retinopathy. Preliminary report. *Archives of Ophthalmology*, *102*(9), 1307–1311.

Bresnick, G. H., & Palta, M. (1987). Oscillatory potential amplitudes. Relation to severity of diabetic retinopathy. *Archives of Ophthalmology*, *105*(7), 929–933.

Bressler, N. M., Beck, R. W., & Ferris, F. L. (2011). Panretinal photocoagulation for proliferative diabetic retinopathy. *The New England Journal of Medicine*, *365*(16), 1520–1526. doi:10.1056/NEJMct0908432

Bressler, N. M., Varma, R., Doan, Q. V., Gleeson, M., Danese, M., Bower, J. K., et al. (2014). Underuse of the health care system by persons with diabetes mellitus and diabetic macular edema in the United States. *JAMA Ophthalmology*, *132*(2), 168–173. doi:10.1001/jamaophthalmol.2013.6426

Brown, D. M., Nguyen, Q. D., Marcus, D. M., Boyer, D. S., Patel, S., Feiner, L., et al. (2013). Long-term outcomes of ranibizumab therapy for diabetic macular edema: The 36-month results from two phase III trials: RISE and RIDE. *Ophthalmology*, *120*(10), 2013–2022. doi:10.1016/j.ophtha.2013.02.034

Brunner, S., Hoellerl, F., Schmid-Kubista, K. E., Zeiler, F., Schernthaner, G., Binder, S., & Schernthaner, G.-H. (2011). Circulating angiopoietic cells and diabetic retinopathy in type 2 diabetes mellitus, with or without macrovascular disease. *Investigative Ophthalmology & Visual Science*, *52*(7), 4655–4662. doi:10.1167/iovs.10-6520

Busik, J. V., Tikhonenko, M., Bhatwadekar, A., Opreanu, M., Yakubova, N., Caballero, S., et al. (2009). Diabetic retinopathy is associated with bone marrow neuropathy and a depressed peripheral clock. *The Journal of Experimental Medicine*, *206*(13), 2897–2906. doi:10.1084/jem.20090889

Byeon, S. H., Chu, Y. K., Lee, H., Lee, S. Y., & Kwon, O. W. (2009). Foveal ganglion cell layer damage in ischemic diabetic maculopathy: Correlation of optical coherence tomographic and anatomic changes. *Ophthalmology*, *116*(10), 1949–59.e8. doi:10.1016/j.ophtha.2009.06.066

Cahoon, J. M., Olson, P. R., Nielson, S., Miya, T. R., Bankhead, P., Mcgeown, J. G., et al. (2014). Acridine orange leukocyte fluorography in mice. *Experimental Eye Research*, *120*, 15–19. doi:10.1016/j.exer.2013.12.002

Campochiaro, P. A., Brown, D. M., Pearson, A., Chen, S., Boyer, D., Ruiz-Moreno, J., et al. (2012). Sustained delivery fluocinolone acetonide vitreous inserts provide benefit for at least 3 years in patients with diabetic macular edema. *Ophthalmology*, *119*(10), 2125–2132. doi:10.1016/j.ophtha.2012.04.030

Campochiaro, P. A., Brown, D. M., Pearson, A., Ciulla, T., Boyer, D., Holz, F. G., et al. (2011). Long-term benefit of sustained-delivery fluocinolone acetonide vitreous inserts for diabetic macular edema. *Ophthalmology*, *118*(4), 626–635.e2. doi:10.1016/j.ophtha.2010.12.028

Campochiaro, P. A., Wykoff, C. C., Shapiro, H., Rubio, R. G., & Ehrlich, J. S. (2014). Neutralization of vascular endothelial growth factor slows progression of retinal nonperfusion in patients with diabetic macular edema. *Ophthalmology*. doi:10.1016/j.ophtha.2014.03.021

Carmeliet, P., Lampugnani, M. G., Moons, L., Breviario, F., Compernolle, V., Bono, F., et al. (1999). Targeted deficiency or cytosolic truncation of the VE-cadherin gene in

mice impairs VEGF-mediated endothelial survival and angiogenesis. *Cell*, *98*(2), 147–157.

Chew, E. Y., Klein, M. L., Ferris, F. L., Remaley, N. A., Murphy, R. P., Chantry, K., et al. (1996). Association of elevated serum lipid levels with retinal hard exudate in diabetic retinopathy. Early Treatment Diabetic Retinopathy Study (ETDRS) Report 22. *Archives of Ophthalmology*, *114*(9), 1079–1084.

Cho, C.-H., Kammerer, R. A., Lee, H. J., Steinmetz, M. O., Ryu, Y. S., Lee, S. H., et al. (2004). COMP-Ang1: A designed angiopoietin-1 variant with nonleaky angiogenic activity. *Proceedings of the National Academy of Sciences of the United States of America*, *101*(15), 5547–5552. doi:10.1073/pnas.0307574101

Cho, C.-H., Sung, H.-K., Kim, K.-T., Cheon, H. G., Oh, G. T., Hong, H. J., et al. (2006). COMP-angiopoietin-1 promotes wound healing through enhanced angiogenesis, lymphangiogenesis, and blood flow in a diabetic mouse model. *Proceedings of the National Academy of Sciences of the United States of America*, *103*(13), 4946–4951. doi:10.1073/pnas.0506352103

Chou, S., Harza, S., Bhatwadekar, A., Li, C. S., Paradiso, L. J., Miller, L. P., et al. (2013). Circulating mononuclear progenitor cells: Differential roles for subpopulations in repair of retinal vascular injury. *Investigative Ophthalmology and Visual Science 54*(4), 3000–3009. doi:10.1167/iovs.12-10280

Ciulla, T. A., Harris, A., McIntyre, N., & Jonescu-Cuypers, C. (2014). Treatment of diabetic macular edema with sustained-release glucocorticoids: Intravitreal triamcinolone acetonide, dexamethasone implant, and fluocinolone acetonide implant. *Expert Opinion on Pharmacotherapy*, *15*(7), 953–959. doi:10.1517/14656566.2014.896899

Cogan, D. G., Toussaint, D., & Kuwabara, T. (1961). Retinal vascular patterns. IV. Diabetic retinopathy. *Archives of Ophthalmology*, *66*, 366–378.

Colella, P., & Auricchio, A. (2012). Gene therapy of inherited retinopathies: A long and successful road from viral vectors to patients. *Human Gene Therapy*, *23*(8), 796–807. doi:10.1089/hum.2012.123

Critser, P. J., & Yoder, M. C. (2010). Endothelial colony-forming cell role in neoangiogenesis and tissue repair. *Current Opinion in Organ Transplantation*, *15*(1), 68–72. doi:10.1097/MOT.0b013e32833454b5

Cunha-Vaz, J. G. (1966). Studies on the permeability of the blood-retinal barrier. II. Breakdown of the blood-retinal barrier by injury. *The British Journal of Ophthalmology*, *50*(8), 454–462.

Davis, S., Papadopoulos, N., Aldrich, T. H., Maisonpierre, P. C., Huang, T., Kovac, L., et

al. (2003). Angiopoietins have distinct modular domains essential for receptor binding, dimerization and superclustering. *Nature Structural Biology*, *10*(1), 38–44. doi:10.1038/nsb880

Diabetic Retinopathy Clinical Research Network, Elman, M. J., Qin, H., Aiello, L. P., Beck, R. W., Bressler, N. M., et al. (2012). Intravitreal ranibizumab for diabetic macular edema with prompt versus deferred laser treatment: Three-year randomized trial results. *Ophthalmology*, *119*(11), 2312–2318. doi:10.1016/j.ophtha.2012.08.022

Dornan, T., Mann, J. I., & Turner, R. (1982). Factors protective against retinopathy in insulin-dependent diabetics free of retinopathy for 30 years. *British Medical Journal (Clinical Research Ed.)*, *285*(6348), 1073–1077.

Du, Y., Veenstra, A., Palczewski, K., & Kern, T. S. (2013). Photoreceptor cells are major contributors to diabetes-induced oxidative stress and local inflammation in the retina. *Proceedings of the National Academy of Sciences*, *110*(41), 16586–16591. doi:10.1073/pnas.1314575110

Elman, M. J., Bressler, N. M., Qin, H., Beck, R. W., Ferris, F. L., Friedman, S. M., et al. (2011). Expanded 2-year follow-up of ranibizumab plus prompt or deferred laser or triamcinolone plus prompt laser for diabetic macular edema. *Ophthalmology*, *118*(4), 609–614. doi:10.1016/j.ophtha.2010.12.033

Fasching, P., Veitl, M., Rohac, M., Streli, C., Schneider, B., Waldhäusl, W., & Wagner, O. F. (1996). Elevated concentrations of circulating adhesion molecules and their association with microvascular complications in insulin-dependent diabetes mellitus. *The Journal of Clinical Endocrinology and Metabolism*, *81*(12), 4313–4317. doi:10.1210/jcem.81.12.8954033

Fernández-Vigo, J., Castro, J., & Macarro, A. (1997). Diabetic iris neovascularization. Natural history and treatment. *Acta Ophthalmologica Scandinavica*, *75*(1), 89–93.

Forbes, J. M., & Cooper, M. E. (2013). Mechanisms of diabetic complications. *Physiological Reviews*, *93*(1), 137–188. doi:10.1152/physrev.00045.2011

Frank, R. N. (2004). Diabetic retinopathy. *The New England Journal of Medicine*, *350*(1), 48–58. doi:10.1056/NEJMra021678

Gastinger, M. J., Singh, R. S. J., & Barber, A. J. (2006). Loss of cholinergic and dopaminergic amacrine cells in streptozotocin-diabetic rat and Ins2Akita-diabetic mouse retinas. *Investigative Ophthalmology & Visual Science*, *47*(7), 3143–3150. doi:10.1167/iovs.05-1376

Gavard, J., Patel, V., & Gutkind, J. (2008). Angiopoietin-1 prevents VEGF-induced endothelial permeability by sequestering Src through mDia. *Developmental Cell*, *14*(1), 25–36. doi:10.1016/j.devcel.2007.10.019

Goldin, A., Beckman, J. A., Schmidt, A. M., & Creager, M. A. (2006). Advanced glycation end products: Sparking the development of diabetic vascular injury. *Circulation*, *114*(6), 597–605. doi:10.1161/CIRCULATIONAHA.106.621854

Group, A. S., Cushman, W. C., Evans, G. W., Byington, R. P., Goff, D. C., Grimm, R. H., et al. (2010a). Effects of intensive blood-pressure control in type 2 diabetes mellitus. *The New England Journal of Medicine*, *362*(17), 1575–1585. doi:10.1056/NEJMoa1001286

Group, A. S., Ginsberg, H. N., Elam, M. B., Lovato, L. C., Crouse, J. R., Leiter, L. A., et al. (2010b). Effects of combination lipid therapy in type 2 diabetes mellitus. *The New England Journal of Medicine*, *362*(17), 1563–1574. doi:10.1056/NEJMoa1001282

Group, A. S., Group, A. E. S., Chew, E. Y., Ambrosius, W. T., Davis, M. D., Danis, R. P., et al. (2010c). Effects of medical therapies on retinopathy progression in type 2 diabetes. *The New England Journal of Medicine*, *363*(3), 233–244. doi:10.1056/NEJMoa1001288

Group, A. T. C. C. R. I. D. S., Gerstein, H. C., Miller, M. E., Byington, R. P., Goff, D. C., Bigger, J. T., et al. (2008). Effects of intensive glucose lowering in type 2 diabetes. *The New England Journal of Medicine*, *358*(24), 2545–2559. doi:10.1056/NEJMoa0802743

Gu, H., Cui, M., Bai, Y., Chen, F., Ma, K., Zhou, C., & Guo, L. (2010). Angiopoietin-1/Tie2 signaling pathway inhibits lipopolysaccharide-induced activation of RAW264.7 macrophage cells. *Biochemical and Biophysical Research Communications*, *392*(2), 178–182. doi:10.1016/j.bbrc.2010.01.009

Hammes, H.-P., Lin, J., Renner, O., Shani, M., Lundqvist, A., Betsholtz, C., et al. (2002). Pericytes and the pathogenesis of diabetic retinopathy. *Diabetes*, *51*(10), 3107–3112.

Hammes, H.-P., Lin, J., Wagner, P., Feng, Y., Hagen, Vom, F., Krzizok, T., et al. (2004). Angiopoietin-2 causes pericyte dropout in the normal retina: Evidence for involvement in diabetic retinopathy. *Diabetes*, *53*(4), 1104–1110.

Hombrebueno, J. R., Chen, M., Penalva, R. G., & Xu, H. (2014). Loss of synaptic connectivity, particularly in second order neurons is a key feature of diabetic retinal neuropathy in the Ins2Akita mouse. *PLoS ONE*, *9*(5), e97970. doi:10.1371/journal.pone.0097970

Huang, H., Gandhi, J. K., Zhong, X., Wei, Y., Gong, J., Duh, E. J., & Vinores, S. A. (2011). TNFalpha is required for late BRB breakdown in diabetic retinopathy, and its inhibition prevents leukostasis and protects vessels and neurons from apoptosis. *Investigative Ophthalmology & Visual Science*, *52*(3), 1336–1344. doi:10.1167/iovs.10-5768

Huang, O. S., Lamoureux, E. L., Tay, W. T., Tai, E. S., Wang, J. J., & Wong, T. Y. (2010). Glycemic and blood pressure control in an Asian Malay population with diabetes and diabetic retinopathy. *Archives of Ophthalmology*, *128*(9), 1185–1190. doi:10.1001/archophthalmol.2010.168

Huang, O. S., Tay, W. T., Tai, E. S., Wang, J. J., Saw, S.-M., Jeganathan, V. S., et al. (2009). Lack of awareness amongst community patients with diabetes and diabetic retinopathy: The Singapore Malay eye study. *Annals of the Academy of Medicine, Singapore*, *38*(12), 1048–1055.

Hughes, D. P., Marron, M. B., & Brindle, N. P. J. (2003). The antiinflammatory endothelial tyrosine kinase Tie2 interacts with a novel nuclear factor-kappaB inhibitor ABIN-2. *Circulation Research*, *92*(6), 630–636. doi:10.1161/01.RES.0000063422.38690.DC

Jacobson, S. G., Cideciyan, A. V., Ratnakaram, R., Heon, E., Schwartz, S. B., Roman, A. J., et al. (2012). Gene therapy for leber congenital amaurosis caused by RPE65 mutations: Safety and efficacy in 15 children and adults followed up to 3 years. *Archives of Ophthalmology*, *130*(1), 9–24. doi:10.1001/archophthalmol.2011.298

Jager, R. D., Aiello, L. P., Patel, S. C., & Cunningham, E. T. (2004). Risks of intravitreous injection: A comprehensive review. *Retina (Philadelphia, Pa)*, *24*(5), 676–698.

Jarajapu, Y. P. R., Hazra, S., Segal, M., Licalzi, S., Jhadao, C., Qian, K., et al. (2014). Vasoreparative dysfunction of CD34+ cells in diabetic individuals involves hypoxic desensitization and impaired autocrine/paracrine mechanisms. *PLoS ONE*, *9*(4), e93965. doi:10.1371/journal.pone.0093965

Jeon, B. H., Khanday, F., Deshpande, S., Haile, A., Ozaki, M., & Irani, K. (2003). Tie-ing the antiinflammatory effect of angiopoietin-1 to inhibition of NF-kappaB. *Circulation Research*, *92*(6), 586–588. doi:10.1161/01.RES.0000066881.04116.45

Joussen, A. M., Poulaki, V., Le, M. L., Koizumi, K., Esser, C., Janicki, H., et al. (2004). A central role for inflammation in the pathogenesis of diabetic retinopathy. *The FASEB Journal*, *18*(12), 1450–1452. doi:10.1096/fj.03-1476fje

Joussen, A. M., Poulaki, V., Tsujikawa, A., Qin, W., Qaum, T., Xu, Q., et al. (2002). Suppression of diabetic retinopathy with angiopoietin-1. *The American Journal of Pathology*, *160*(5), 1683–1693. doi:10.1016/S0002-9440(10)61115-7

Klein, B. E., Klein, R., Moss, S. E., & Palta, M. (1995). A cohort study of the relationship of diabetic retinopathy to blood pressure. *Archives of Ophthalmology*, *113*(5), 601–606.

Klein, R., Klein, B. E., & Moss, S. E. (1992). Epidemiology of proliferative diabetic

retinopathy. *Diabetes Care*, *15*(12), 1875–1891.

Klein, R., Klein, B. E., Moss, S. E., Davis, M. D., & DeMets, D. L. (1984). The Wisconsin epidemiologic study of diabetic retinopathy. III. Prevalence and risk of diabetic retinopathy when age at diagnosis is 30 or more years. *Archives of Ophthalmology*, *102*(4), 527–532.

Klein, R., Knudtson, M. D., Lee, K. E., Gangnon, R., & Klein, B. E. K. (2008). The Wisconsin Epidemiologic Study of Diabetic Retinopathy: XXII the twenty-five-year progression of retinopathy in persons with type 1 diabetes. *Ophthalmology*, *115*(11), 1859–1868. doi:10.1016/j.ophtha.2008.08.023

Klein, R., Knudtson, M. D., Lee, K. E., Gangnon, R., & Klein, B. E. K. (2009). The Wisconsin Epidemiologic Study of Diabetic Retinopathy XXIII: the twenty-five-year incidence of macular edema in persons with type 1 diabetes. *Ophthalmology*, *116*(3), 497–503. doi:10.1016/j.ophtha.2008.10.016

Ko, F., Vitale, S., Chou, C.-F., Cotch, M. F., Saaddine, J., & Friedman, D. S. (2012). Prevalence of nonrefractive visual impairment in US adults and associated risk factors, 1999-2002 and 2005-2008. *JAMA: The Journal of the American Medical Association*, *308*(22), 2361–2368. doi:10.1001/jama.2012.85685

Lee, J., Kim, K. E., Choi, D.-K., Jang, J. Y., Jung, J.-J., Kiyonari, H., et al. (2013). Angiopoietin-1 guides directional angiogenesis through integrin αvβ5 signaling for recovery of ischemic retinopathy. *Science Translational Medicine*, *5*(203), 203ra127–203ra127. doi:10.1126/scitranslmed.3006666

Lee, S., Kim, W., Moon, S.-O., Sung, M. J., Kim, D. H., Kang, K. P., et al. (2007). Renoprotective effect of COMP-angiopoietin-1 in db/db mice with type 2 diabetes. *Nephrology, Dialysis, Transplantation: Official Publication of the European Dialysis and Transplant Association - European Renal Association*, *22*(2), 396–408. doi:10.1093/ndt/gfl598

Li, G., Veenstra, A. A., Talahalli, R. R., Wang, X., Gubitosi-Klug, R. A., Sheibani, N., & Kern, T. S. (2012). Marrow-derived cells regulate the development of early diabetic retinopathy and tactile allodynia in mice. *Diabetes*, *61*(12), 3294–3303. doi:10.2337/db11-1249

Lieth, E., Antonetti, D. A., Barber, A. J., Gardner, T. W., & Penn State Retina Research Group. (2000). Retinal neurodegeneration: Early pathology in diabetes. *Clinical & Experimental Ophthalmology*, *28*(1), 3–8.

Limb, G. A., Webster, L., Soomro, H., Janikoun, S., & Shilling, J. (1999). Platelet expression of tumour necrosis factor-alpha (TNF-alpha), TNF receptors and intercellular adhesion molecule-1 (ICAM-1) in patients with proliferative diabetic retinopathy. *Clinical and Experimental Immunology*, *118*(2), 213–218.

Liu, J., & Feener, E. P. (2013). Plasma kallikrein-kinin system and diabetic retinopathy. *Biological Chemistry*, *394*(3), 319–328. doi:10.1515/hsz-2012-0316

Maguire, A. M., Simonelli, F., Pierce, E. A., Pugh, E. N., Mingozzi, F., Bennicelli, J., et al. (2008). Safety and efficacy of gene transfer for Leber's congenital amaurosis. *The New England Journal of Medicine*, *358*(21), 2240–2248. doi:10.1056/NEJMoa0802315

Maisonpierre, P. C., Aldrich, T. H., Suri, C., Jones, P. F., Bartunkova, S., Wiegand, S. J., et al. (1997). Angiopoietin-2, a natural antagonist for Tie2 that disrupts in vivo angiogenesis. *Science (New York, N.Y.)*, *277*(5322), 55–60.

McLenachan, S., Chen, X., McMenamin, P. G., & Rakoczy, E. P. (2013). Absence of clinical correlates of diabetic retinopathy in the Ins2Akita retina. *Clinical & Experimental Ophthalmology*, *41*(6), 582–592. doi:10.1111/ceo.12084

Medina, R. J., O'Neill, C. L., Humphreys, M. W., Gardiner, T. A., & Stitt, A. W. (2010a). Outgrowth endothelial cells: Characterization and their potential for reversing ischemic retinopathy. *Investigative Ophthalmology & Visual Science*, *51*(11), 5906–5913. doi:10.1167/iovs.09-4951

Medina, R. J., O'Neill, C. L., O'Doherty, T. M., Wilson, S. E. J., & Stitt, A. W. (2012). Endothelial progenitors as tools to study vascular disease. *Stem Cells International*, *2012*, 346735. doi:10.1155/2012/346735

Medina, R. J., O'Neill, C. L., Sweeney, M., Guduric-Fuchs, J., Gardiner, T. A., Simpson, D. A., & Stitt, A. W. (2010b). Molecular analysis of endothelial progenitor cell (EPC) subtypes reveals two distinct cell populations with different identities. *BMC Medical Genomics*, *3*, 18. doi:10.1186/1755-8794-3-18

Mitchell, P., Wong, T. Y., & Diabetic Macular Edema Treatment Guideline Working Group. (2014). Management paradigms for diabetic macular edema. *American Journal of Ophthalmology*, *157*(3), 505–13.e1–8. doi:10.1016/j.ajo.2013.11.012

Mizutani, M., Kern, T. S., & Lorenzi, M. (1996). Accelerated death of retinal microvascular cells in human and experimental diabetic retinopathy. *The Journal of Clinical Investigation*, *97*(12), 2883–2890. doi:10.1172/JCI118746

Muni, R. H., Kohly, R. P., Lee, E. Q., Manson, J. E., Semba, R. D., & Schaumberg, D. A. (2013). Prospective study of inflammatory biomarkers and risk of diabetic retinopathy in the diabetes control and complications trial. *JAMA Ophthalmology*, *131*(4), 514–521. doi:10.1001/jamaophthalmol.2013.2299

Murata, T., Ishibashi, T., Khalil, A., Hata, Y., Yoshikawa, H., & Inomata, H. (1995). Vascular endothelial growth factor plays a role in hyperpermeability of diabetic retinal vessels. *Ophthalmic Research*, *27*(1), 48–52.

Navaratna, D., McGuire, P. G., Menicucci, G., & Das, A. (2007). Proteolytic degradation of VE-cadherin alters the blood-retinal barrier in diabetes. *Diabetes*, *56*(9), 2380–2387. doi:10.2337/db06-1694

Nguyen, Q. D., Brown, D. M., Marcus, D. M., Boyer, D. S., Patel, S., Feiner, L., et al. (2012). Ranibizumab for diabetic macular edema: results from 2 phase III randomized trials: RISE and RIDE. *Ophthalmology*, *119*(4), 789–801. doi:10.1016/j.ophtha.2011.12.039

Nguyen, Q. D., Shah, S. M., Khwaja, A. A., Channa, R., Hatef, E., Do, D. V., et al. (2010). Two-year outcomes of the ranibizumab for edema of the mAcula in diabetes (READ-2) study. *Ophthalmology*, *117*(11), 2146–2151. doi:10.1016/j.ophtha.2010.08.016

O'Neill, C. L., O'Doherty, M. T., Wilson, S. E., Rana, A. A., Hirst, C. E., Stitt, A. W., & Medina, R. J. (2012). Therapeutic revascularisation of ischaemic tissue: The opportunities and challenges for therapy using vascular stem/progenitor cells. *Stem Cell Research & Therapy*, *3*(4), 31. doi:10.1186/scrt122

Papapetropoulos, A., Fulton, D., Mahboubi, K., Kalb, R. G., O'Connor, D. S., Li, F., et al. (2000). Angiopoietin-1 inhibits endothelial cell apoptosis via the Akt/survivin pathway. *The Journal of Biological Chemistry*, *275*(13), 9102–9105.

Partanen, J., Armstrong, E., Mäkelä, T. P., Korhonen, J., Sandberg, M., Renkonen, R., et al. (1992). A novel endothelial cell surface receptor tyrosine kinase with extracellular epidermal growth factor homology domains. *Molecular and Cellular Biology*, *12*(4), 1698–1707.

Patel, J. I., Hykin, P. G., Gregor, Z. J., Boulton, M., & Cree, I. A. (2005). Angiopoietin concentrations in diabetic retinopathy. *The British Journal of Ophthalmology*, *89*(4), 480–483. doi:10.1136/bjo.2004.049940

Procopio, W. N., Pelavin, P. I., Lee, W. M., & Yeilding, N. M. (1999). Angiopoietin-1 and -2 coiled coil domains mediate distinct homo-oligomerization patterns, but fibrinogen-like domains mediate ligand activity. *The Journal of Biological Chemistry*, *274*(42), 30196–30201.

Prusky, G. T., Alam, N. M., Beekman, S., & Douglas, R. M. (2004). Rapid quantification of adult and developing mouse spatial vision using a virtual optomotor system. *Investigative Ophthalmology & Visual Science*, *45*(12), 4611–4616. doi:10.1167/iovs.04-0541

Quaggin, S. E. (2012). Turning a blind eye to anti-VEGF toxicities. *The Journal of Clinical Investigation*, *122*(11), 3849–3851. doi:10.1172/JCI65509

Rein, D. B. (2013). Vision problems are a leading source of modifiable health

expenditures. *Investigative Ophthalmology & Visual Science*, *54*(14), ORSF18–22. doi:10.1167/iovs.13-12818

Rein, D. B., Zhang, P., Wirth, K. E., Lee, P. P., Hoerger, T. J., McCall, N., et al. (2006). The economic burden of major adult visual disorders in the United States. *Archives of Ophthalmology*, *124*(12), 1754–1760. doi:10.1001/archopht.124.12.1754

Ritter, M. R., Banin, E., Moreno, S. K., Aguilar, E., Dorrell, M. I., & Friedlander, M. (2006). Myeloid progenitors differentiate into microglia and promote vascular repair in a model of ischemic retinopathy. *The Journal of Clinical Investigation*, *116*(12), 3266–3276. doi:10.1172/JCI29683

Romeo, G., Liu, W.-H., Asnaghi, V., Kern, T. S., & Lorenzi, M. (2002). Activation of nuclear factor-kappaB induced by diabetes and high glucose regulates a proapoptotic program in retinal pericytes. *Diabetes*, *51*(7), 2241–2248.

Salm, M., Belsky, D., & Sloan, F. A. (2006). Trends in cost of major eye diseases to Medicare, 1991 to 2000. *American Journal of Ophthalmology*, *142*(6), 976–982. doi:10.1016/j.ajo.2006.07.057

Sander, B., Hamann, P., & Larsen, M. (2008). A 5-year follow-up of photocoagulation in diabetic macular edema: The prognostic value of vascular leakage for visual loss. *Graefe's Archive for Clinical and Experimental Ophthalmology = Albrecht Von Graefes Archiv Für Klinische Und Experimentelle Ophthalmologie*, *246*(11), 1535–1539. doi:10.1007/s00417-008-0892-6

Shaw, J. E., Sicree, R. A., & Zimmet, P. Z. (2010). Global estimates of the prevalence of diabetes for 2010 and 2030. *Diabetes Research and Clinical Practice*, *87*(1), 4–14. doi:10.1016/j.diabres.2009.10.007

Shin, H. Y., Lee, Y. J., Kim, H. J., Park, C.-K., Kim, J. H., Wang, K. C., et al. (2010). Protective role of COMP-Ang1 in ischemic rat brain. *Journal of Neuroscience Research*, *88*(5), 1052–1063. doi:10.1002/jnr.22274

Simonelli, F., Maguire, A. M., Testa, F., Pierce, E. A., Mingozzi, F., Bennicelli, J. L., et al. (2010). Gene therapy for Leber's congenital amaurosis is safe and effective through 1.5 years after vector administration. *Molecular Therapy: The Journal of the American Society of Gene Therapy*, *18*(3), 643–650. doi:10.1038/mt.2009.277

Singh, R., Barden, A., Mori, T., & Beilin, L. (2001). Advanced glycation end-products: A review. *Diabetologia*, *44*(2), 129–146. doi:10.1007/s001250051591

Sivaskandarajah, G. A., Jeansson, M., Maezawa, Y., Eremina, V., Baelde, H. J., & Quaggin, S. E. (2012). Vegfa protects the glomerular microvasculature in diabetes. *Diabetes*, *61*(11), 2958–2966. doi:10.2337/db11-1655

Sjølie, A. K., & Green, A. (1987). Blindness in insulin-treated diabetic patients with age at onset less than 30 years. *Journal of Chronic Diseases*, *40*(3), 215–220.

Stitt, A. W., O'Neill, C. L., O'Doherty, M. T., Archer, D. B., Gardiner, T. A., & Medina, R. J. (2011). Vascular stem cells and ischaemic retinopathies. *Progress in Retinal and Eye Research*, *30*(3), 149–166. doi:10.1016/j.preteyeres.2011.02.001

Stratton, I. M., Kohner, E. M., Aldington, S. J., Turner, R. C., Holman, R. R., Manley, S. E., & Matthews, D. R. (2001). UKPDS 50: Risk factors for incidence and progression of retinopathy in Type II diabetes over 6 years from diagnosis. *Diabetologia*, *44*(2), 156–163. doi:10.1007/s001250051594

Suri, C., Jones, P. F., Patan, S., Bartunkova, S., Maisonpierre, P. C., Davis, S., et al. (1996). Requisite role of angiopoietin-1, a ligand for the TIE2 receptor, during embryonic angiogenesis. *Cell*, *87*(7), 1171–1180.

Tadros, A., Hughes, D. P., Dunmore, B. J., & Brindle, N. P. J. (2003). ABIN-2 protects endothelial cells from death and has a role in the antiapoptotic effect of angiopoietin-1. *Blood*, *102*(13), 4407–4409. doi:10.1182/blood-2003-05-1602

Takakura, N., Huang, X. L., Naruse, T., Hamaguchi, I., Dumont, D. J., Yancopoulos, G. D., & Suda, T. (1998). Critical role of the TIE2 endothelial cell receptor in the development of definitive hematopoiesis. *Immunity*, *9*(5), 677–686.

The Diabetes Control and Complications Trial Research Group. (1993). The effect of intensive treatment of diabetes on the development and progression of long-term complications in insulin-dependent diabetes mellitus. The Diabetes Control and Complications Trial Research Group. *The New England Journal of Medicine*, *329*(14), 977–986. doi:10.1056/NEJM199309303291401

Thurston, G. (2002). Complementary actions of VEGF and angiopoietin-1 on blood vessel growth and leakage. *Journal of Anatomy*, *200*(6), 575–580.

Thurston, G., Rudge, J. S., Ioffe, E., Zhou, H., Ross, L., Croll, S. D., et al. (2000). Angiopoietin-1 protects the adult vasculature against plasma leakage. *Nature Medicine*, *6*(4), 460–463. doi:10.1038/74725

Tiruppathi, C., Malik, A. B., Del Vecchio, P. J., Keese, C. R., & Giaever, I. (1992). Electrical method for detection of endothelial cell shape change in real time: Assessment of endothelial barrier function. *Proceedings of the National Academy of Sciences of the United States of America*, *89*(17), 7919–7923.

Traktuev, D. O., Merfeld-Clauss, S., Li, J., Kolonin, M., Arap, W., Pasqualini, R., et al. (2008). A population of multipotent CD34-positive adipose stromal cells share pericyte and mesenchymal surface markers, reside in a periendothelial location, and stabilize endothelial networks. *Circulation Research*, *102*(1), 77–85.

doi:10.1161/CIRCRESAHA.107.159475

van Dijk, H. W., Kok, P. H. B., Garvin, M., Sonka, M., Devries, J. H., Michels, R. P. J., et al. (2009). Selective loss of inner retinal layer thickness in type 1 diabetic patients with minimal diabetic retinopathy. *Investigative Ophthalmology & Visual Science*, *50*(7), 3404–3409. doi:10.1167/iovs.08-3143

Vinores, S. A., Xiao, W.-H., Shen, J., & Campochiaro, P. A. (2007). TNF-alpha is critical for ischemia-induced leukostasis, but not retinal neovascularization nor VEGF-induced leakage. *Journal of Neuroimmunology*, *182*(1-2), 73–79. doi:10.1016/j.jneuroim.2006.09.015

White, N. H., Sun, W., Cleary, P. A., Danis, R. P., Davis, M. D., Hainsworth, D. P., et al. (2008). Prolonged effect of intensive therapy on the risk of retinopathy complications in patients with type 1 diabetes mellitus: 10 years after the Diabetes Control and Complications Trial. *Archives of Ophthalmology*, *126*(12), 1707–1715. doi:10.1001/archopht.126.12.1707

Wild, S., Roglic, G., Green, A., Sicree, R., & King, H. (2004). Global prevalence of diabetes: Estimates for the year 2000 and projections for 2030. *Diabetes Care*, *27*(5), 1047–1053.

Wilkinson, C. P., Ferris, F. L., Klein, R. E., Lee, P. P., Agardh, C. D., Davis, M., et al. (2003). Proposed international clinical diabetic retinopathy and diabetic macular edema disease severity scales. *Ophthalmology*, *110*(9), 1677–1682. doi:10.1016/S0161-6420(03)00475-5

Wong, T. Y., Mwamburi, M., Klein, R., Larsen, M., Flynn, H., Hernandez-Medina, M., et al. (2009). Rates of progression in diabetic retinopathy during different time periods: A systematic review and meta-analysis. *Diabetes Care*, *32*(12), 2307–2313. doi:10.2337/dc09-0615

Xie, L., Zhu, X., Hu, Y., Li, T., Gao, Y., Shi, Y., & Tang, S. (2008). Mitochondrial DNA oxidative damage triggering mitochondrial dysfunction and apoptosis in high glucose-induced HRECs. *Investigative Ophthalmology & Visual Science*, *49*(9), 4203–4209. doi:10.1167/iovs.07-1364

Yau, J. W. Y., Rogers, S. L., Kawasaki, R., Lamoureux, E. L., Kowalski, J. W., Bek, T., et al. (2012). Global prevalence and major risk factors of diabetic retinopathy. *Diabetes Care*, *35*(3), 556–564. doi:10.2337/dc11-1909

Yellowlees Douglas, J., Bhatwadekar, A. D., Li Calzi, S., Shaw, L. C., Carnegie, D., Caballero, S., et al. (2012). Bone marrow-CNS connections: Implications in the pathogenesis of diabetic retinopathy. *Progress in Retinal and Eye Research*, *31*(5), 481–494. doi:10.1016/j.preteyeres.2012.04.005

Yin, L., Greenberg, K., Hunter, J. J., Dalkara, D., Kolstad, K. D., Masella, B. D., et al. (2011). Intravitreal injection of AAV2 transduces macaque inner retina. *Investigative Ophthalmology & Visual Science*, *52*(5), 2775–2783. doi:10.1167/iovs.10-6250

Zhang, P., Zhang, X., Brown, J., Vistisen, D., Sicree, R., Shaw, J., & Nichols, G. (2010). Global healthcare expenditure on diabetes for 2010 and 2030. *Diabetes Research and Clinical Practice*, *87*(3), 293–301. doi:10.1016/j.diabres.2010.01.026

Zhang, X., Bao, S., Hambly, B. D., & Gillies, M. C. (2009). Vascular endothelial growth factor-A: a multifunctional molecular player in diabetic retinopathy. *The International Journal of Biochemistry & Cell Biology*, *41*(12), 2368–2371. doi:10.1016/j.biocel.2009.07.011

Zhu, W., London, N. R., Gibson, C. C., Davis, C. T., Tong, Z., Sorensen, L. K., et al. (2012). Interleukin receptor activates a MYD88-ARNO-ARF6 cascade to disrupt vascular stability. *Nature*, *492*(7428), 252–255. doi:10.1038/nature11603

CHAPTER 2

ACRIDINE ORANGE LEUKOCYTE FLUOROGRAPHY IN MICE*

*Reprinted with permission from Experimental Eye Research and Elsevier Publishing Cahoon, JM. *et al.* Acridine orange leukocyte fluorography in mice. Experimental Eye Research 120, 15-19.

Experimental Eye Research 120 (2014) 15–19

Contents lists available at ScienceDirect

Experimental Eye Research

journal homepage: www.elsevier.com/locate/yexer

Methods in eye research

Acridine orange leukocyte fluorography in mice☆

Judd M. Cahoon [a,*], Paul R. Olson [a], Spencer Nielson [a], Tadashi R. Miya [a], Peter Bankhead [b], J. Graham McGeown [b], Timothy M. Curtis [b], Balamurali K. Ambati [a]

[a] Department of Ophthalmology and Visual Science, John A Moran Eye Center, University of Utah, Salt Lake City, UT 84109, United States
[b] Centre for Vision and Vascular Science, Queen's University of Belfast, Institute of Clinical Sciences, Block A, Royal Victoria Hospital Belfast, Ireland

ARTICLE INFO

Article history:
Received 29 May 2013
Accepted in revised form 4 December 2013
Available online 12 December 2013

Keywords:
retina
leukocyte
inflammation
acridine orange
blood flow

ABSTRACT

Simultaneous non-invasive visualization of blood vessels and nerves in patients can be obtained in the eye. The retinal vasculature is a target of many retinopathies. Inflammation, readily manifest by leukocyte adhesion to the endothelial lining, is a key pathophysiological mechanism of many retinopathies, making it a valuable and ubiquitous target for disease research. Leukocyte fluorography has been extensively used in the past twenty years; however, fluorescent markers, visualization techniques, and recording methods have differed between studies. The lack of detailed protocol papers regarding leukocyte fluorography, coupled with lack of uniformity between studies, has led to a paucity of standards for leukocyte transit (velocity, adherence, extravasation) in the retina. Here, we give a detailed description of a convenient method using acridine orange (AO) and a commercially available scanning laser ophthalmoscope (SLO, HRA-OCT Spectralis) to view leukocyte behavior in the mouse retina. Normal mice are compared to mice with acute and chronic inflammation. This method can be readily adopted in many research labs.

1. Introduction

The eye uniquely lends itself to simultaneous non-invasive visualization of blood vessels and nerves in patients. Many retinopathies affect the retinal vasculature, in turn compromising neural function. Inflammation is a key pathophysiological mechanism of many retinopathies, making it a valuable and ubiquitous target for disease research. Leukocyte adherence to the endothelial lining of blood vessels is a key component of inflammation. Leukocyte fluorography has been extensively used in the past twenty years (Janssen et al., 1994; Nishiwaki et al., 1995, 1996; Iwama et al., 2008; Miyahara et al., 2004); however, fluorescent markers, visualization techniques, and recording methods have differed between studies. To date there have been no detailed protocol papers relating to leukocyte fluorography in mice, resulting in a paucity of standards for leukocyte transit (velocity, adherence, extravasation) in the retina. We describe a convenient method using acridine orange (AO) and a commercially available scanning laser ophthalmoscope (SLO, HRA-OCT Spectralis) to view leukocyte behavior in the mouse retina and demonstrate that leukocyte rolling and adhesion can be visualized in acute and chronic inflammation.

Acridine orange (AO) is a cell permeable metachromatic fluorescent dye that has been widely used to assess apoptotic cells, measure leukocyte adhesion, and quantify vascular flow (as it binds white but not red blood cells) (Janssen et al., 1994). After binding double-stranded DNA, AO emits green fluorescence with spectral properties similar to sodium fluorescein (peak excitation at 502 nm and emission at 522 nm). Although a tried and tested technique, in vivo AO leukocyte fluorography (AOLF) has been predominantly reserved for studies equipped with a customized in-house scanning laser ophthalmoscope on larger rodent models (Barouch et al., 2000; Joussen et al., 2001). Even when AOLF was used with commercially available SLOs, a video monitoring system developed in-house developed was required for recording and analysis (Miyamoto et al., 1998). While leukocyte fluorography has been tested in mice, it has either relied on alternative dyes which required removal of leukocytes prior to staining and then re-introducing the leukocytes back into the mouse (Xu et al., 2003), or relied on in house video recording devices that required separate set up (Iwama et al., 2008; Miyahara et al., 2004). This paper presents a method with simple administration of the fluorescent agent (tail vein injection of AO) and a commercially available imaging system (Heidelberg Spectralis) which contains within its software

☆ Study supported by NEI RO1EY01796-01A1.
* Corresponding author. Tel.: +1 801 213 2550.
E-mail addresses: judd.cahoon@hsc.utah.edu, judd.cahoon@utah.edu (J. M. Cahoon).

0014-4835/$ – see front matter © 2013 Elsevier Ltd. All rights reserved.
http://dx.doi.org/10.1016/j.exer.2013.12.002

video recording capabilities. Standards for arteriole, capillary, and venule leukocyte velocity are compared to previously reported data as well as mouse models of acute (intravitreal injection of VEGF) and chronic (diabetes > four months) inflammation.

2. Materials and supplies

2.1. Mice

All animals were treated in accordance with IACUC approval. Three cohorts of mice obtained from Jackson laboratory were used in this study. Male C57Bl6/J mice were compared to Ins2Akita heterozygote male mice (diabetic, >600 mg/dL blood glucose), and C57Bl6/J mice treated with intravitreal injections of VEGF (200 ng/2 μL) to study chronic and acute inflammation, respectively. All mice were aged 20–25 weeks. Mice injected intravitreally with VEGF were observed the following day.

2.2. Scanning laser ophthalmoscope

Heidelberg Spectralis: HRA-OCT Spectralis (Heidelberg, Germany) running software version 1.6.4.0 was used with a 488 nm argon blue laser with a standard 500 nm long-pass filter.

2.3. Anesthetic

Isoflurane a mixture of 3% Isoflurane/O_2 mixture in a closed canister at a flow rate of 1.0 Lpm. Anesthesia was maintained with 1.5% isoflurane/O_2 mixture at same flow rate.

2.4. Fluorescent agent

Acridine orange was purchased from Acros organics Acridine orange (AO (Acros Organics, Geel, Belgium), 0.10%/PBS) and filtered with a 0.22 μm filter.

2.5. Video analysis

Video images acquired by Heidelberg Spectralis were transferred to .avi format using the included software. AVI files were then opened in ImageJ using and analyzed with a plug in developed by Peter Bankhead.

3. Detailed methods

3.1. Imaging mouse retina

Mice were anesthetized by an initial inhalation of 3% Isoflurane/O_2 mixture in a closed canister at a flow rate of 1.0 Lpm. Anesthesia was maintained with 1.5% isoflurane/O_2 mixture at same flow rate and mice were placed on a heated water pad (37 °C). Pupils were dilated with a 1% tropicamide solution and afterward hydrated periodically with saline solution to prevent corneal desiccation. Acridine orange (AO (Acros Organics, Geel, Belgium), 0.10%/PBS) was filtered with a 0.22 μm filter. The solution (0.05 mL/min for a total of 1 min) was then injected into the tail vein of mice. Imaging was accomplished using HRA-OCT Spectralis (Heidelberg, Germany) with a 488 nm argon blue laser with a standard 500 nm long-pass filter. Images were acquired from both eyes with a 55 ° lens while restricting the visual field to a 25 ° digital zoom to visualize an area of 3.3 mm × 3.3 mm. Reducing the visual field shortened the time required to obtain horizontal scans therefore increasing the frame rate. Utilizing the movie mode on the Heidelberg HRA OCT Spectralis, videos were captured at 15.4 frames per second imaging in High Speed mode. Endothelial staining of AO allowed for identification of larger retinal vessels in which leukocytes were manually focused upon. To control for minor eye movements, either induced by the operator or the mouse, video frames were registered after acquisition. Arteries and veins were distinguished by leukocyte transit away from and toward the optic disc, respectively. Arteries and veins, of which there were typically six each, were defined as emanating from the optic nerve. Arterioles were defined as branches coming from the central retinal arteries and leading to capillaries. Capillaries connected the arterioles to the venules, which drained back into the central retinal veins. Images focused on the superior quadrant of the retina between artery, capillary bed, and vein. After acquiring videos, animals were transferred to a recovery heat pad and monitored until regaining full consciousness.

3.2. Analysis of videos

Videos were exported in .avi format from Heidelberg proprietary software and opened in ImageJ software. Relevant leukocytes were determined by those present in at least three frames in the field of view and 3 disc diameters away from the optic disc. At least three leukocytes were tracked in each vessel type (3 per artery/iole, vein/ule, and capillary) in each eye and in each mouse ($n = 18$). Using a Cell Analyzer Plugin (developed by Peter Bankhead) leukocytes were tracked in consecutive frames. Distances in pixels were calculated and converted using Heidelberg's automated scaling metadata to microns (1.22 microns/pixel) after adjusting for murine corneal radius of curvature of 1.4 mm. Multiplying distance traveled between frames by 15.4 yielded individual velocities and averages were calculated.

Leukocyte engagement and subsequent rolling along the endothelium was also recorded and tracked using the Cell Analyzer Plugin. Rolling leukocytes exhibited much slower transit times and followed the vessel wall. Leukocytes were determined to be rolling if they maintained contact with the vessel wall and could be tracked for greater than 5 consecutive frames (with many exceeding 10 frames).

3.3. In vitro leukocyte rolling

To determine whether acridine orange affected leukocyte-endothelial interaction dynamics we tested human leukocyte rolling over human retinal microvascular endothelial cells (HrMVEC, human primary cells from Cell Systems, Kirkland, WA) in vitro (a system wherein leukocytes are visible without acridine orange labeling). HrMVECs were cultured in parallel-plate fibronectin-coated flow chambers (Ibidi u-slide VI 0.4) until 80% confluent and then exposed to TNF-α (10 ng/mL) or vehicle control for three hours to elicit an inflammatory and pro-adhesive response to leukocytes. Leukocytes, obtained from venous whole blood of healthy human donors, were isolated as described previously (Zhu et al., 2012), diluted in warmed ultrasaline (Lonza) to 1 × 106/ml and exposed to acridine orange (0.15%) or vehicle control. Leukocyte solution was then pumped through the parallel plate flow chambers using a syringe pump (Harvard Apparatus) at 1 dyn/cm2 (typical venous shear stress). Leukocyte adhesion and rolling was monitored using differential interference contrast microscopy (DIC). DIC images were acquired at a rate of 1/second for 1 min and the number of leukocytes adhered or rolling on the endothelial monolayer was quantified as leukocytes/frames/second. At least four independent flow wells were averaged to achieve the reported values (mean ± SD).

3.4. Results

In C57Bl6/J mice, leukocyte velocity was greatest in the arteries and veins (18.07 ± 3 mm/s and 17.7 ± 2 mm/s, respectively).

Table 1
Leukocyte velocity in C57Bl6/J mice is given in each area of the vascular tree. Leukocyte transit times of diabetic Ins2Akita mice and C57Bl6/J treated with intravitreal injections of VEGF are given as well. Diabetic mice had slower leukocyte velocities in the arterioles, capillaries, venules, and veins ($p < 0.0001$), while VEGF-injected mice experienced slower transit times in the capillaries, only ($p < 0.001$).

	Velocity (mm/sec)					
		Artery	Arteriole	Capillary	Venule	Vein
Mouse type	C57Bl6/J	18.1 ± 3	6.9 ± 1	1.7 ± 0.4	8.5 ± 1	17.7 ± 2
	Ins2Akita	12.8 ± 1	3.7 ± 0.8*	0.7 ± 0.2*	2.7 ± 0.5*	3.6 ± 0.4*
	C57Bl6/J + VEGF	12.5 ± 1.1	7.2 ± 0.8	0.7 ± 0.1*	6.4 ± 1	13.7 ± 1

* = $p < 0.001$.

Velocity decreased in arterioles and venules (6.9 ± 1 mm/s and 8.5 ± 1.1 mm/s, respectively) and was slowest in the capillaries (1.7 ± 0.3 mm/s). These values were significantly decreased in the Ins2Akita mice and the mice injected with VEGF (Table 1, Fig. 1). The number of rolling leukocytes in the venules and veins of normal C57Bl6/J mice averaged 0.3 ± 0.8 within the field of view (FOV) (3 mm × 3 mm) over a five minute observation period, compared with 13.5 ± 5.1 in the diabetic Ins2Akita mice and 8 ± 1.4 in the VEGF-injected mice (Fig. 2). Data are shown in Table 1 (mean ± standard deviation, $n = 18$ C57Bl6/J mice, 9 Ins2Akita mice, 7 VEGF-injected C57Bl6/J mice).

3.5. Evaluation of extravasated leukocytes

To determine whether leukocytes had left the vasculature and crossed into the retina, static images of the retina were taken 30 min after injection of acridine orange. By this time, leukocytes were not visible traveling in the blood vessels (due to the washout effect (Iwama et al., 2008), and leukocytes appeared outside major vessels). The number of leukocytes counted in the still image was taken to represent the number of leukocytes that left the vasculature and extravasated into the retina. 1.48 ± 1.04 leukocytes migrated out of the vasculature and into the FOV in normal C57Bl6/J mice, as analyzed thirty minutes after AO injection. VEGF injection dramatically increased leukocyte extravasation (13 ± 6.3 leukocytes). Ins2Akita mice also demonstrated increased leukocyte extravasation (7.1 ± 3.3 leukocytes). Leukocyte extravasation was confirmed using confocal microscopy to visualize leukocytes (CD11b, BD Biosciences, San Jose, California) and vessels (isolectin GS-IB_4, Life Technologies, Carlsbad, California) on retinal flatmount (Fig. 3). It should be noted that confocal microscopic imaging revealed more extravasated leukocytes than could be observed with the ophthalmoscope.

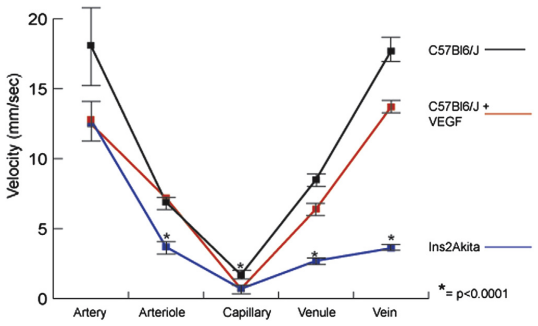

Fig. 1. Graph demonstrating leukocyte velocity in each segment of the vascular tree. Leukocyte velocity was slower in diabetic Ins2Akita mice compared to normal mice in all areas except the central retinal arteries. VEGF injection decreased leukocyte transit time in the capillaries.

3.6. In vitro leukocyte rolling

While TNF-α increased leukocyte adhesion and rolling in vitro, acridine orange had no effect on leukocyte adhesion or rolling in either the inflammatory (TNF-α+) (36 ± 5, without acridine orange vs. 31 ± 6, with acridine orange leukocyte frames/sec) or non-inflammatory (TNF-α−) (4 ± 1, without acridine orange vs. 3 ± 1, with acridine orange leukocyte frames/sec) conditions ($n = 4$ wells per condition; $p = 0.68$ between AO + and AO −)(Fig. 4). Acridine orange did not affect leukocyte adhesion to the endothelium in the presence or absence of TNF-alpha.

4. Potential pitfalls and troubleshooting

4.1. Eye opacity

Visualization became limited after cataracts began to form due to continued anesthesia. This limited visualization for each mouse to a temporal window of 5 min. Several methods were employed to reduce cataract formation: 1) mice were placed on a heated water pad during imaging, 2) moisture of mouse eyes was maintained with periodic drops of phosphate buffered saline and wicked away with a cotton tip applicator to allow for clear visualization, 3) imaging time was limited to 5 min maximum. By following these practices, clarity persisted allowing for useful imaging.

4.2. Continuous tail vein injections

To maintain a continuous flow of acridine orange into the mouse we employed use of a butterfly catheter needle (25 gauge) attached

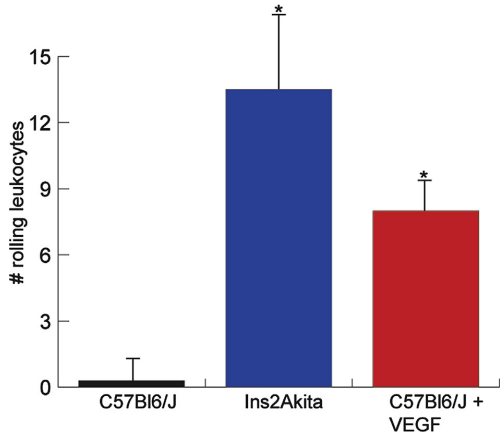

Fig. 2. The number of rolling leukocytes counted over a five minute observation period following acridine orange administration. Leukocyte rolling was increased in diabetic Ins2Akita mice and mice injected with VEGF.

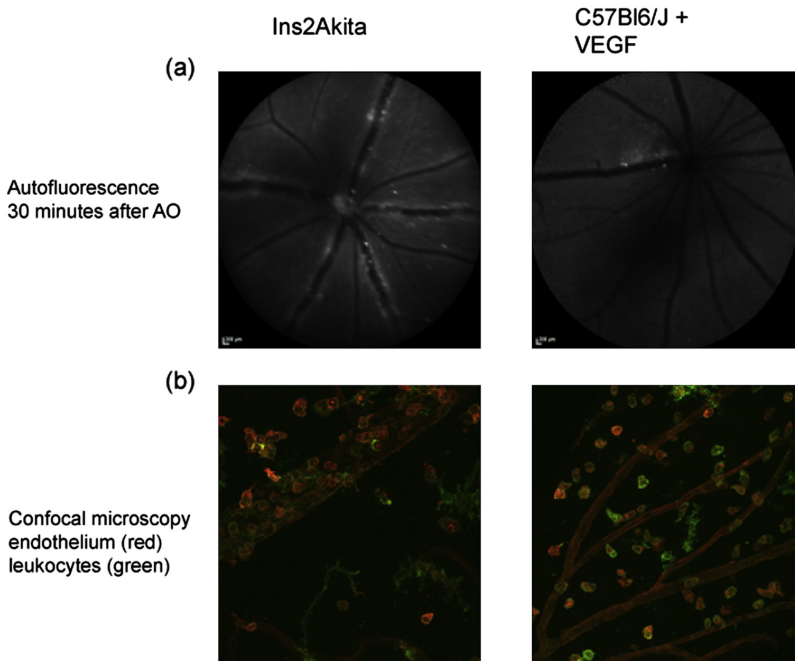

Fig. 3. Leukocyte extravasation was seen 30 min after acridine orange administration with the scanning laser ophthalmoscope and was confirmed with confocal microscopy.

to a 1 mL syringe. After the needle was placed into the tail vein (confirmed with low resistance when pressure was applied to the plunger) the needle was taped in place allowing for a small bolus to be applied every 30 s. If too many leukocytes were observed in the FOV, making counting and tracking difficult, AO solution could be injected intraperitoneally to dilute the concentration and allow for a slower absorption into the circulation.

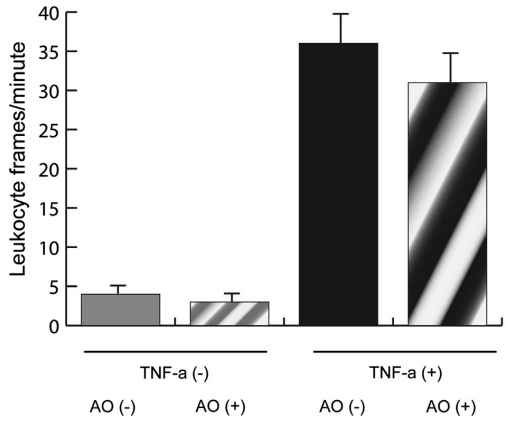

Fig. 4. To determine whether acridine orange altered leukocyte endothelial interactions, human leukocytes were rolled across a human retinal microvascular endothelial cell monolayer at a constant rate. Leukocytes could be visualized under microscope and adhering leukocytes were counted in each frame. Results are shown as leukocyte frames/minute for each condition. While TNF-α increased leukocyte adhesion, acridine orange did not alter leukocyte adhesion in either the presence or absence of TNF-α.

4.3. Speed of recording

To increase the frame rate High Speed mode was selected and FOV was narrowed to a 3 mm × 3 mm area of the retina; this allowed us to record at 15.4 frames/sec.

5. Discussion

Here we present a detailed description of the established method of following leukocytes in vivo. Leukocytes can be easily visualized and tracked after tail vein injection of acridine orange in mice using a commercially available system (HRA-OCT Spectralis), mitigating the need for custom-built in house video monitoring systems making this technique feasible for many laboratories that already routinely image the mouse retina. By defining the normal parameters of leukocyte behavior in vivo in the mouse retina, this technique establishes baseline characteristics against which leukocyte behavior in inflammatory stress models or therapeutic models can be compared. Previously reported data for average leukocyte velocity in arterioles, venues, and capillaries comes from a study by Xu et al., in Balb/C mice and B10. RIII mice using C-AM labeled leukocytes (Xu et al., 2002). However, results reported here, though slightly slower, are still in alignment with these results despite a different background of mouse and leukocyte fluorescent agent.

There are some limitations to our study that merit future mechanistic investigation and technical enhancements. Higher magnification and resolution would enable assessment of firmly adherent cells. It is possible that some of the “extravasated leukocytes” are en face capillaries, but this is unlikely as we observed carefully for flow within these structures by using different angles of visualization. Extravasated cells retain acridine orange longer than endothelial cells mainly due to the washout effect (Xu et al.,

2003). Extravasated cells may be a specific subset of leukocytes and not representative of leukocytes in general. Elucidating this and characterizing the surface markers of extravasated leukocytes would require separating retinal interstitial tissue from retinal vessels, or performing acridine orange leukography in the relatively avascular retina of rabbits. Most importantly, assessing the impact of retinal vascular hyperpermeability on extravasation in models of retinal disease that disrupt the blood-retinal barrier would have the most translational value.

Future studies with this approach could explore in vivo studies of leukocyte dynamics in diabetic retinopathy, retinal vein occlusion, uveitis, or other inflammatory conditions. If dynamic leukocyte behavior was significantly different in these conditions, it would be easy to envision developing a system where imaging these parameters in patients (with a non-toxic leukocyte fluorophore as opposed to acridine orange) could be of diagnostic, prognostic, or disease monitoring value. Tagging leukocytes and endothelial or neural cells with different fluorophores would enable high-resolution imaging of leukocyte interactions with other retinal components with an appropriate multi-spectal imaging system. Further, labeling of leukocytes with long-wavelength fluorophores would theoretically facilitate imaging of leukocyte dynamics in the pigmented choroid. In conclusion, leukocytes can be easily visualized and tracked after tail vein injection of acridine orange in mice using a commercially available system (HRA-OCT Spectralis), bypassing the need for complex in house video monitoring, making this technique feasible for many laboratories that already routinely image the mouse retina.

Acknowledgments

We thank Bonnie Archer for proofreading the manuscript. We thank Andrew Weyrich, Guy Zimmerman, Robert Campbell for isolating leukocytes. We thank Christopher Gibson and Dean Li for assistance with the leukocyte rolling assay. Supported in part by an Unrestricted Grant from Research to Prevent Blindness, Inc., New York, NY, to the Department of Ophthalmology & Visual Sciences, University of Utah.

Appendix A. Supplementary data

Supplementary data related to this article can be found at http://dx.doi.org/10.1016/j.exer.2013.12.002.

References

Barouch, F.C., Miyamoto, K., Allport, J.R., Fujita, K., Bursell, S.E., Aiello, L.P., Luscinskas, F.W., Adamis, A.P., 2000. Integrin-mediated neutrophil adhesion and retinal leukostasis in diabetes. Investig. Ophthalmol. Vis. Sci. 41, 1153–1158.

Iwama, D., Miyahara, S., Tamura, H., Miyamoto, K., Hirose, F., Yoshimura, N., 2008. Lack of inducible nitric oxide synthases attenuates leukocyte-endothelial cell interactions in retinal microcirculation. Br. J. Ophthalmol. 92, 694–698.

Janssen, G.H., Tangelder, G.J., Oude Egbrink, M.G., Reneman, R.S., 1994. Spontaneous leukocyte rolling in venules in untraumatized skin of conscious and anesthetized animals. Am. J. Physiol. 267, H1199–H1204.

Joussen, A.M., Murata, T., Tsujikawa, A., Kirchof, B., Bursell, S.E., Adamis, A.P., 2001. Leukocyte-mediated endothelial cell injury and death in the diabetic retina. Am. J. Pathol. 158, 147–152.

Miyahara, S., Kiryu, J., Miyamoto, K., Katuta, H., Hirose, F., Tamura, H., Musashi, K., Honda, Y., Yoshimura, N., 2004. In vivo three-dimensional evaluation of leukocyte behavior in retinal microcirculation of mice. Investig. Ophthalmol. Vis. Sci. 45, 4197–4201.

Miyamoto, K., Hiroshiba, N., Tsujikawa, A., Ogura, Y., 1998. In vivo demonstration of increased leukocyte entrapment in retinal microcirculation of diabetic rats. Investig. Ophthalmol. Vis. Sci. 39, 2190–2194.

Nishiwaki, H., Ogura, Y., Kimura, H., Kiryu, J., Honda, Y., 1995. Quantitative evaluation of leukocyte dynamics in retinal microcirculation. Investig. Ophthalmol. Vis. Sci. 36, 123–130.

Nishiwaki, H., Ogura, Y., Kimura, H., Kiryu, J., Miyamoto, K., Matsuda, N., 1996. Visualization and quantitative analysis of leukocyte dynamics in retinal microcirculation of rats. Investig. Ophthalmol. Vis. Sci. 37, 1341–1347.

Xu, H., Manivannan, A., Goatman, K.A., Liversidge, J., Sharp, P.F., forrester, J.V., Crane, I.J., 2002. Improved leukocyte tracking is mouse retinal and choroidal circulation. Exp. Eye Res. 74 (3), 403–410.

Xu, H., Forrester, J.V., Liversidge, J.I., Crane, J., 2003. Leukocyte trafficking in experimental autoimmune uveitis: breakdown of blood-retinal barrier and upregulation of cellular adhesion molecules. Investig. Ophthalmol. Vis. Sci. 44, 226–234.

Zhu, W., London, N.R., Gibson, C.C., Davis, C.T., Tong, Z., Sorensen, L.K., Shi, D.S., Guo, J., Smith, M.C.P., Grossman, A.H., Thomas, K.R., Li, D.Y., 2012. Interleukin receptor activates a MYD88-ARNO-ARF6 cascade to disrupt vascular stability. Nature 492, 252–255.

CHAPTER 3

COMP-ANG1 AND ENDOTHELIAL COLONY-FORMING CELLS RESTORE DIABETIC RETINAL NEUROVASCULATURE

3.1 Abstract

Diabetic retinopathy is the leading cause of blindness in the working-age population in the US. Hyperglycemia induces neuroglial dysfunction in the retina, which occurs in unison with vascular cell damage leading to breakdown of the blood retinal barrier, vasodegeneration, and ischemia. Currently, no therapies exist for normalizing the vasculature in diabetic retinopathy. Here, we show that a single intravitreal dose of adeno-associated virus serotype 2 encoding a stable, soluble form of Ang1 (AAV2.COMP-Ang1) ameliorated structural and functional hallmarks of diabetic retinopathy with sustained effects observed through six months. AAV2.COMP-Ang1 single-dose gene therapy modulated the expression of vascular markers, such as VE-cadherin and VEGF-A, which were expressed in levels comparable to nondiabetic controls, and preserved retinal vascular integrity in the diabetic mouse. Furthermore, AAV2.COMP-Ang1 prevented retinal thinning and ganglion cell layer dropout and largely preserved visual tracking and electroretinographic response. In mice with established diabetic retinopathy, COMP-Ang1 enhanced the therapeutic benefit of intravitreally-delivered endothelial colony-forming cells by promoting integration into the vasculature, which significantly stemmed further visual decline. AAV2.COMP-Ang1 can prevent neural and vascular pathology in early diabetic retinopathy and promote vascular regeneration and stabilize visual function in late diabetic retinopathy.

3.2 Introduction

Diabetes affects 25.8 million people in the United States and its prevalence is expected to triple in the next 20 years (Wong et al., 2009; Yau et al., 2012). Diabetic

retinopathy (DR) is the leading cause of blindness in the working-age population (Wild, Roglic, Green, Sicree, & King, 2004). The leading cause of vision loss in DR is diabetic macular edema (DME), largely induced by vascular hyperpermeability associated with breakdown of the blood retinal barrier (BRB) (Murata et al., 1995). DME is currently treated by laser photocoagulation and monthly intravitreal injections of agents that block vascular endothelial growth factor (VEGF). These treatments fail to improve vision in a significant number of patients (Brown et al., 2013), and have risks of retinal burns, detachment, hemorrhage, infection, or pain (Jager, Aiello, Patel, & Cunningham, 2004). Current treatment of DME only slows, but does not stop, progression (Campochiaro, Wykoff, Shapiro, Rubio, & Ehrlich, 2014). Moreover, since VEGF is neurotrophic, its blockade in the long-term has been associated with retinal toxicity in rodents and potentially in patients (Quaggin, 2012). This project advances a new approach that works by reversing retinal vascular damage and restoring normal perfusion to improve vision in diabetic retinopathy.

The underlying pathogenesis of DR is largely due to hyperglycemia (Dornan, Mann, & Turner, 1982). Hyperglycemia increases inflammatory responses leading to leukocyte adhesion, microvascular occlusion, and consequent hypoxia (Adamis et al., 2001a; Joussen et al., 2004). Further, hyperglycemia induces pericyte loss, compromising endothelial stability and blood retinal barrier (BRB) integrity. Eventual capillary degeneration leads to retinal nonperfusion, exacerbating retinal hypoxia (Mizutani, Kern, & Lorenzi, 1996). Consequent pathological VEGF-induced angiogenesis is uncoordinated and results in immature, leaky vessels with inadequate perfusion, creating a vicious cycle of hypoxia-driven VEGF secretion (Aiello et al., 1994; Hammes et al.,

2004). Retinal ganglion cell loss, neuronal dysfunction, and changes in vision are also seen in patients with DR and this occurs in unison with vascular pathology (Byeon, Chu, Lee, Lee, & Kwon, 2009; Gastinger, Singh, & Barber, 2006; van Dijk et al., 2009). As a therapeutic goal, vascular stabilization could promote normal perfusion of the metabolically demanding retinal neuropile and prevent sight-threatening sequelae of ischemia.

Patients with DR have decreased vitreous Angiopoietin 1 (Ang1) (J. I. Patel, Hykin, Gregor, Boulton, & Cree, 2005). Ang1, via the Tie2 endothelial receptor, induces vessel quiescence and maturation, and decreases vascular leakage by preventing VEGF-induced degradation of vascular endothelial (VE)-cadherin, a transmembrane protein in the adherens junction between endothelial cells that promotes vascular integrity and decreases vascular permeability (Aldrich et al., 1996; Gavard, Patel, & Gutkind, 2008; Thurston et al., 2000). Further, Ang1 promotes survival of damaged vascular endothelial cells through PI3K/Akt signaling (Augustin, Young Koh, Thurston, & Alitalo, 2009). Thus, restoration of Ang1 signaling could serve as a potential treatment to prevent endothelial loss, retinal ischemia, and abnormal VEGF expression in DR (Joussen et al., 2002). Pharmaceutical development of Ang1 as a viable therapy has been hindered by its insolubility and aggregation. Ten years ago, a novel, stable, soluble and more potent version of Ang1, cartilage oligo matrix protein Ang1 (COMP-Ang1), was developed to overcome the limitations of native Ang1 (Cho et al., 2004).

Acellular capillaries, a hallmark of diabetic retinopathy, lead to nonperfusion, and could theoretically be recellularized and refunctionalized by endothelial progenitor cells (EPCs) (Medina, O'Neill, Sweeney, Guduric-Fuchs, Gardiner, Simpson, et al., 2010b).

However, CD34+ EPCs isolated from diabetic patients have a decreased ability to associate with the existing vascular networks ("Circulating mononuclear progenitor cells: differential roles for subpopulations in repair of retinal vascular injury," 2013). The term EPC encapsulates a diverse group of cell-types with myeloid, haematopoietic or endothelial characteristics (Stitt et al., 2011) and this explains the conflicting clinical trial outcomes using these cells in cardiovascular disease (O'Neill et al., 2012). A unique EPC subtype, known as endothelial colony-forming cells (ECFCs, also known as outgrowth endothelial cells (OECs)), has been shown to encompass true endothelial progenitors which fully integrate into blood vessels and serve to regenerate damaged vasculature in the ischemic retina (Medina, O'Neill, Humphreys, Gardiner, & Stitt, 2010a), as well as other ischemic models (Alphonse et al., 2014). These cells have yet to be investigated as possible reparative cells in the context of the damaged diabetic retinal vasculature.

To model DR, we used the type 1 diabetic Ins2Akita mouse, which harbors a mutation in the insulin gene that prevents proper insulin secretion, inducing hyperglycemia (Barber et al., 2005; Gastinger et al., 2006; Huang et al., 2011). Progressive retinal abnormalities begin 12 weeks after the onset of hyperglycemia and include apoptosis (demonstrated by endothelial and ganglion cell loss) and functional deficits (increased vascular permeability and decreased neuronal function) (Akimov & Rentería, 2012).

We hypothesized that constitutive expression of COMP-Ang1 could prevent vascular endothelial destabilization in a model of early diabetic retinopathy and restore lost vasculature when administered in combination with ECFCs. Here, we show that constitutive expression of COMP-Ang1 via the adeno-associated virus serotype 2

(AAV2) viral vector, a safe and effective vector for retinal disease (Maguire et al., 2008), delivered before the onset of the retinopathy in Ins2Akita mice prevents vascular structural and functional breakdown, accompanied by preservation of neurovascular structure and function. Additionally, we found that COMP-Ang1 increases ECFC tubulogenesis and migration in vitro. Finally, we demonstrate COMP-Ang1 can increase ECFC integration into the aged diabetic Ins2Akita retina and prevent further visual decline.

3.3 Material and methods

C57BL/6-Ins2^{Akita}/J (Ins2Akita) and its background strain, C57BL6/J, mice were obtained from The Jackson Laboratory (Sacramento, USA) and bred in our pathogen-free animal facility. Mice heterozygous for the *Ins2* mutation experience hypoinsulinemia and hyperglycemia by four weeks of age. This research protocol was approved by the Institutional Animal Care and Use Committee of the University of Utah and conforms to the standards in the ARVO Statement for the Use of Animals in Ophthalmic and Vision research. Blood sugar level was measured by using OneTouch® Ultra®2 (LIFESCAN Johnson & Johnson Company, Milpitas, CA, USA). We used only male Ins2Akita with blood sugar levels greater than 600 mg/dL or age-matched controls.

Plasmids, pAAV2.COMP-Ang1 and pAAV2.AcGFP, were made. Cassettes from these were integrated into viral vectors driven by the CMV promoter, to generate AAV2.COMP-Ang1 and AAV2.AcGFP. By integrating cDNA of COMP-Ang1 to pAAV-MCS (Agilent Technologies, Santa Clara, USA), pAAV2.COMP-Ang1 was generated. As a control, pAAV2.AcGFP was also generated using AcGFP cDNA from pIRES2-AcGFP1 (Clontech Laboratories, Mountain View, USA). Each serotype 2 AAV

vector was generated in the Vector Core Gene Therapy Center, University of Massachusetts Medical School.

Each mouse was anesthetized with 0.025 mL Avertin (1.25% tribromoethanol)/gram of body weight intraperitoneally. At two months of age, mice were randomly assigned to receive 2.0 x 10^9 AAV2 particles or the same volume of PBS (2 µl) injected into the vitreous cavity of both eyes with a 33-gauge micro syringe (Hamilton Company, Reno, USA).

Primer sequences for PCR are: COMP-Ang1 F 5`-GCTCTGTTTTCCTGCTGTCC-3` COMP-Ang1 R 5`-GTGATGGAATGTGACGCTTG -3` and, as an internal control, glyceraldehyde 3-phosphate dehydrogenase (GAPDH): GAPDH F 5`-AACTTTGGGATTGTGGAAGGG -3` GAPDH R 5`-ACCAGTGGATGCAGGGATGAT -3`.

At six months of age the retina was harvested and placed in 200 µl of RIPA buffer (Sigma-Aldrich, St. Louis, USA) containing a protease and phosphatase inhibitor cocktail (Roche Diagnostics Corporation, Indianapolis, USA). Samples were subjected to immunoprecipitation using ANTI-FLAG M2 Affinity Gel (Sigma-Aldrich) following the manufacturer's instructions. We detected COMP-Ang1 protein using ANTI-FLAG M2 antibody (Sigma-Aldrich). For detection of other proteins, we used anti-VEGF-A (1:200, Santa Cruz Biotechnology, Inc, Santa Cruz, USA), anti-VE cadherin (1:1000, Abcam, Cambridge, USA), anti-GAPDH (1:3000, Abcam) and anti-phospho-Src (PY419, 1 µg/mL, R&D) and anti-β-actin (1:3000, Abcam) as a primary antibody.

Eyes were fixed with 4% paraformaldehyde for two hours at 4º C, and incubated in sucrose overnight. After embedding in optimal cutting temperature compound (Sakura,

Torrance, USA) globes were cut in 10μm sections. Sections were stained with anti-VE cadherin antibody (1:200, Abcam, Cambridge, USA) for 40 minutes at 37ºC, washed with PBS and stained with AlexaFluor 546 conjugated secondary antibody for 30 minutes at 37º C. Following DAPI staining sections were mounted with anti-fading reagents.

Eyes were placed in 4% paraformaldehyde/PBS at 4ºC for two hours. Preparations were stained with 1:200 α-SMA antibody conjugated with Cy3 (Sigma-Aldrich, St. Louis, USA) and 5μg/ml Alexa 647 conjugated isolectin GS-IB4 (Invitrogen Corporation, Carlsbad, USA) in blocking buffer overnight at 4º C. After washing, the retina was flatmounted on a glass slide. Fluorescence images were captured with scanning laser confocal microscopy (Olympus America Inc. Center Valley, USA).

Measurements of transendothelial electrical resistance were performed with the electrical cell–substrate impedance sensing (ECIS) system (Applied Biophysics, Troy, USA). HrMVECs were seeded (50,000 cells/well) onto fibronectin-coated gold microelectrodes in ECIS culture wells (8W10E+) and incubated overnight at 37°C in EBM-2 media supplemented with EGM2-MV until cell resistance reached a plateau. Cells were serum starved for one hour until resistance was stabilized (1200 Ω). Treatments were added to each well, and monitoring was continued for 21 hours. The data from triplicate wells were averaged and presented as normalized resistance versus time.

Evans Blue (EB) (Sigma-Aldrich) assay was used to assess retinal permeability. Animals were administered Evans Blue (20mg/kg) through tail vein injection. After four hours, animals were sacrificed and retinae were harvested in formamide at 70ºC for 18 hours. Samples were centrifuged for two hours at 40,000 g in a 0.2μm filter and EB

concentration was detected spectrophotometrically by subtracting absorbance at 620 nm from 740 nm. Green fluorescent protein (GFP) conjugated microspheres (100 nm in diameter) were injected into the tail vein of mice (100 μL/20 gram mouse). Mouse eyes were imaged immediately after injection, as well as 30 minutes after injection to observe any residual extravasation. Because we were unable to distinguish GFP microspheres in mice treated with AAV2.GFP, we utilized the ICG modality on Heidelberg Spectralis to visualize 100 nanometer microspheres (Magsphere) conjugated with the near infrared fluorophore ZW800 (Flare Foundation).

Leukocyte-endothelial interaction dynamics were tested using human leukocytes rolled over human retinal microvascular endothelial cells (HrMVEC) *in vitro*. HrMVECs were cultured in parallel-plate fibronectin-coated flow chambers (Ibidi u-slide VI 0.4) until 80% confluent and then exposed to TNF-α (10ng/mL) or vehicle control for three hours to elicit an inflammatory and pro-adhesive response to leukocytes. Leukocytes were isolated as described previously in accordance with IRB protocol (Zhu et al., 2012), diluted in warmed ultrasaline (Lonza) to 1 x 10^6/ml. Leukocyte solution was then pumped through the parallel plate flow chambers using a syringe pump (Harvard Apparatus) at 1 dynes/cm^2 (typical venous shear stress). Differential interference contrast (DIC) images were acquired at a rate of 1/second for one minute and the number of leukocytes adhered or rolling on the endothelial monolayer was quantified as leukocytes/frames/second. At least three independent flow wells were averaged to achieve the reported values (mean +/- stdev).

Mice were anesthetized by an initial inhalation of 3% Isoflurane/O2 mixture in a closed canister at a flow rate of 1.0 Lpm. Pupils were dilated with a 1% tropicamide

solution and afterwards hydrated periodically with saline solution to prevent corneal desiccation. Acridine orange (AO (Acros Organics, Geel, Belgium), 0.10%/PBS) was filtered with a 0.22 μm filter. The solution (0.05mL/min for a total of one minute) was then injected into the tail vein of mice. Imaging was accomplished using HRA-OCT Spectralis (Heidelberg, Germany) with a 488nm argon blue laser with a standard 500nm long-pass filter. Images were acquired from both eyes with a 55 degree utilizing the movie mode on the Heidelberg HRA OCT Spectralis.

Each mouse was anesthetized as described above and pupils were dilated with a drop of 1% tropicamide. Using Spectralis® HRA+OCT (Heidelberg Engineering GmbH, Heidelberg, Germany), fluorescence images were captured to determine AcGFP expression in the retina. Retinal thickness of each mouse was determined *in vivo* using optical coherence tomography (OCT). Retinal thickness was measured 250μm relative to the optic nerve head determined by measurements from the OCT-derived *en face* image. Retinal thickness was measured in the four retinal quadrants and averaged to produce a single value for each retina.

Optomotor reflex-based spatial frequency threshold tests were conducted in a visuomotor behavior measuring system (OptoMotry; CerebralMechanics, Lethbridge, AB, Canada). Tracking was defined as a reproducible smooth pursuit with a velocity and direction concordant with the stimulus. Trials of each direction and spatial frequency were repeated until the presence or absence of the tracking response could be established unequivocally. Spatial frequency of the stimulus was stepped up or down with the staircase method to find the behavioral threshold, corresponding to the visual acuity for the behavior. Rotation speed (12°/s) and contrast (100%) were kept constant.

Electroretinography (ERG) was performed on dark adapted mice anesthetized in dim red light with ketamine/xylazine (10 mg/kg) and placed on a controlled warming plate (TC-1000, CWE Instruments, Ardmore, PA) that maintained temperature. ERGs were measured (UTAS E-3000; LKC Technologies, Gaithersburg, MD) between a gold corneal and a stainless-steel scalp electrode with a 0.3 to 500-Hz band-pass filter. Scotopic ERGs were recorded with flash intensities increasing from -3.62 to -1.61 log(cd s/m^2). The photoflash unit was calibrated by LKC Technologies to deliver 2.5 cd s/m^2 at 0 dB flash intensity.

Fresh human cord blood was obtained under full ethical approval at the Northern Ireland Blood Transfusion Service from healthy volunteers (Belfast, United Kingdom). Mononuclear cells (MNCs) were obtained by density gradient fractionation. To obtain ECFCs, MNCs were resuspended in complete medium (EGM-2 MV; Lonza Ltd.) supplemented with 10% FBS and seeded on 24-well culture plates precoated with rat tail collagen type 1 (BD Biosciences, Bedford, UK) at a density of 1×10^7 cells/mL. Three different clones of ECFCs were used for each experiment. For *in vivo* testing, one clone type was chosen and used in all mice. Cells were labeled with QTracker from Invitrogen according to manufacturer's instructions (Qdot 655) before being delivered via intravitreal injection. At six months, mice were treated with intravitreal injection of AAV2.COMP-Ang1, AAV2.AcGFP, or PBS. Two weeks after delivery of the virus mice were then injected with the $1x10^5$ ECFCs (labeled with QTracker 655, Invitrogen).

All data are presented as mean ± stdev. For statistical analysis between two samples we used a two-tailed Student's t-test, α level 0.05. ANOVA was used for comparison between four groups, $p<0.05$ was considered significant, followed by Tukey

post hoc analysis to determine differences between groups.

3.4 Results

To achieve constitutive expression of COMP-Ang1 in the mouse retina, we delivered AAV2 encoding COMP-Ang1 (AAV2.COMP-Ang1) through intravitreous injections. AAV2 has been safe and effective in clinical trials with intravitreal use (Simonelli et al., 2010). As revealed by *in vivo* confocal fluorescence imaging and *ex vivo* evaluation of retinal flat mounts, *Aequorea coerulescens* green fluorescent protein (AcGFP) fluorescence was observed following AAV2.AcGFP particle injection. Fluorescence was initially observed one-week postinjection and persisted through six months, the endpoint of our first cohort of mice. AcGFP fluoresced in all retinal quadrants at the level of the ganglion cell layer, as previously reported (Yin et al., 2011). COMP-Ang1 mRNA and protein expression was confirmed by reverse transcriptase polymerase chain reaction (RT-PCR) and immunoblotting from the mouse retina, respectively.

Two of the principal features of diabetic retinopathy are pericyte and capillary dropout with consequent vascular hyperpermeability and ischemia (Cogan, Toussaint, & Kuwabara, 1961). We observed that a single injection of AAV2.COMP-Ang1 delivered intravitreally at age two months prevented the retinal vessel loss observed in Ins2Akita mice at age six months (Figure 3.1a). Endothelial staining decreased in the PBS and AAV2.AcGFP treated Ins2Akita mice compared to WT, ($P<0.001$) (Figure 3.1b). AAV2.COMP-Ang1 restored retinal endothelial coverage to ($p=0.02$ vs. AAV2.AcGFP).

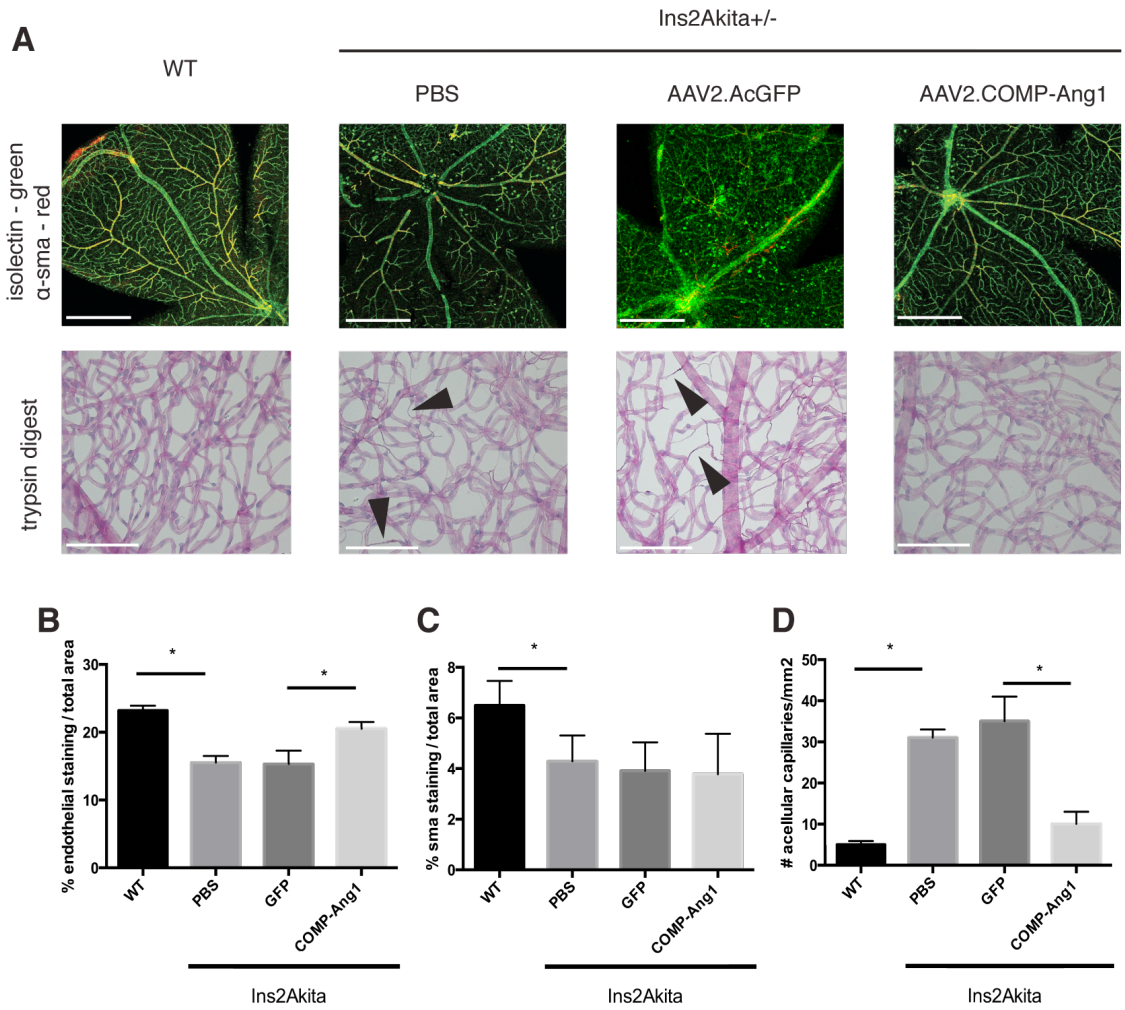

Figure 3.1**:** COMP-Ang1 mitigates diabetic retinal capillary dropout. (a) Representative retinal flatmounts prepared from six month-old mice and stained for isolectin (endothelial cell marker, green) and α-SMA (smooth muscle marker, red). Ins2Akita mice experienced pericyte and endothelial dropout; the latter was prevented with a single intravitreous dose of AAV2.COMP-Ang1. Scale bars = 600 μm (top). Trypsin digest featuring of retinas representative of each group. Black arrow heads denote acellular capillaries (bottom). (b) Quantification using ImageJ of endothelial coverage and (c) pericyte coverage. (d) Acellular capillaries were manually counted and averaged over an area 1mm^2. Eight eyes were used in each analysis, data are mean ± stdev. *$p<0.001$, ANOVA. Post hoc comparisons with a Tukey test to compare means of each group. Scale bars: 100 μm (b).

Pericyte coverage in diabetic Ins2Akita mice decreased compared to controls and was not rescued by AAV2.COMP-Ang1 (Figure 3.1c). These data suggest that AAV2.COMP-Ang1 provides Ang1 endothelial-trophic signaling in lieu of pericytes, which are known to be the major source of endogenous Ang1 in the capillary unit (Aldrich et al., 1996). Trypsin digest preparations confirmed that acellular capillaries were reduced in diabetic mice with COMP-Ang1 treatment compared to control treated diabetics (Figure 3.1a,c) ($p<0.05$).

To assess whether the improved vascular morphology was accompanied by improved function, we determined whether COMP-Ang1 enhanced barrier function in human retinal microvascular endothelial cells (HrMVECs) and the mouse retina. COMP-Ang1 increased, and VEGF decreased, the transepithelial resistance of HrMVECs, as measured by electric cell-substrate impedance sensing (ECIS) (Figure 3.2a) (Tiruppathi, Malik, Del Vecchio, Keese, & Giaever, 1992). While retinal vascular permeability was not marked on fluorescein angiography (McLenachan, Chen, McMenamin, & Rakoczy, 2013), breakdown of the BRB was quantified using Evans Blue permeability into the retina (Adamis, Xu, & Qaum, 2001b) and this was elevated in control-treated Ins2Akita diabetic mice relative to wildtype (WT) mice. Intravitreal AAV2.COMP-Ang1-treatment in Ins2Akita diabetic mice restored Evan's blue permeability to baseline levels comparable to that observed in the WT retina (Figure 3.2b). These findings were further supported by two separate qualitative assessments of vascular permeability *in vivo*. Fluorescent microspheres (100 nm in diameter; labeled with GFP or ZW800 (an NIR fluorophore), whose emission wavelengths are detectable by the Heidelberg Spectralis confocal scanning laser ophthalmoscope in the FA or ICG modes, respectively, were

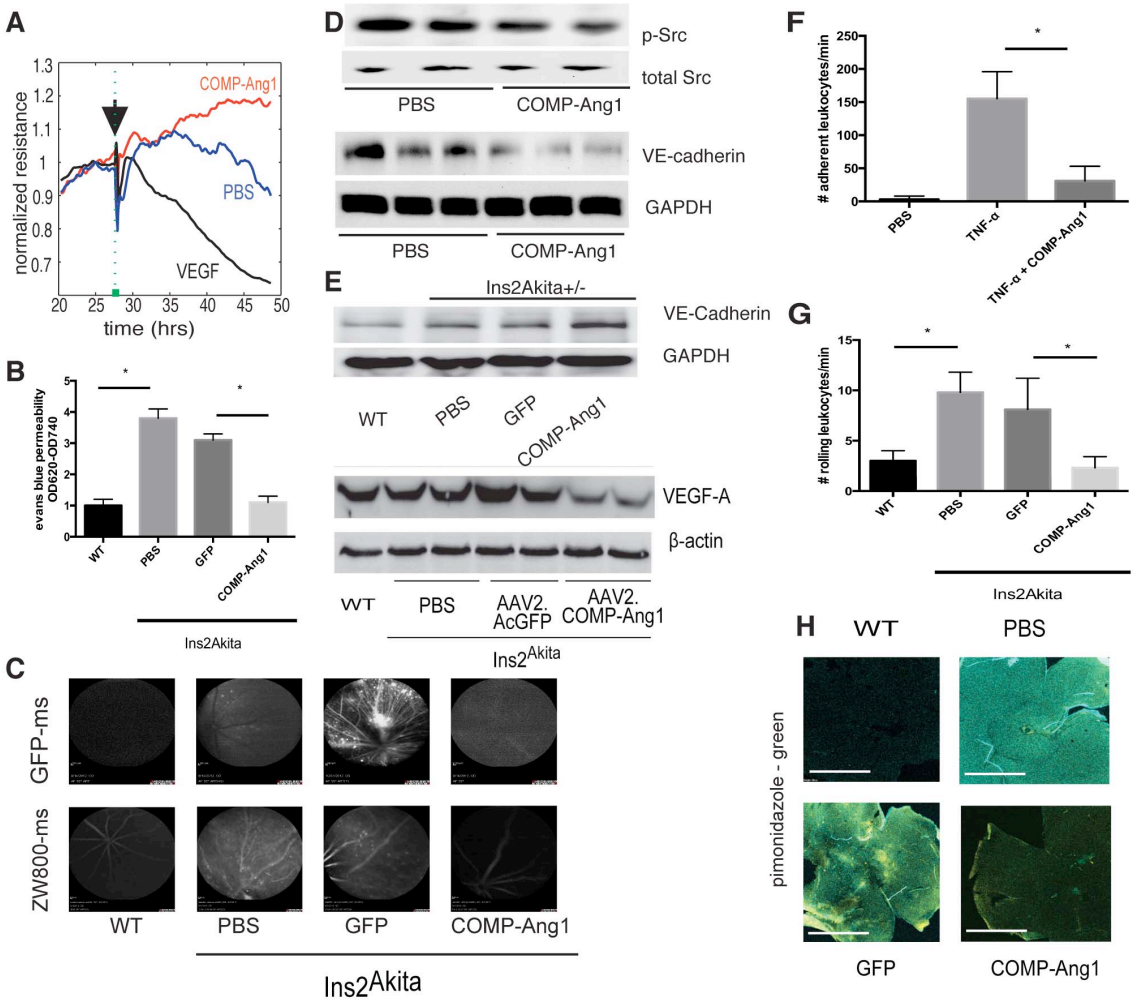

Figure 3.2**:** COMP-Ang1 enhances barrier function and reduces ischemia. (a) Graph of ECIS of HrMVECs with COMP-Ang1, VEGF, or PBS added to the media. COMP-Ang1 increased resistance of HrMVECs (n=3). (b) Evans Blue extravasation from the retina of Ins2Akita mice was increased compared to control; treatment with AAV2.COMP-Ang1 returned vascular hyperpermeabilty to control levels. *P<0.001 compared to C57BL/6-J, **P=0.02 compared to AAV2.AcGFP. (c) GFP or the NIR fluorophore ZW800 were conjugated to aminated latex microspheres (GFP-ms, or ZW800–ms; 100 nm in diameter) and injected into the tail vein of three mice per group. Leakage was captured using the FA or ICG imaging modality on Spectralis, respectively. (d) Increased VE-cadherin and decreased phosphorylated Src expression in HrMVEC treated with COMP-Ang1 compared to controls (n=3). (e) Ins2Akita mouse retinas have increased VE-cadherin and decreased VEGF-A concentrations in mice treated with AAV2.COMP-Ang1. (f) COMP-Ang1 reduced TNF-α induced leukocyte rolling in cultured HrMVECs. (g) COMP-Ang1 prevents leukostasis and inflammation (h) Representative retinas (four mice per group) from mice treated with hypoxyprobe (pimonidazole). COMP-Ang1 reduced hypoxia in diabetic mouse retinas. Scale bars: 600 μm (h) *P<0.001, ANOVA. Post hoc comparisons with a Tukey test to compare means of each group.

observed. Microsphere leakage was increased in the diabetic mice and prevented by COMP-Ang1 administration (Figure 3.2c). This indicates that retinal vascular leakage can be suppressed despite persistent pericyte dropout.

To clarify the molecular underpinnings of COMP-Ang1-mediated enhancement of BRB integrity, we determined its influence on Src phosphorylation and VE-cadherin expression in human retinal microvascular endothelial cells (HrMVECs). VEGF-A induces vascular leakage through Src-mediated downregulation of VE-cadherin, while Ang1 promotes VE-cadherin expression (GAVARD et al., 2008; Thurston, 2002). As expected, COMP-Ang1 decreased Src phosphorylation and increased VE-cadherin in HrMVECs (Figure 3.2d). These findings were consistent with retinal levels of VE-cadherin in Ins2Akita mice (Figure 3.2e). Interestingly, COMP-Ang1 treatment also reduced VEGF-A levels in the retina of Ins2Akita mice (Figure 3.2e). Collectively and consistent with prior reports on Ang1 activity, these mechanistic data indicate that COMP-Ang1 likely reduces vascular endothelial permeability through decreased Src phosphorylation and increased VE-cadherin. Decreases in VEGF-A retinal protein could be mediated by a decrease in retinal hypoxia, as shown by pimonidazole staining (Figure 3.2h)**.** COMP-Ang1-mediated perfusion enhancement was associated with reduced retinal VEGF-A expression, contributing further to vascular stability.

The Ins2Akita mouse, like patients with DR, experiences inflammatory responses to diabetes (Huang et al., 2011). Leukocyte adhesion to the vascular wall is mediated, in part, by TNF-α (Vinores, Xiao, Shen, & Campochiaro, 2007). We determined that COMP-Ang1 decreased TNF-α induced leukocyte adherence to an endothelial monolayer *in vitro* (Figure 3.2f). Furthermore, acridine orange leukocyte fluorography (Cahoon et

al., 2014) indicated that COMP-Ang1 reduces leukocyte adherence in the capillaries of the mouse retina (Figure 3.2g). Increased leukocyte rolling in the diabetic retina was suppressed with AAV2.COMP-Ang1 treatment.

Consistent with previous reports (Joussen et al., 2002), our data support that constitutive delivery of Ang1 can suppress the vascular dysfunction in diabetic mice. However, whether this therapy improves retinal neuronal health has yet to be elucidated.

To determine whether promoting a more robust vascular network in diabetic mice correlated with improved retinal structure, we assessed the effects of COMP-Ang1 on retinal ganglion cell layer loss (van Dijk et al., 2009) by examining retinal cross-sections (*ex vivo*) and retinal thickness (*in vivo* using optical coherence tomography (OCT)) between AAV2.COMP-Ang1 injected Ins2Akita mice and control mice (Figure 3.3a). Retinal thickness of Ins2Akita mice treated with either PBS or AAV2.AcGFP declined compared to C57BL/6JL6 mice ($P<0.0001$), but was preserved by AAV2.COMP-Ang1 treatment ($P=0.006$ vs. AAV2.AcGFP) (Figure 3.3b). This was followed up with *ex vivo* cross sections of retina labeled for nuclei staining (Figure 3.3c). Ganglion cell layer nuclei were counted in each group. AAV2.COMP-Ang1 treatment prevented loss of ganglion cell layer nuclei in Ins2Akita mice (Figure 3.3d), suggesting that this therapy may be beneficial in preventing diabetes-induced retinal ganglion cell death. Further, we saw no evidence of toxicity or cell loss in the rest of the retina due to AAV2.COMP-Ang1.

Finally, we assessed whether AAV2.COMP-Ang1 could preserve retinal physiological function in addition to inducing structural and vascular improvements. We tested whether AAV2.COMP-Ang1 could rescue visual tracking behavior and retinal

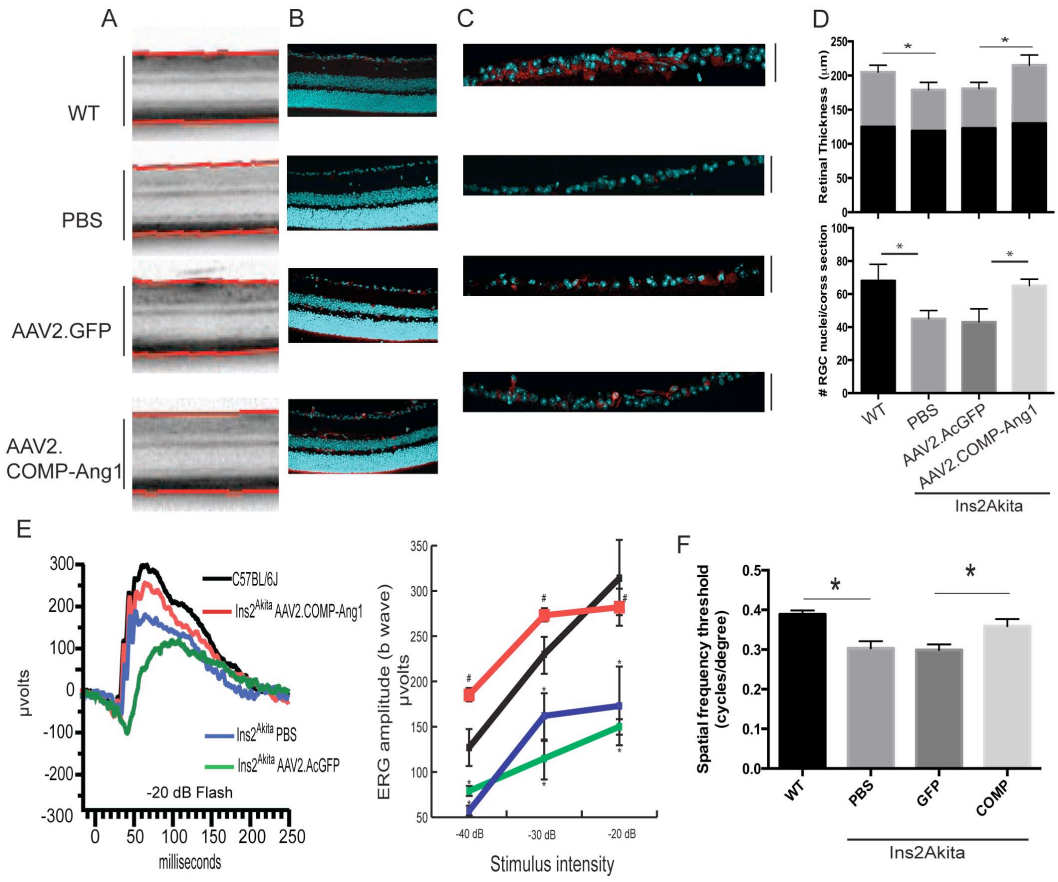

Figure 3.3: COMP-Ang1 prevents diabetes-induced retinal ganglion cell layer degeneration and stabilizes visual function. (a) Representative figures from optical coherence tomography (OCT) measuring retinal thickness. The red line indicates the retinal surface and Bruch's membrane. Scale bars = 200 µm. (b) Cross sections of six month-old retina from WT, or Ins2Akita mice treated with PBS, AAV2.AcGFP, or AAV2.COMP-Ang1 stained with DAPI. (c) View of the ganglion cell layer from mice stained for VE-cadherin (red) or nuclei (DAPI, blue) demonstrating increased VE-cadherin and nuclear staining. Scale bars 30 µm (right). (d) Quantification of retinal thickness from OCT showing that AAV2.COMP-Ang1 prevented diabetes-induced retinal thinning as measured *in vivo* (*p<0.0001 vs. WT, P=0.006 vs. AAV2.AcGFP). AAV2.COMP-Ang1 prevented diabetes-induced inner retinal layer loss (*p=0.03 ANOVA, with post hoc Tukey test). (e) Representative example of ERG response from all groups of mice. Electrical retinal response was elicited and the amplitude of b-wave during scotopic conditions at -3.62 log (Cd s/m^2), -2.62 log (Cd s/m^2), -1.62 log (Cd s/m^2), intensity was recorded. Decreased amplitudes were recorded in Ins2Akita mice treated with PBS or AAV2.AcGFP compared to WT mice and AAV2.COMP-Ang1 prevented the decrease in amplitude. *p=0.0001, ANOVA. Assessing visual acuity was accomplished by testing optomotor tracking response of Ins2Akita mice treated with AAV2.COMP-Ang1 or control compared to WT. (f) Ins2Akita mice exhibited decreased optokinetic tracking response (units = cycles/degree). AAV2.COMP-Ang1 prevented the decrease in visual response; six mice from each group were tested, data are mean ± stdev. *P<0.001, ANOVA.

electrical responses, which are impaired in diabetic retinopathy (Bresnick, Korth, Groo, & Palta, 1984). AAV2.COMP-Ang1 treatment, compared to AAV2.AcGFP or PBS, prevented the diabetes-induced reduction in electroretinographic (ERG) scotopic b-wave amplitudes in Ins2Akita mice (Figure 3.3e), which would be impaired due to anomalous photoreceptor-bipolar communication (Hombrebueno, Chen, Penalva, & Xu, 2014). Furthermore, AAV2.COMP-Ang1 treatment prevented the diabetes-induced reduction in visual tracking response as measured by using the optomotor head tracking response task to determine spatial visual thresholds (Barabas et al., 2011) (Figure 3.3f). These spatial resolution and electroretinographic findings demonstrate that AAV2.COMP-Ang1 can preserve retinal function in the face of prolonged diabetes.

Thus far, our data demonstrate a protective role for COMP-Ang1 when delivered early (age two months) to the diabetic mouse retina. In ischemic retina, successful regeneration has been shown using intravitreal delivery of ECFCs in the oxygen-induced retinopathy model (Medina, O'Neill, Humphreys, Gardiner, & Stitt, 2010a) but their potential has not yet been explored in the diabetic retina. Ang1 promotes differentiation of embryonic or induced pluripotent stem cells into vasculogenic cells, which undergo vascular engraftment and facilitate vessel regeneration. Hence, there is clear potential for COMP-Ang1 to mobilize or enhance the normal function of these endogenous, reparative cells.

To serve as an effective treatment clinically, we tested the ability of COMP-Ang1 to enhance ECFC function *in vitro* and promote their integration into the diabetic retinal vasculature *in vivo*. We sought to determine whether COMP-Ang1 would improve the functional benefit of treatment with ECFCs, which express high levels of the

Angiopoietin-1 receptor, Tie2 (Medina, O'Neill, Sweeney, Guduric-Fuchs, Gardiner, Simpson, et al., 2010b).

We demonstrated that COMP-Ang1 increases migration and tubulogenesis of ECFCs *in vitro*, as assessed by scratch migration assay and matrigel tube formation assay, respectively (Figure 3.4a,b). To explore the potential of *in vivo* retinal vascular repair, diabetic mice at six months of age were given intravitreal injections of AAV2.COMP-Ang1 or controls (AAV2.AcGFP or PBS). Two weeks later, labeled ECFCs (Qdot-655, Invitrogen) were administered intravitreally. In one cohort of mice, retinas were harvested 72 hours after injection of ECFCs, stained for endothelial cells, and mounted flat for confocal analysis. COMP-Ang1 enhanced ECFC integration into the diabetic retina (Figure 3.4c). Three-dimensional reconstruction of confocal immunofluorescence images demonstrates enhanced ECFC engraftment onto retinal vessels in diabetic mice treated with AAV2.COMP-Ang1 relative to control. A second cohort of mice was followed for two months to determine whether this combination therapy achieved significant visual outcomes. The optokinetic tracking response was stabilized in mice treated with COMP-Ang1 and ECFCs, yet declined in control mice, which received ECFCs after administration of either PBS or AAV.GFP (Figure 3.4d).

3.5 Discussion

We demonstrated the salutary effects of COMP-Ang1 in ameliorating these pivotal pathogenic events in diabetes and hallmarks of diabetic macular edema and ischemia. AAV2.COMP-Ang1 reduced VEGF-A and increased VE-cadherin expression in Ins2Akita mice, consistent with a model of vascular normalization. Strikingly, structural and functional indices of endothelial homeostasis were restored by

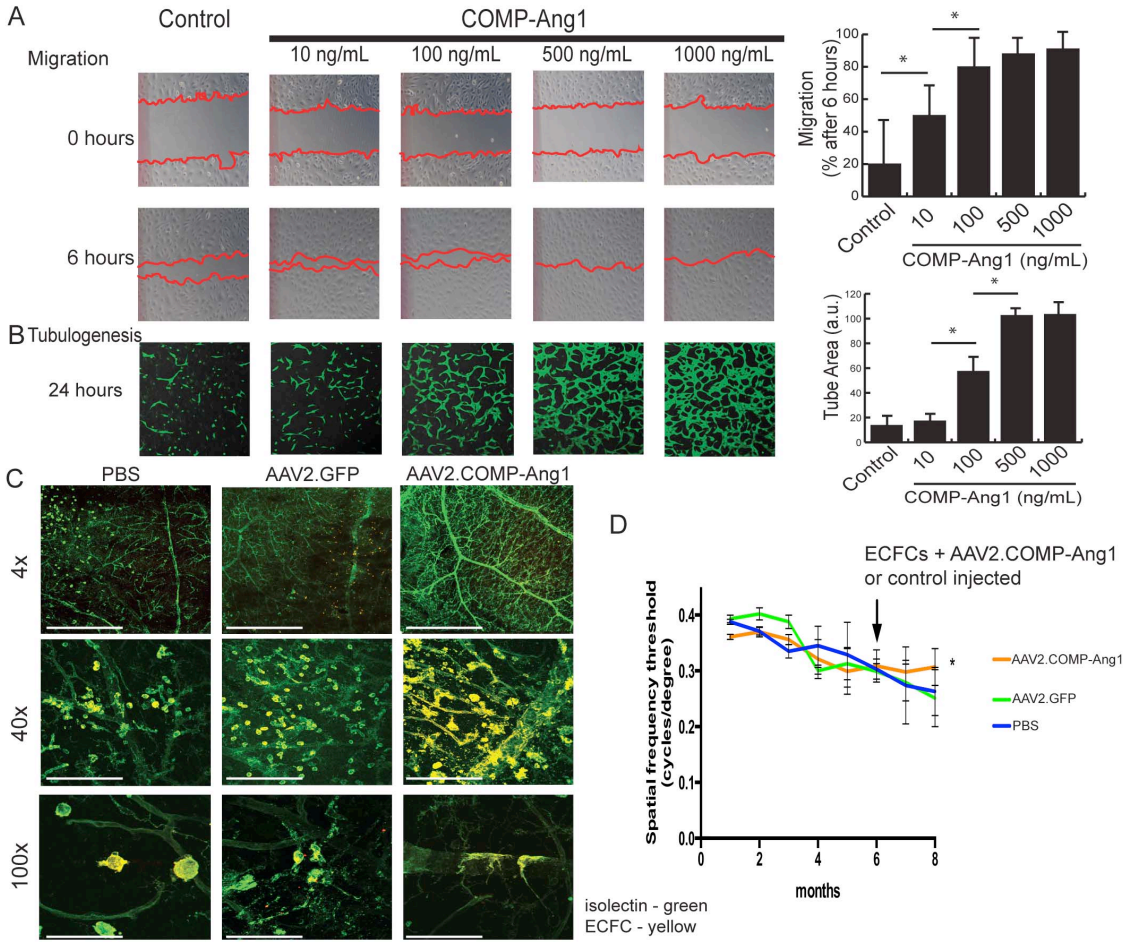

Figure 3.4**:** COMP-Ang1 enhances ECFC engraftment into the diabetic retina and prevents further visual decline. (a) Endothelial colony-forming cells (ECFCs) were plated on collagen-coated wells and assayed for migration potential under increasing doses of COMP-Ang1. (b) Additionally, 3D tube formation was tested in matrigel. COMP-Ang1 increased migration and tube formation in a dose dependent manner with maximal effects exerted at 500 ng/mL. (c) ECFCs were injected in aged diabetic mice (six months, arrow) after the mice had been treated with COMP-Ang1 or control. ECFCs were labeled with qdots (655) and injected intravitreally. Three days later retinas were harvested and stained for blood vessels (isolectin 546) and flatmounted for confocal analysis. COMP-Ang1 increased ECFC integration into the diabetic retinal vasculature (see also Supplemental Video). (d) Mice treated with COMP-Ang1 or control plus ECFCs were analyzed for visual tracking ability. COMP-Ang1 plus ECFCs prevented further declines in spatial frequency threshold. *$p<0.05$, *in vitro* experiments were performed in triplicate on three different ECFC clones (total of nine experiments per condition). *In vivo* experiments were performed on five mice per group (ten eyes). Scale bars: 600 µm (top), 150 µm (middle), and 90 µm (bottom). *$P<0.001$, ANOVA. Post hoc comparisons with a Tukey test to compare means of each group.

AAV2.COMP-Ang1 despite concomitant pericyte loss in the capillaries, which is often present prior to onset of therapy in diabetics. This indicates a potential role for AAV2.COMP-Ang1 in arresting vascular dysfunction and disruption. Furthermore, AAV2.COMP-Ang1 preserved the retinal ganglion cell layer, the loss of which is an integral cause of decreased vision in diabetic retinopathy.

Based on our data, our working model is that AAV2.COMP-Ang1 normalizes the vasculature by decreasing Src phosphorylation and increasing and VE-cadherin stability, enhancing vascular integrity and preventing the endothelial cell loss seen in Ins2Akita mice. These processes result in normalized vasculature, enhanced perfusion, reduced hypoxia-driven VEGF production (further contributing to vascular stability) and reduced ganglion cell layer loss. The decrease in VEGF production could derive from either COMP-Ang1 mediated decrease in retinal hypoxia or via inhibition of macrophage-produced VEGF (J. Lee et al., 2013). Recently, Ang-1 has demonstrated neuroprotective effects in the CNS (Shin et al., 2010). In this study, AAV2.COMP-Ang1 restored visual acuity and ERG responsiveness, which often decrease in diabetic patients.

Most intriguingly, from a perspective of reparative therapy for advanced diabetic retinopathy, we found that COMP-Ang1 increases ECFC vasculogenic capabilities and promotes their integration into and engraftment with the diabetic retinal vessels. This was functionally relevant as the combination of AAV2.COMP-Ang1 and ECFCs stemmed further visual decline in mice with advanced diabetes, as determined by visual tracking response.

This work compliments the recent findings of those published by Lee et. al (J. Lee et al., 2013) that angiopoietin-1 can help recover from oxygen-induced retinopathy and

laser-induced CNV. Our manuscript advances the field by 1) showing that sustainable delivery can be achieved with a single intravitreal injection, 2) testing the effects of COMP-Ang1 in a model of diabetic retinopathy, and most importantly 3) showing that COMP-Ang1 can enhance the regenerative capacity of endothelial progenitor cells in a retina with advanced diabetes.

Engineered COMP-Ang1 avoids the issues of aggregation and insolubility, and we have shown here that COMP-Ang1 gene therapy can replace deficient Ang1 secretion by pericytes, which are lost in diabetic retinopathy. In conclusion, we suppressed retinal vascular leakage, preserved retinal morphology, and prevented diabetes-induced deficits in visual acuity and retinal function in the diabetic Ins2Akita mouse retina with a single intravitreous injection, which afforded long-term expression of COMP-Ang1 delivered by AAV2. Furthermore, COMP-Ang1 enhanced ECFC integration into the retina of mice with advanced diabetes, stemming further visual decline. This therapy suppresses the pathognomonic features of nonproliferative diabetic retinopathy and, in contrast to existing therapies, decreases the nonperfusion and ischemia critical to the genesis of proliferative diabetic retinopathy. Our data indicate that COMP-Ang1 has significant potential to prevent retinal vascular endothelial cell damage during diabetes. Moreover, enhanced expression of this vasotrophic growth factor enhances the established vasoregenerative properties of ECFCs delivered to the diabetic retina as cell therapy. COMP-Ang1 could prove useful for vascular normalization in diabetic retinopathy and other conditions, which entail vascular ischemia. Further studies will focus on type 2 diabetes and larger animal models of diabetic retinopathy.

3.6 Acknowledgments

We thank Srinivas P. Sangly (Indiana CTSI), Jayakrishna Ambati (University of Kentucky), Valeria Tarallo and Derick Holt (University of Utah) for insightful and constructive discussions. We would like to acknowledge Andrew Weyrich, Guy Zimmerman, and Robert Campbell from the University of Utah for isolating leukocytes.

This work was partly supported by NEI 5R01EY017950, NEI 5R01EY017182, and the University of Utah T-32 Neuroscience Training Grant 5T32DC008553-05, the University of Utah Metabolism T-32 Training Grant 5T32DK091317, and the P30EY14800 NIH grant. Further support was provided in part by an Unrestricted Grant from Research to Prevent Blindness, Inc., New York, NY, to the Department of Ophthalmology & Visual Sciences, University of Utah. Judd Cahoon, Hironori Uehara, Ling Luo, Jackie Simonis, Tom Olsen, Bradlee Duncan, Tina Mamalis, and Paul Olson performed animal studies; Judd Cahoon, Hironori Uehara, Kortnie Walker, and Vai Jessop performed cell culture studies; Judd Cahoon and Paul Olson performed visual functional studies; Judd Cahoon, Chistopher Gibson, Dean Li, and Kortnie Walker performed trans-endothelial resistance studies; Gou Young Koh, Hironori Uehara, and Guangping Gao developed the plasmids and viral vectors; Judd Cahoon and Bala Ambati prepared and wrote the manuscript.

3.6 References

Adamis, A. P., Joussen, A. M., Murata, T., Tsujikawa, A., Kirchhof, B., & Bursell, S. E. (2001a). Leukocyte-mediated endothelial cell injury and death in the diabetic retina. *The American Journal of Pathology*, *158*(1), 147–152. doi:10.1016/S0002-9440(10)63952-1

Adamis, A. P., Xu, Q., & Qaum, T. (2001b). Sensitive blood-retinal barrier breakdown quantitation using Evans Blue. *Investigative Ophthalmology & Visual Science*, *42*(3), 789–794.

Aiello, L. P., Avery, R. L., Arrigg, P. G., Keyt, B. A., Jampel, H. D., Shah, S. T., et al. (1994). Vascular endothelial growth factor in ocular fluid of patients with diabetic retinopathy and other retinal disorders. *The New England Journal of Medicine*, *331*(22), 1480–1487. doi:10.1056/NEJM199412013312203

Akimov, N. P., & Rentería, R. C. (2012). Spatial frequency threshold and contrast sensitivity of an optomotor behavior are impaired in the Ins2Akita mouse model of diabetes. *Behavioural Brain Research*, *226*(2), 601–605. doi:10.1016/j.bbr.2011.09.030

Aldrich, T. H., Davis, S., Jones, P. F., Acheson, A., Compton, D. L., Jain, V., et al. (1996). Isolation of angiopoietin-1, a ligand for the TIE2 receptor, by secretion-trap expression cloning. *Cell*, *87*(7), 1161–1169.

Alphonse, R. S., Vadivel, A., Fung, M., Shelley, W. C., Critser, P. J., Ionescu, L., et al. (2014). Existence, functional impairment, and lung repair potential of endothelial colony-forming cells in oxygen-induced arrested alveolar growth. *Circulation*, *129*(21), 2144–2157. doi:10.1161/CIRCULATIONAHA.114.009124

Augustin, H. G., Young Koh, G., Thurston, G., & Alitalo, K. (2009). Control of vascular morphogenesis and homeostasis through the angiopoietin–Tie system. *Nature Reviews Molecular Cell Biology*, *10*(3), 165–177. doi:10.1038/nrm2639

Barabas, P., Huang, W., Chen, H., Koehler, C. L., Howell, G., John, S. W. M., et al. (2011). Missing optomotor head-turning reflex in the DBA/2J mouse. *Investigative Ophthalmology & Visual Science*, *52*(9), 6766–6773. doi:10.1167/iovs.10-7147

Barber, A. J., Antonetti, D. A., Kern, T. S., Reiter, C. E. N., Soans, R. S., Krady, J. K., et al. (2005). The Ins2Akita mouse as a model of early retinal complications in diabetes. *Investigative Ophthalmology & Visual Science*, *46*(6), 2210–2218. doi:10.1167/iovs.04-1340

Bresnick, G. H., Korth, K., Groo, A., & Palta, M. (1984). Electroretinographic oscillatory potentials predict progression of diabetic retinopathy. Preliminary report. *Archives of Ophthalmology*, *102*(9), 1307–1311.

Brown, D. M., Nguyen, Q. D., Marcus, D. M., Boyer, D. S., Patel, S., Feiner, L., et al. (2013). Long-term outcomes of ranibizumab therapy for diabetic macular edema: The 36-month results from two phase III trials: RISE and RIDE. *Ophthalmology*, *120*(10), 2013–2022. doi:10.1016/j.ophtha.2013.02.034

Byeon, S. H., Chu, Y. K., Lee, H., Lee, S. Y., & Kwon, O. W. (2009). Foveal ganglion cell layer damage in ischemic diabetic maculopathy: Correlation of optical coherence tomographic and anatomic changes. *Ophthalmology*, *116*(10), 1949–59.e8. doi:10.1016/j.ophtha.2009.06.066

Cahoon, J. M., Olson, P. R., Nielson, S., Miya, T. R., Bankhead, P., Mcgeown, J. G., et al. (2014). Acridine orange leukocyte fluorography in mice. *Experimental Eye Research*, *120*, 15–19. doi:10.1016/j.exer.2013.12.002

Campochiaro, P. A., Wykoff, C. C., Shapiro, H., Rubio, R. G., & Ehrlich, J. S. (2014). Neutralization of vascular endothelial growth factor slows progression of retinal nonperfusion in patients with diabetic macular edema. *Ophthalmology*. doi:10.1016/j.ophtha.2014.03.021

Cho, C.-H., Kammerer, R. A., Lee, H. J., Steinmetz, M. O., Ryu, Y. S., Lee, S. H., et al. (2004). COMP-Ang1: A designed angiopoietin-1 variant with nonleaky angiogenic activity. *Proceedings of the National Academy of Sciences of the United States of America*, *101*(15), 5547–5552. doi:10.1073/pnas.0307574101

Chou, S., Harza, S., Bhatwadekar, A., Li, C. S., Paradiso, L. J., Miller, L. P., et al. (2013). Circulating mononuclear progenitor cells: Differential roles for subpopulations in repair of retinal vascular injury. *Investigative Ophthalmology and Visual Science 54*(4), 3000–3009. doi:10.1167/iovs.12-10280

Cogan, D. G., Toussaint, D., & Kuwabara, T. (1961). Retinal vascular patterns. IV. Diabetic retinopathy. *Archives of Ophthalmology*, *66*, 366–378.

Dornan, T., Mann, J. I., & Turner, R. (1982). Factors protective against retinopathy in insulin-dependent diabetics free of retinopathy for 30 years. *British Medical Journal (Clinical Research Ed.)*, *285*(6348), 1073–1077.

Gastinger, M. J., Singh, R. S. J., & Barber, A. J. (2006). Loss of cholinergic and dopaminergic amacrine cells in streptozotocin-diabetic rat and Ins2Akita-diabetic mouse retinas. *Investigative Ophthalmology & Visual Science*, *47*(7), 3143–3150. doi:10.1167/iovs.05-1376

Gavard, J., Patel, V., & Gutkind, J. (2008). Angiopoietin-1 prevents VEGF-induced endothelial permeability by sequestering Src through mDia. *Developmental Cell*, *14*(1), 25–36. doi:10.1016/j.devcel.2007.10.019

Hammes, H.-P., Lin, J., Wagner, P., Feng, Y., Hagen, Vom, F., Krzizok, T., et al. (2004). Angiopoietin-2 causes pericyte dropout in the normal retina: Evidence for involvement in diabetic retinopathy. *Diabetes*, *53*(4), 1104–1110.

Hombrebueno, J. R., Chen, M., Penalva, R. G., & Xu, H. (2014). Loss of synaptic connectivity, particularly in second order neurons is a key feature of diabetic retinal neuropathy in the Ins2Akita mouse. *PLoS ONE*, *9*(5), e97970. doi:10.1371/journal.pone.0097970

Huang, H., Gandhi, J. K., Zhong, X., Wei, Y., Gong, J., Duh, E. J., & Vinores, S. A. (2011). TNFalpha is required for late BRB breakdown in diabetic retinopathy, and its

inhibition prevents leukostasis and protects vessels and neurons from apoptosis. *Investigative Ophthalmology & Visual Science*, *52*(3), 1336–1344. doi:10.1167/iovs.10-5768

Jager, R. D., Aiello, L. P., Patel, S. C., & Cunningham, E. T. (2004). Risks of intravitreous injection: A comprehensive review. *Retina (Philadelphia, Pa)*, *24*(5), 676–698.

Joussen, A. M., Poulaki, V., Le, M. L., Koizumi, K., Esser, C., Janicki, H., et al. (2004). A central role for inflammation in the pathogenesis of diabetic retinopathy. *The FASEB Journal*, *18*(12), 1450–1452. doi:10.1096/fj.03-1476fje

Joussen, A. M., Poulaki, V., Tsujikawa, A., Qin, W., Qaum, T., Xu, Q., et al. (2002). Suppression of diabetic retinopathy with angiopoietin-1. *The American Journal of Pathology*, *160*(5), 1683–1693. doi:10.1016/S0002-9440(10)61115-7

Lee, J., Kim, K. E., Choi, D.-K., Jang, J. Y., Jung, J.-J., Kiyonari, H., et al. (2013). Angiopoietin-1 guides directional angiogenesis through integrin αvβ5 signaling for recovery of ischemic retinopathy. *Science Translational Medicine*, *5*(203), 203ra127–203ra127. doi:10.1126/scitranslmed.3006666

Maguire, A. M., Simonelli, F., Pierce, E. A., Pugh, E. N., Mingozzi, F., Bennicelli, J., et al. (2008). Safety and efficacy of gene transfer for Leber's congenital amaurosis. *The New England Journal of Medicine*, *358*(21), 2240–2248. doi:10.1056/NEJMoa0802315

McLenachan, S., Chen, X., McMenamin, P. G., & Rakoczy, E. P. (2013). Absence of clinical correlates of diabetic retinopathy in the Ins2Akita retina. *Clinical & Experimental Ophthalmology*, *41*(6), 582–592. doi:10.1111/ceo.12084

Medina, R. J., O'Neill, C. L., Humphreys, M. W., Gardiner, T. A., & Stitt, A. W. (2010a). Outgrowth endothelial cells: Characterization and their potential for reversing ischemic retinopathy. *Investigative Ophthalmology & Visual Science*, *51*(11), 5906–5913. doi:10.1167/iovs.09-4951

Medina, R. J., O'Neill, C. L., Sweeney, M., Guduric-Fuchs, J., Gardiner, T. A., Simpson, D. A., & Stitt, A. W. (2010b). Molecular analysis of endothelial progenitor cell (EPC) subtypes reveals two distinct cell populations with different identities. *BMC Medical Genomics*, *3*, 18. doi:10.1186/1755-8794-3-18

Mizutani, M., Kern, T. S., & Lorenzi, M. (1996). Accelerated death of retinal microvascular cells in human and experimental diabetic retinopathy. *The Journal of Clinical Investigation*, *97*(12), 2883–2890. doi:10.1172/JCI118746

Murata, T., Ishibashi, T., Khalil, A., Hata, Y., Yoshikawa, H., & Inomata, H. (1995). Vascular endothelial growth factor plays a role in hyperpermeability of diabetic

retinal vessels. *Ophthalmic Research*, *27*(1), 48–52.

O'Neill, C. L., O'Doherty, M. T., Wilson, S. E., Rana, A. A., Hirst, C. E., Stitt, A. W., & Medina, R. J. (2012). Therapeutic revascularisation of ischaemic tissue: The opportunities and challenges for therapy using vascular stem/progenitor cells. *Stem Cell Research & Therapy*, *3*(4), 31. doi:10.1186/scrt122

Patel, J. I., Hykin, P. G., Gregor, Z. J., Boulton, M., & Cree, I. A. (2005). Angiopoietin concentrations in diabetic retinopathy. *The British Journal of Ophthalmology*, *89*(4), 480–483. doi:10.1136/bjo.2004.049940

Quaggin, S. E. (2012). Turning a blind eye to anti-VEGF toxicities. *The Journal of Clinical Investigation*, *122*(11), 3849–3851. doi:10.1172/JCI65509

Shin, H. Y., Lee, Y. J., Kim, H. J., Park, C.-K., Kim, J. H., Wang, K. C., et al. (2010). Protective role of COMP-Ang1 in ischemic rat brain. *Journal of Neuroscience Research*, *88*(5), 1052–1063. doi:10.1002/jnr.22274

Simonelli, F., Maguire, A. M., Testa, F., Pierce, E. A., Mingozzi, F., Bennicelli, J. L., et al. (2010). Gene therapy for Leber's congenital amaurosis is safe and effective through 1.5 years after vector administration. *Molecular Therapy: The Journal of the American Society of Gene Therapy*, *18*(3), 643–650. doi:10.1038/mt.2009.277

Stitt, A. W., O'Neill, C. L., O'Doherty, M. T., Archer, D. B., Gardiner, T. A., & Medina, R. J. (2011). Vascular stem cells and ischaemic retinopathies. *Progress in Retinal and Eye Research*, *30*(3), 149–166. doi:10.1016/j.preteyeres.2011.02.001

Thurston, G. (2002). Complementary actions of VEGF and angiopoietin-1 on blood vessel growth and leakage. *Journal of Anatomy*, *200*(6), 575–580.

Thurston, G., Rudge, J. S., Ioffe, E., Zhou, H., Ross, L., Croll, S. D., et al. (2000). Angiopoietin-1 protects the adult vasculature against plasma leakage. *Nature Medicine*, *6*(4), 460–463. doi:10.1038/74725

Tiruppathi, C., Malik, A. B., Del Vecchio, P. J., Keese, C. R., & Giaever, I. (1992). Electrical method for detection of endothelial cell shape change in real time: Assessment of endothelial barrier function. *Proceedings of the National Academy of Sciences of the United States of America*, *89*(17), 7919–7923.

van Dijk, H. W., Kok, P. H. B., Garvin, M., Sonka, M., Devries, J. H., Michels, R. P. J., et al. (2009). Selective loss of inner retinal layer thickness in type 1 diabetic patients with minimal diabetic retinopathy. *Investigative Ophthalmology & Visual Science*, *50*(7), 3404–3409. doi:10.1167/iovs.08-3143

Vinores, S. A., Xiao, W.-H., Shen, J., & Campochiaro, P. A. (2007). TNF-alpha is critical for ischemia-induced leukostasis, but not retinal neovascularization nor VEGF-

induced leakage. *Journal of Neuroimmunology*, *182*(1-2), 73–79. doi:10.1016/j.jneuroim.2006.09.015

Wild, S., Roglic, G., Green, A., Sicree, R., & King, H. (2004). Global prevalence of diabetes: Estimates for the year 2000 and projections for 2030. *Diabetes Care*, *27*(5), 1047–1053.

Wong, T. Y., Mwamburi, M., Klein, R., Larsen, M., Flynn, H., Hernandez-Medina, M., et al. (2009). Rates of progression in diabetic retinopathy during different time periods: A systematic review and meta-analysis. *Diabetes Care*, *32*(12), 2307–2313. doi:10.2337/dc09-0615

Yau, J. W. Y., Rogers, S. L., Kawasaki, R., Lamoureux, E. L., Kowalski, J. W., Bek, T., et al. (2012). Global prevalence and major risk factors of diabetic retinopathy. *Diabetes Care*, *35*(3), 556–564. doi:10.2337/dc11-1909

Yin, L., Greenberg, K., Hunter, J. J., Dalkara, D., Kolstad, K. D., Masella, B. D., et al. (2011). Intravitreal injection of AAV2 transduces macaque inner retina. *Investigative Ophthalmology & Visual Science*, *52*(5), 2775–2783. doi:10.1167/iovs.10-6250

Zhu, W., London, N. R., Gibson, C. C., Davis, C. T., Tong, Z., Sorensen, L. K., et al. (2012). Interleukin receptor activates a MYD88-ARNO-ARF6 cascade to disrupt vascular stability. *Nature*, *492*(7428), 252–255. doi:10.1038/nature11603

CHAPTER 4

DUAL SUPRESSION OF HEMANGIOGENESIS AND LYMPHANGIOGENESIS BY SPLICE-SHIFTING MORPHOLINOS TARGETING VASCULAR ENDOTHELIAL GROWTH FACTOR RECEPTOR 2 (KDR)*

Hironori Uehara was the first author of this manuscript and designed the study. My role in this manuscript was performing mouse retinal and corneal staining and analysis (Figure 4 E-K; Figure 5 C-D).

*Reprinted with permission from FASEB and Elsevier Publishing. Uehara, H. et al. Dual suppression of hemangiogenesis and lymphangiogenesis by splice-shifting morpholinos targeting vascular endothelial growth factor receptor 2 (KDR). *FASEB J. 27*, 76-85 (2013)

The FASEB Journal • Research Communication

Dual suppression of hemangiogenesis and lymphangiogenesis by splice-shifting morpholinos targeting vascular endothelial growth factor receptor 2 (KDR)

Hironori Uehara,* YangKyung Cho,*,† Jackie Simonis,* Judd Cahoon,* Bonnie Archer,* Ling Luo,* Subrata K. Das,* Nirbhai Singh,* Jayakrishna Ambati,‡ and Balamurali K. Ambati*,[1]

*Moran Eye Center, University of Utah, Salt Lake City, Utah, USA; †St. Vincent Hospital, Catholic University of Korea, Suwon, Republic of Korea; and ‡Department of Ophthalmology and Visual Sciences, University of Kentucky College of Medicine, Lexington, Kentucky, USA

ABSTRACT **The *KDR* gene, which participates in angiogenesis and lymphangiogenesis, produces two functionally distinct protein products, membrane-bound KDR (mbKDR) and its isoform, soluble KDR (sKDR). Since sKDR does not have a tyrosine kinase domain and does not dimerize, it is principally an antagonist of lymphangiogenesis by sequestering VEGF-C. Alternative polyadenylation of exon 30 or intron 13 leads to the production of mbKDR or sKDR, respectively, yet the regulatory mechanisms are unknown. Here we show that an antisense morpholino oligomer directed against the exon 13-intron 13 junction increases sKDR (suppressing lymphangiogenesis) and decreases mbKDR (inhibiting hemangiogenesis). The latent polyadenylation site in intron 13 of *KDR* is activated by blocking the upstream 5′ splicing site with an antisense morpholino oligomer. Intravitreal morpholino injection suppressed laser choroidal neovascularization while increasing sKDR. In the mouse cornea, subconjunctival injection of the morpholino-inhibited corneal angiogenesis and lymphangiogenesis, and suppressed graft rejection after transplantation. Thus, this morpholino can be used for concurrent suppression of hemangiogenesis and lymphangiogenesis. This study offers new insight into the mechanisms and potential therapeutic modulation of alternative polyadenylation.—Uehara, H., Cho, YK., Simonis, J., Cahoon, J., Archer, B., Luo, L., Das, S. K., Singh, N., Ambati, J., Ambati, B. K. Dual suppression of hemangiogenesis and lymphangiogenesis by splice-shifting morpholinos targeting vascular endothelial growth factor receptor 2 (KDR). *FASEB J.* 27, 76–85 (2013). www.fasebj.org**

Key Words: alternative polyadenylation · corneal graft rejection

Blood vessel network formation (vasculogenesis and angiogenesis) are necessary for maintenance of the body in vertebrates (1). Many diseases (*e.g.*, cancer, rheumatoid arthritis, macular degeneration, diabetic retinopathy) are due to uncontrolled neovascularization (2–6). Vascular endothelial cell growth factor A (VEGF-A) and KDR [also referred to as vascular endothelial growth factor receptor 2 (VEGFR2)] play central roles in physiological and pathological angiogenesis (7, 8). The *KDR* gene produces 2 functionally distinct protein products, membrane-bound KDR (mbKDR) and its isoform soluble KDR (sKDR) by alternative polyadenylation (9, 10). The mbKDR has an extracellular domain consisting of 7 immunoglobulin domains, a transmembrane domain, and tyrosine kinase domains (7, 8) and is the primary angiogenic receptor for VEGF-A. While mbKDR is composed of 30 exons in humans and mice, sKDR is produced by utilization of polyadenylation signals within intron 13 in mice. Since sKDR does not have tyrosine kinase domains and has much more affinity for VEGF-C than VEGF-A, it is an antagonist of VEGF-C, the key driver of lymphangiogenesis (9, 10). Thus, the membrane-bound isoform of KDR is prohemangiogenic, while the soluble isoform of KDR is antilymphangiogenic.

Abbreviations: cDNA, complementary DNA; CNV, choroidal neovascularization; DPBS, Dulbecco's phosphate-buffered saline; EST, expressed sequence tag; HUVEC, human umbilical vein endothelial cell; KDR_MOe13, morpholino oligomer targeting exon 13-intron 13 junction in human KDR; mbKDR, membrane-bound KDR; moKDR_MOe13, morpholino oligomer targeting exon 13-intron 13 junction in mouse KDR; RACE, rapid amplification of cDNA ends; sKDR, soluble KDR; STD_MO, standard morpholino; TFMS, trifluoromethanesulfonic acid; UTR, untranslated region; VEGF-A, vascular endothelial cell growth factor A; VEGFR2, vascular endothelial growth factor receptor 2 (also referred to as KDR)

[1] Correspondence: Moran Eye Center, University of Utah, 65 Mario Capecchi Dr., Salt Lake City, UT 84132, USA. E-mail: bala.ambati@utah.edu

doi: 10.1096/fj.12-213835

This article includes supplemental data. Please visit *http://www.fasebj.org* to obtain this information.

0892-6638/13/0027-0076 © FASEB

Here we report that a morpholino antisense oligomer can shift splicing of KDR pre-mRNA from the membrane to the soluble isoform in human umbilical vein endothelial cells (HUVECs). The induced sKDR requires utilization of a polyadenylation signal in intron 13, which is usually not activated in HUVECs. In addition, morpholino intravitreal injection suppressed laser choroidal neovascularization while increasing vitreous sKDR. Furthermore, in a mouse corneal suturing model, injection of the morpholino into the subconjunctival space suppressed corneal angiogenesis and lymphangiogenesis, and suppressed graft rejection in mouse corneal transplantation. Our results indicate that exon recognition by splicing factors affects subsequent polyadenylation signal activation and that by modifying it, latent polyadenylation signals can be activated, inducing alternative isoforms of proteins. We believe that this study elucidates alternative polyadenylation and that modification of this mechanism could potentially be a new drug target.

MATERIALS AND METHODS

Morpholino oligomer and primer sequences

Morpholino oligomers were purchased from Gene Tools (Philomath, OR, USA). Sequences of the morpholino oligomers and primers are listed in **Table 1**.

Cell cultures, morpholino delivery, and total RNA extraction

HUVECs (Lonza, Walkersville, MD, USA) were cultured in endothelial basal medium (EBM) with endothelial growth medium SingleQuot Kit supplements and growth factors (Lonza) according to the manufacturer's instructions. To prevent loss of endothelial cell properties, cell cultures were limited to passages 4 to 7. As a mouse endothelial cell, MS-1 (American Type Culture Collection, Manassas, VA, USA) were cultured in 5% FBS/DMEM. Morpholinos were delivered by nucleofection (Amaxa, Gaithersburg, MD, USA) using Basic Nucleofector Kit for Primary Mammalian Endothelial Cells (Amaxa) program A-034 for HUVECs and MS-1 cells. For one nucleofection, 1×10^6 cells were used and plated on a 6-well plate. Total RNA was extracted using the RNeasy mini kit (Qiagen, Valencia, CA, USA) with DNaseI treatment.

Complementary DNA (cDNA) synthesis and real-time PCR

cDNAs were synthesized from 400 ng total RNA using the Omniscript RT kit (Qiagen) and Oligo-dT primer (dT20) according to the manufacturer's instructions. Real-time PCR was performed using the QuantiTect SYBR Green PCR Kit (Qiagen) and 1 μl of cDNA. Real-time PCR conditions: 95°C for 10 min, followed by 40 cycles of 94°C for 15 s, 55°C for 30 s, and 72°C for 30 s.

3′ rapid amplification of cDNA ends (RACE)

cDNA was synthesized using cloning_R1. PCR was performed using the LongRange PCR Kit (Qiagen). PCR conditions were 93°C for 3 min, 35 cycles of 93°C for 15 s, 55°C for 30 s, and 68°C for 6 min using KDR_F and cloning_R2. Specific bands were subjected to DNA sequencing. To determine endogenous 3′ untranslated region (UTR) of sKDR mRNA, total RNA extracted from one human cornea was obtained from the Utah Lions Eye Bank (Salt Lake City, UT, USA). cDNA was synthesized with the same above method, and PCR was performed using cloning_F(1042-1061), which is designed in human *KDR* intron 13, and cloning_R2.

TABLE 1. *Morpholino oligomer and primer sequences*

Oligomer or primer	Sequence
Morpholino oligomer	
KDR_MOe13 (human)	5′-gatccagaattgtctccctacCTAG-3′
moKDR_MOe13 (mouse)	5′-cacccagggatgcctccatacCTAG-3′
PCR primer for human	
sKDR_F (exon13)	5′-TTCTTGGCTGTGCAAAAGTG-3′
sKDR_R (intron13)	5′-TCTTCAGTTCCCCTCCATTG-3′
mbKDR_F (exon15)	5′-GAGAGTTGCCCACACCTGTT-3′
mbKDR_R (exon17)	5′-CAACTGCCTCTGCACAATGA-3′
KDRexon10_F	5′-CCTACCAGTACGGCACCACT-3′
GAPDH_F	5′-CAGCCTCAAGATCATCAGCA-3′
GAPDH_R	5′-TGTGGTCATGAGTCCTTCCA-3′
PCR primer for mouse	
Mouse sKDR_F	5′-ACCAAGGCGACTATGTTTGC-3′
Mouse sKDR_R	5′-CAATTCTGTCACCCAGGGAT-3′
Mouse mbKDR_F	5′-ACCATTGAAGTGACTTGCCC-3′
Mouse mbKDR_R	5′-CCGGTTCCCATCTCTCAGTA-3′
Mouse GAPDH_F	5′-AACTTTGGCATTGTGGAAGGGCTC-3′
Mouse GAPDH_R	5′-ACCAGTGGATGCAGGGATGATGTT-3′
3′RACE primer	
Cloning_R1	5′-GGCCACGCGTCGACTAGTACTTTTTTTTTTTTTTTTV-3′
Cloning_R2	5′-GGCCACGCGTCGACTAGTAC-3′
Cloning_F(1042-1061)	5′-CCAGCATCCTTCAAGTCACA-3′

Upper and lower case in morpholino oligomer sequences correspond to exon and intron, respectively. Morpholino oligomer sequences were synthesized.

Flow cytometry

At 3 d after nucleofection, cells were treated with trypsin-EDTA and incubated in mouse anti-KDR antibody (ab9530, 1:1000; Abcam, Cambridge, MA, USA) with 10% FBS and 1% sodium azide/PBS for 60 min. After 3 washes, the cells were incubated in Alexa Fluor 647 conjugated anti-mouse IgG (Invitrogen, Carlsbad, CA, USA) for 30 min. The cells were washed 3 times, and fluorescence was detected by a FACScan Analyzer (BD Biosciences, San Jose, CA).

Western blot for sKDR and mbKDR from HUVECs

After nucleofection, cells were cultured in a 75-cm^2 flask for 3 d without changing the medium. The medium was collected, and cell debris was removed by centrifugation. Trichloroacetic acid (Fisher Scientific, Pittsburgh, PA, USA) was added to the supernatant; final concentration of trichloroacetic acid was 10%. After incubation for 30 min on ice, they were centrifuged at 12 000 *g* 4°C for 5 min. Supernatants were discarded, and cold acetone was added to the pellet. Centrifugation was repeated, the acetone was discarded, and 800 μl of RIPA buffer was added. Samples were sonicated and subjected to SDS-PAGE under reducing conditions. The same primary antibody in flow cytometry was used for immunobloting.

Deglycosylation of sKDR

Culture medium (2 ml) from HUVECs treated with morpholino oligomer targeting exon 13-intron 13 junction in human KDR (KDR_MOe13; 2 d culture) was freeze dried. Each sample was treated by 200 μl cold Dulbecco's phosphate-buffered saline (DPBS) or trifluoromethanesulfonic acid (TFMS) for 10 and 20 min. After adding 1 ml of cold 1 M Tris-Cl buffer (pH 8.8), the proteins were condensed with trichloroacetic acid precipitation. The pellet was dissolved with 100 μl of RIPA buffer. The same antibody for sKDR detection in Western blot was used.

Intravitreous injection of morpholino and Western blot for sKDR and mbKDR from mouse eye

On d 0 and 3, 2 μl of 100 ng/μl morpholino oligomer targeting exon 13-intron 13 junction in mouse KDR (moKDR_MOe13), standard morpholino (STD_MO), or DPBS was injected intravitreously. On d 4, retinal total RNA was extracted with the RNeasy mini kit with DNaseI treatment for real-time RT-PCR. For Western blot of mbKDR, on d 4, retina was dissolved in RIPA buffer. For Western blot of sKDR, on d 4, intraocular solution was obtained from 6 eyes by pipette. After centrifugation, supernatant was used for further experiments. For detection, biotin-conjugated anti-KDR (BAF644; R&D Systems, Minneapolis, MN, USA) was used at 1 μg/μl.

Laser-induced choroidal neovascularization (CNV)

Laser photocoagulation and CNV measurement were described previously (11). Briefly, laser photocoagulation (532 nm, 150 mV, 100 ms, 100 μm) was performed on both eyes (2–5 spots/eye). Laser CNVs were stained with 5 μg/ml Alexa488 -onjugated isolectin GS-IB4 (Invitrogen), and observed by laser confocal microscope (Olympus America, Center Valley, CA, USA). Supplemental Fig. S1 summarizes the condition of intravitreous injection in each experiment. After photocoagulation, on d 1 and 4, 2 μl of 100 ng/μl STD_MO or moKDR_MOe13, 500 ng/μl goat IgG (AB-108-C; R&D Systems), 500 ng/μl goat anti-mouse VEGF-A IgG (AF-493-NA; R&D Systems), or 2 ng/μl SU1498 (572888; EMD Chemicals, Gibbstown, NJ, USA) was injected intravitreously.

TUNEL assay

TUNEL assay was performed using Click-iT TUNEL Alexa Fluor 594 Imaging Assay (C10246; Invitrogen). DPBS, STD_MO, or moKDR_MOe13 was injected into normal mouse eyes or laser-photocoagulated eyes (1 d postlaser) as described above. After 2 d, the eyes were fixed with 4% paraformaldehyde for 2 h at 4°C, and incubated in 15% sucrose for 2 h and 30% sucrose overnight. After embedding in optimal cutting temperature (OCT) compound (Sakura Finetek, Torrance, CA, USA), they were cut into 12-μm sections. Staining for apoptosis was conducted with the manufacturer's protocol. DNase-I treated section was used for positive control.

Transmission electron microscopy

To examine the integrity of fenestration in choriocapillaris after intravitreous moKDR_MOe13 injection, we examined the choroid with a transmission electron microscope, following previously described methods (12, 13).

Mouse corneal injury and observation of CD31 and LYVE-1 in cornea flat mount

Experimental conditions are listed in Supplemental Fig. S1. Under anesthesia, 15 μl of moKDR_MOe13 (40 ng/μl), STD_MO (40 ng/μl), or DPBS was injected subconjunctivally into 2 different places. The corneas were fixed in acetone at room temperature for 20 min. After 4 washes in PBST (0.1% Tween20/PBS), the corneas were incubated in 3% BSA/PBS at 4°C for 3 d. Then corneas were incubated in 3%BSA/PBS with FITC-conjugated rat anti-CD31 antibody (553372, 1:500; BD Biosciences) and rabbit anti-LYVE-1 (ab14917, 1:200; Abcam) overnight at 4°C. After 3 washes, the corneas were incubated in 3% BSA/PBS with Alexa Fluor 546-conjugated goat anti-rabbit IgG (A11071, 1:2000; Invitrogen) for 1 h at room temperature. After 4 washes, corneas were mounted on glass slides with Fluoro-gel (Electron Microscopy Sciences, Hatfield, PA, USA). Fluorescence was observed by fluorescence microscope (Carl Zeiss MicroImaging, Thornwood, NY, USA). The data for each suture were calculated separately by ImageJ (U.S. National Institutes of Health, Bethesda, MD, USA).

Mouse corneal transplantation

Mouse corneal transplantation was described previously (9, 14). The donor cornea was marked with 2 mm trephine, the anterior chamber was penetrated using a knife (ClearCut; Alcon, Hünenberg, Switzerland), and the cornea was cut with Vannas scissors and then placed in balanced salt solution. The recipient mouse was anesthetized with ketamine (100 mg/kg body weight) and xylazine (20 mg/kg body weight). To dilate the pupil and anesthetize the cornea, 1% tropicamide ophthalmic solution and 0.5% proparacaine ophthalmic solution were used. The recipient's right cornea was marked with 1.5 mm trephine and removed by the same method as the donor cornea. Viscoelastic material (Healon,1% sodium hyaluronate; Abbott Medical Optics, North Chicago, IL, USA) was used during recipient cornea dissection. The donor graft was sutured into the recipient bed using interrupted sutures (11-0 nylon, CS160-6; Ethicon, Somerville, NJ, USA). After the transplantation, the eye was covered with 0.5% erythromycin ophthalmic ointment, and the lid was sutured with 8-0 coated vicryl (BV130-5; Ethicon). All sutures

remained for the first postoperative week. We injected 15 μl moKDR_MOe13 (40 ng/μl), STD_MO (40 ng/μl), or DPBS subconjunctivally on the day of transplantation and postoperative 1, 2, 3, and 4 wk (Supplemental Fig. S1). The corneal opacity was examined weekly using an operating microscope by the end point (8 wk). The opacity was graded (from 0 to 5) to determine graft rejection (15). Opacity of grade 3 or more was considered to be graft rejection. At 8 wk, corneas were harvested and subjected for CD31 and LYVE1 stain using the method described above.

RESULTS

Blocking exon 13-intron 13 junction in KDR leads to increased sKDR and decreased mbKDR at the mRNA level

At first, we examined whether modulation of splicing can lead to sKDR up-regulation and mbKDR down-regulation. To modulate splicing, we used antisense morpholino oligomers that bind mRNA or pre-mRNA with high specificity to inhibit translation and affect alternative splicing (16, 17). Antisense morpholino oligomers were designed corresponding to the junction of exon 13-intron 13 (KDR_MOe13; **Fig. 1*A*** and the sequences in Table 1). Although the human sKDR mRNA structure was not well characterized, we utilized the expressed sequence tag (EST) database and found the sequence of the initial 365 nt of intron 13, which include a stop codon at 48–50 nt. In addition, 2 polyadenylation sites (AAUAAA) are found in intron 13 (Fig. 1*A*). To introduce morpholino into cultured cells, we performed nucleofection. Fluorescent conjugated morpholino was used to confirm transfection into HUVECs (Fig. 1*B*). At 2 d after morpholino transfection, sKDR and mbKDR mRNA in HUVECs were examined by RT-PCR (Fig. 1*C* and

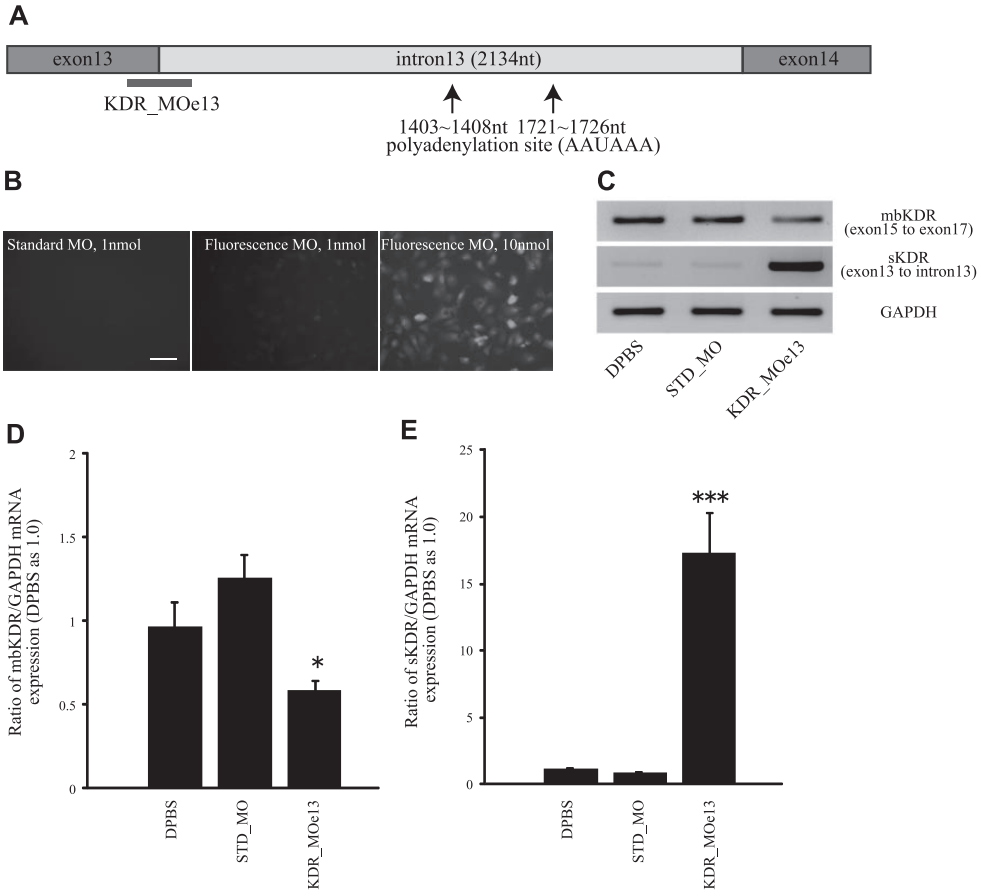

Figure 1. KDR_MOe13 decreases mbKDR mRNA and increases sKDR mRNA. *A*) Schematic design of KDR_MOe13. *B*) Fluorescent morpholinos can be observed after nucleofection. Indicated amounts of each morpholino were nucleofected into HUVECs. Scale bar = 100 μm. *C*) RT-PCR indicates mbKDR mRNA decrease and sKDR mRNA increase after KDR_MOe13. *D*, *E*) Quantitative real-time PCR shows 40% decrease of mbKDR and 17-fold increase of sKDR mRNA. All results were normalized by GAPDH and compared with DPBS-transfected HUVECs by 2-tailed Student's *t* test; $n = 6$/group. Bars represent means ± SE. $^*P < 0.05$, $^{***}P < 0.001$ *vs.* DPBS-transfected HUVECs.

Supplemental Fig. S2). mbKDR mRNA decreased in HUVECs transfected with KDR_MOe13 compared with DPBS- or STD_MO-transfected HUVECs. On the other hand, sKDR mRNA was increased by KDR_MOe13. To quantify these results, real-time PCR was performed (Fig. 1*D*, *E*). We found that KDR_MOe13 down-regulates mbKDR mRNA by 40% compared with STD_MO or DPBS ($P<0.05$). In contrast, sKDR mRNA showed a 17-fold increase ($P<0.001$) with KDR_MOe13.

KDR_MOe13 increased sKDR and decreased mbKDR protein

Next, we examined mbKDR protein expression by Western blot. KDR_MOe13 reduced mbKDR protein expression compared to DPBS and STD_MO (**Fig. 2*A***). On flow cytometry, in DPBS- and STD_MO-transfected HUVECs, 83.3 and 81.0% were mbKDR positive, respectively, while KDR_MOe13 decreased mbKDR positive cells to 40.7% (Fig. 2*B*). To confirm sKDR protein expression, we performed Western blot from culture medium of KDR_MOe13-transfected HUVECs using an antibody recognizing KDR extracellular domains (Fig. 2*C*, *D*). Although the predicted molecular mass of human sKDR is ~76 kD, 150-kD bands were detected from the culture medium of HUVECs transfected with KDR_MOe13. Based on previous studies, mbKDR can be glycosylated, increasing the molecular mass from 150 to 230 kD (18). In addition, sKDR has been detected at 160 kDa, although it was not reported whether this was derived from alternative polyadenylation or proteolytic cleavage from mbKDR (10). To confirm glycosylation of sKDR, we attempted deglycosylation of sKDR in medium from KDR_MOe13-treated HUVECs using TFMS (Fig. 2*E*). We found that the observed size of sKDR decreased from 150 to ~70 kDa, confirming glycosylation of sKDR.

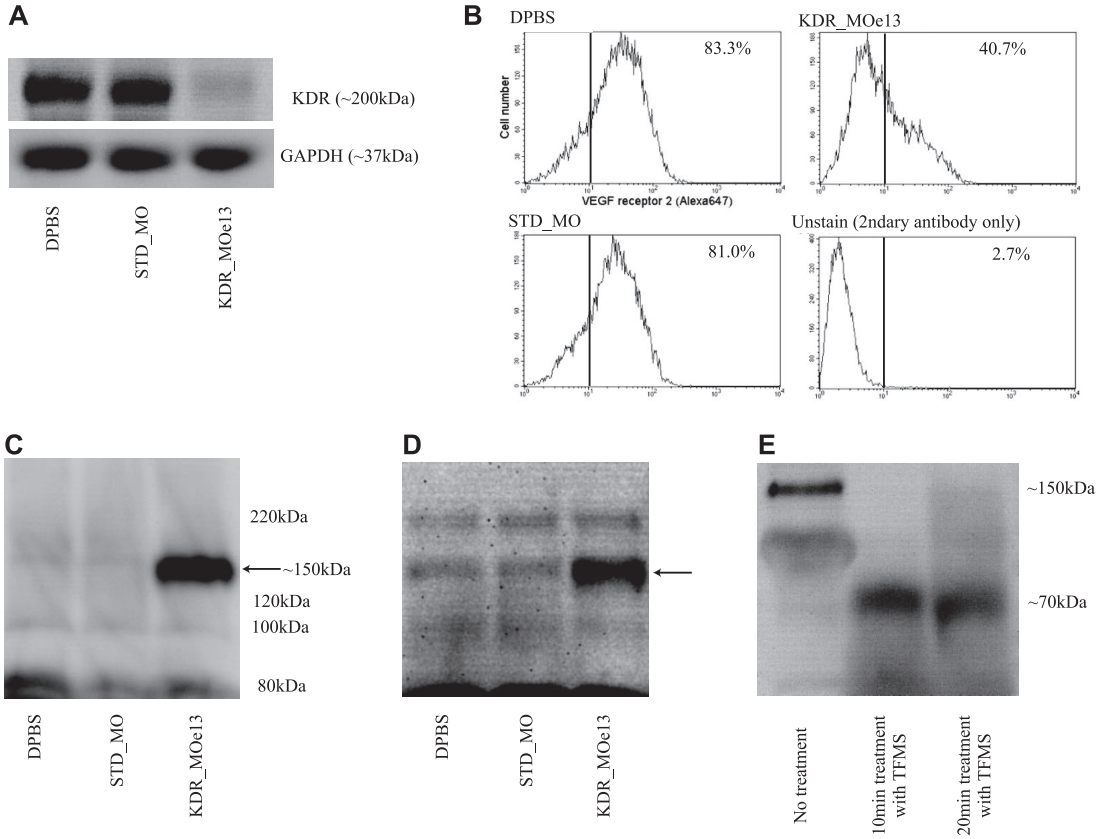

Figure 2. KDR_MOe13 decreases mbKDR protein and increases sKDR protein. *A*) KDR_MOe13 decreased mbKDR protein expression, as detected on Western blot. *B*) Flow cytometry demonstrates that KDR_MOe13 decreases mbKDR cell surface expression. HUVECs stained with only secondary antibody were used as a negative control. *C*) Western blot from concentrated culture medium shows that KDR_MOe13 induced sKDR (150-kDa band). *D*) sKDR protein detection from conditioned culture medium without concentration. We exposed for a long period and enhanced the image. The 150-kDa band (arrow) was detected from KDR_MOe13-transfected HUVEC culture medium strongly. *E*) Deglycosylation of sKDR by TFMS. After deglycosylation, sKDR induced by KDR_MOe13 was observed at approximately calculated molecular weight (~70 kDa).

Polyadenylation signal induced by KDR_MOe13 is the same polyadenylation site as in endogenous sKDR found in human cornea

Next, to determine the 3′ UTR of sKDR mRNA induced by morpholinos, 3′ RACE was performed (**Fig. 3*A***). A strong band (~1600 bp) was detected from KDR_MOe13-transfected HUVECs. Based on the sequence of this band, sKDR mRNA utilizes a polyadenylation site located in the 1403- to 1408-nt range of intron 13 (Fig. 3*C*). Based on this, we sought to identify the 3′ UTR of sKDR from human corneal total RNA (Fig. 3*B*). Corneal tissue is known to predominantly express sKDR (9). We found that in the human cornea, sKDR mRNA utilizes the same polyadenylation site that KDR_MOe13 induces (Fig. 3*C*).

KDR_MOe13 suppressed experimental hemangiogenesis and lymphangiogenesis *in vivo*

Because KDR_MOe13 decreases mbKDR and increases sKDR, we predicted that KDR_MOe13 can inhibit hemangiogenesis and lymphangiogenesis *in vivo*. Therefore, we created moKDR_MOe13, which targets the exon 13-intron 13 junction of mouse *KDR*. By RT-PCR, we found that moKDR_MOe13 increased sKDR mRNA and decreased mbKDR mRNA in mouse MS-1 cells (**Fig. 4*A***). To administer morpholinos *in vivo*, we developed morpholinos conjugated with dendrimer at the 3′ position (vivomorpholino; ref. 19). Vivomorpholino possesses guanidinium head groups, which are predicted to help morpholino transport into cells through binding with the phosphates of phospholipids. To determine moKDR_MOe13 function *in vivo*, each morpholino or DPBS was injected intravitreously, and the retinal total RNA was subjected to real-time RT-PCR for sKDR and mbKDR mRNA (Fig. 4*B*). moKDR_MOe13 significantly increased the sKDR/mbKDR mRNA ratio. Next, we examined mbKDR and sKDR retinal and vitreous protein by Western blot. Consistent with real-time PCR results, moKDR_MOe13 decreased retinal mbKDR protein (Fig. 4*C*) and increased vitreous sKDR protein (Fig. 4*D*). Next, we examined whether moKDR_MOe13 inhibits laser-induced CNV. Each morpholino or DPBS was injected intravitreously on d 1 and 4 after laser photocoagulation, and laser CNV volumes were examined on d 7. Figure 4*E* shows representative images of laser CNV with DPBS, STD_MO, and moKDR_MOe13. moKDR_MOe13 significantly suppressed laser CNV compared with STD_MO ($P<0.05$) and DPBS ($P<0.01$) (Fig. 4*F*). In addition, moKDR_MOe13 treatment was comparable to anti-VEGF-A IgG and KDR kinase inhibitor (SU1498) treatment (Fig. 4*G*). We also assessed apoptosis using TUNEL assay (Supplemental Fig. S3). Mild apoptosis was observed after treatment with moKDR_MOe13 and STD_MO. Furthermore, after morpholino intravitreous injection, fenestration in

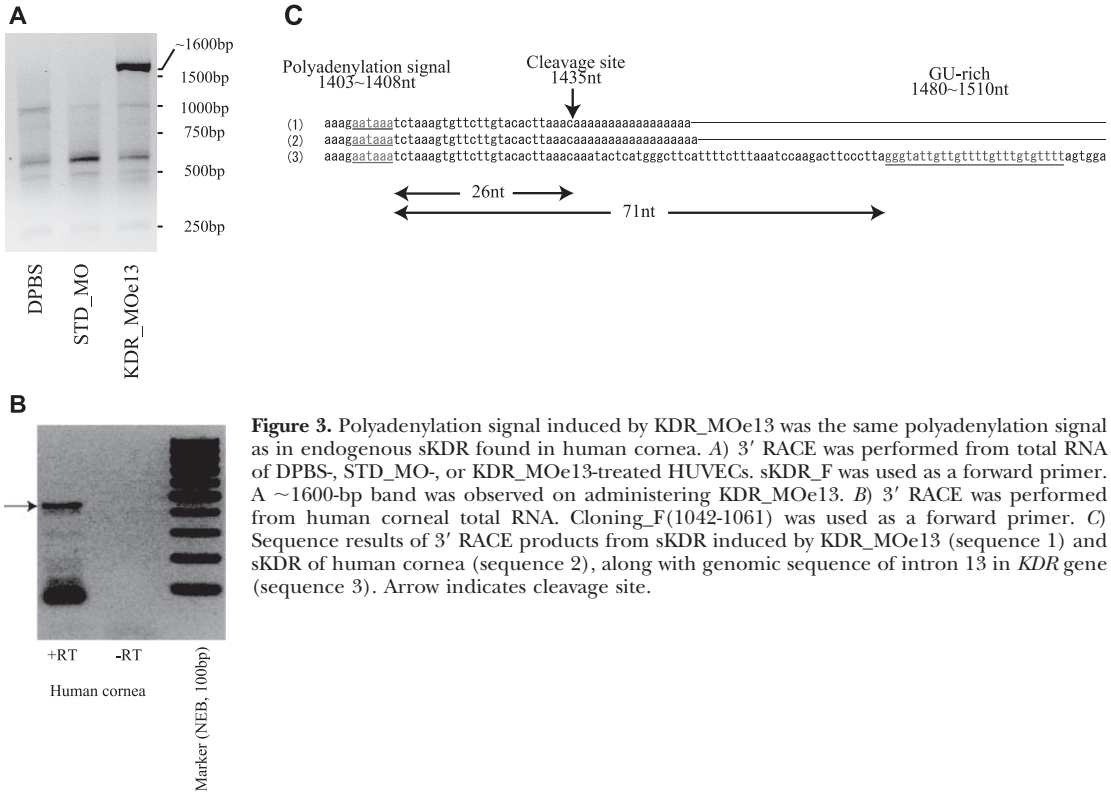

Figure 3. Polyadenylation signal induced by KDR_MOe13 was the same polyadenylation signal as in endogenous sKDR found in human cornea. *A*) 3′ RACE was performed from total RNA of DPBS-, STD_MO-, or KDR_MOe13-treated HUVECs. sKDR_F was used as a forward primer. A ~1600-bp band was observed on administering KDR_MOe13. *B*) 3′ RACE was performed from human corneal total RNA. Cloning_F(1042-1061) was used as a forward primer. *C*) Sequence results of 3′ RACE products from sKDR induced by KDR_MOe13 (sequence 1) and sKDR of human cornea (sequence 2), along with genomic sequence of intron 13 in *KDR* gene (sequence 3). Arrow indicates cleavage site.

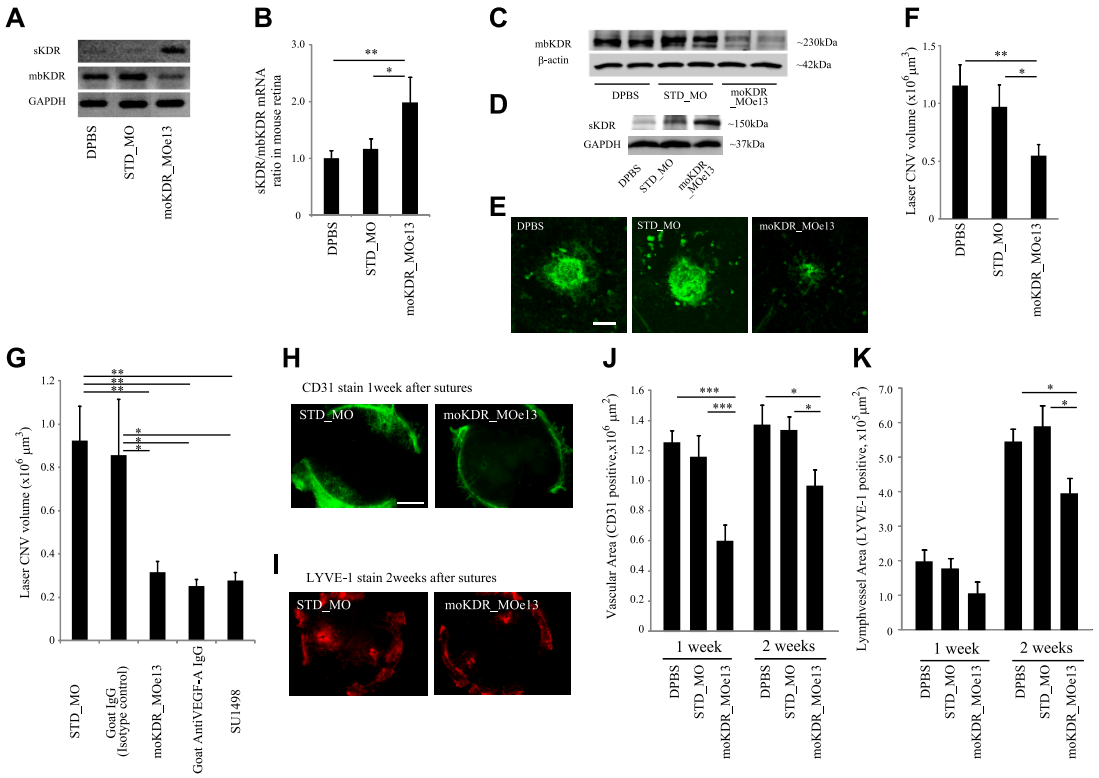

Figure 4. moVEGFR2_MOe13 suppresses experimental neovascularization and lymphangiogenesis in mice. *A*) RT-PCR from MS-1 cells shows that moKDR_MOe13 decreases mbKDR mRNA and increases sKDR. *B*) Real-time PCR indicates that intravitreous injection of moKDR_MOe13 increases sKDR/mbKDR mRNA ratio in mouse retina (n=4). *C, D*) moKDR_MOe13 decreased mbKDR protein and increased sKDR protein *in vivo*, as demonstrated by Western blots of mouse retina and vitreous. *E*) Representative images of laser-induced CNV. *F*) moKDR_MOe13 suppressed laser-induced CNV relative to PBS or standard nonspecific morpholino (n=11–17). *G*) moKDR_MOe13 suppressed laser-induced CNV volume by comparable amounts relative to anti-mouse VEGF-A antibody and the KDR kinase inhibitor SU1498 (n=14–18). ANOVA: P = 0.000255. *H, I*) Representative images of corneal neovascularization 1 wk after suture (*H*) and corneal lymphangiogenesis 2 wk after sutures (*I*). *J, K*) moKDR_MOe13 suppressed neovascularization at 1 and 2 wk (*J*), and decreased lymphangiogenesis at 2 wk (*K*) compared with the controls. Scale bars = 100 μm. P values were calculated by 2-tailed Student's t test (n=13–16). Bars represent means ± SE. $^*P < 0.05$, $^{**}P < 0.01$, $^{***}P < 0.001$.

choriocapirallis was not affected by either moKDR_MOe13 or control (Supplemental Fig. S4). For a second model of angiogenesis, we used the corneal suture model. For the 1-wk subarm, each morpholino or DPBS was injected subconjunctivally 1 d before and 4 d after suturing; the corneas were harvested 7 d postsuturing. For the 2-wk subarm, each morpholino or DPBS was injected subconjunctivally 1 d prior and 4, 7, and 10 d after suturing; corneas were harvested at 14 d. CD31 and LYVE-1 were used as markers of neovascularization and lymphangiogenesis, respectively. Figure 4*H, I* displays representative images of CD31-stained corneas at 1 wk and LYVE-1-stained corneas at 2 wk. Figure 4*J, K* displays the mean area of neovascularization and lymphangiogenesis in each group. moKDR_MOe13 suppressed suture-induced neovascularization by 52.2% (1 wk) and 29.6% (2 wk) compared to DPBS (P<0.001 and 0.05, respectively). moKDR_MOe13 did not suppress lymphangiogenesis 1 wk postsuturing but suppressed lymphangiogenesis by 27.8% 2 wk postsuturing, compared to DPBS (P<0.05).

KDR_MOe13 reduced graft rejection after mouse corneal transplantation

Finally, we examined whether moKDR_MOe13 suppressed murine corneal transplant rejection, which is pathologically dependent on both hemangiogenesis and lymphangiogenesis. After cornea transplantation, moKDR_MOe13, STD_MO, or DPBS was injected subconjunctivally. The corneas were observed with the stereomicroscope (**Fig. 5*A***). We found that moKDR_MOe13 increased graft survival compared with DPBS and STD_MO (Fig. 5*B*, log rank test: P=0.0186 and 0.0610, respectively). Figure 5*C* shows the representative images of CD31 and LYVE-1 stained cornea at the end point (8 wk). Concordantly, moKDR_MOe13 signifi-

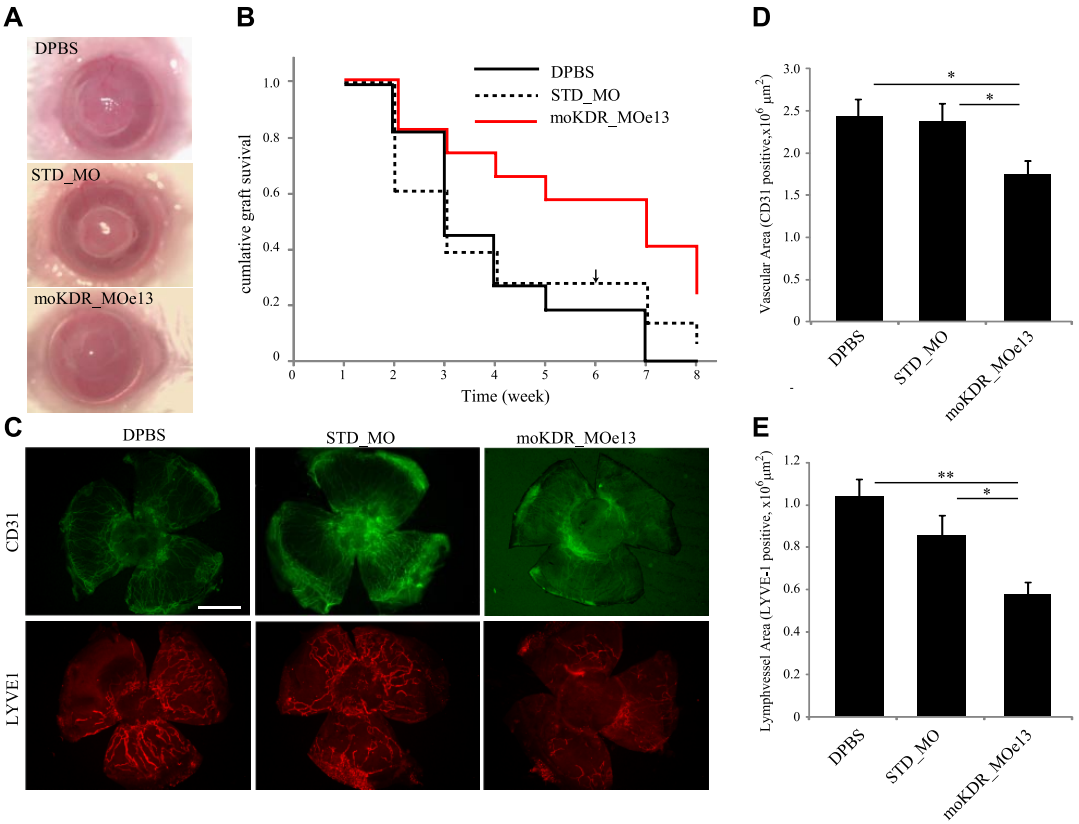

Figure 5. moKDR_MOe13 suppresses graft rejection in mouse corneal transplantation. *A*) Representative stereomicroscope images 3 wk after corneal transplantation show that corneal transplants treated with moKDR_MOe13 were clear and had less inflammation than the others. *B*) Cumulative graft survival rate. moKDR_MOe13 increased graft survival rate compared with DPBS and STD_MO (log rank test: P=0.0186 and 0.0610, respectively). Arrow indicates censored data. *C*) Representative images of corneal neovascularization and lymphangiogenesis in mouse corneal transplants at 8 wk. Scale bar = 1 mm. *D*, *E*) moKDR_MOe13 suppressed neovascularization (*D*) and lymphangiogenesis (*E*) in mouse corneal transplants at 8 wk. P values were calculated by 2-tailed Student's t test (n=11–17). Bars represent means ± SE. *$P < 0.05$, **$P < 0.01$).

cantly reduced neovascularization and lymphangiogenesis (Fig. 5*D*, *E*).

DISCUSSION

Generally, alternative splicing produces a variety of isoforms from a single gene and contributes diversity. For example, the *VEGF-A* gene produces VEGF121, VEGF165, VEGF189, and VEGF206 by alternative splicing, and the products may contribute to forming the gradient of VEGF-A (20–22). Compared with alternative splicing, alternative polyadenylation is not yet well understood despite its importance. In humans and mice, EST database analysis indicated that ~60% of mRNA may result from alternative polyadenylation (23). We can divide alternative polyadenylation into 2 classes. In the first class, the 3′ UTR has ≥2 polyadenylation sites. Depending on which polyadenylation site is used, the length of 3′ UTR changes. The difference of 3′ UTR length affects stability and localization of mRNA (24–26). In the second class, the active polyadenylation site exists in a different exon or intron. The example of this type of alternative polyadenylation is the immunoglobulin system in B cells (27, 28). This type of polyadenylation is believed to be associated with an alternative splicing event (29). The *KDR* gene would represent this type of alternative polyadenylation.

In this study, we demonstrate that the latent polyadenylation site in intron 13 of *KDR* can be activated by blocking the upstream 5′ splicing site (exon 13-intron 13 junction) using KDR_MOe13, which decreased mbKDR and increased sKDR at mRNA and protein levels. The polyadenylation site induced by KDR_MOe13 is normally inactive in HUVECs, preferentially excluding intron 13 during physiological splicing. KDR_MOe13 likely competes with U1snRNPs at the exon 13-intron 13 junction. U1snRNPs may inhibit downstream polyadenylation and are among the key components for the splicing event, although U1snRNP-

independent RNA splicing has been demonstrated (30–32). It is probable that KDR_MOe13 activates the latent polyadenylation signal by inhibiting U1snRNP binding to the exon 13-intron 13 junction.

Interestingly, the polyadenylation site induced by KDR_MOe13 is the same polyadenylation site as in endogenous sKDR found in human cornea. The sequence around the polyadenylation site indicates that a cleavage site (CA dinucleotides) and a GU-rich region are located 26 and 71 nt downstream of AAUAAA, respectively (Fig. 3*C*). These sequence components are similar to typical polyadenylation signals (29, 33). Without any direct modification of the polyadenylation mechanism, KDR_MOe13 activates the latent polyadenylation signal. Thus, mbKDR-preferred cells, such as HUVECs, are still able to recognize the latent polyadenylation signal. This indicates that endogenous sKDR may be produced by splicing factor control, rather than polyadenylation mechanism modification. To understand altenative polyadenylation events, splicing factors should be focused rather than polyadenylation mechanisms themselves.

sKDR protein induced by KDR_MOe13 was processed (glycosylation) and exported to culture medium *in vitro*. These results indicated that sKDR has similar binding capacity of mbKDR to VEGF-C and inhibits it in extracellularly. We have shown the effectiveness of morpholinos *in vivo* by using moKDR_MOe13 to suppress corneal neovascularization and lymphangiogenesis in a suture injury model in mice. These results suggested also that sKDR induced by KDR_MOe13 has binding capacity to VEGF-C.

siRNA therapies to block angiogenesis are currently under development. We propose the use of morpholinos to shift the functionality of proangiogenic mbKDR to antiangiogenic sKDR as an alternative avenue for developing antiangiogenic therapies. siRNAs can knock down target mRNA but lacks the distinct advantage that morpholinos have in being able to not only knock down an undesirable protein, but also produce a desirable protein at the same time. The dual effect of knocking down one protein, while concurrently increasing the translation of another, could offer therapeutic advantages in the ability to more precisely regulate protein levels. In addition, unlike siRNA, morpholinos are of neutral charge and induce a lesser inflammatory response and less off target binding.

We used a vivomorpholino *in vivo* study, although the dendrimer that enables cell entry has been reported to have mild toxicity (34), and we found some toxicity (Supplemental Fig. S3). To advance this further toward clinical translation, in future studies, we will test cell-penetrating peptides such as polyarginine or cholesterol conjugation (to avoid use of dendrimers). Future investigations will also explore the distribution and duration of morpholinos *in vivo* using novel but currently unavailable vivomorpholinos with fluorophores. To target delivery of morpholinos, nanoparticles may also be employed.

Another potential application for our morpholino-targeting KDR would be the area of oncology. Solid tumors rely on both hemangiogenesis and lymphangiogenesis for growth and metastasis. The approach described herein holds great potential for solid tumor therapy as it simultaneously suppresses formation of both blood and lymphatic vessels.

A recent report showed that polyadenylation activation could induce soluble isoforms of several receptor tyrosine kinases, including *KDR* (35). We confirm the concept of activating a latent polyadenylation signal using morpholino oligomers and demonstrate *in vivo* utility in suppressing hemangiogenesis and lymphangiogenesis with therapeutic effect in 3 models of blinding disorders, including macular degeneration, corneal injury, and corneal transplant rejection. This has applications not only for antiangiogenesis or eye disease by targeting KDR but also in other conditions where regulatory manipulation of splicing and polyadenylation could have therapeutic valence. FJ

This work was supported by a Research to Prevent Blindness Physician Scientist Award, a U.S. Department of Veterans Affairs Merit Award, and U.S. National Eye Institute grant R01EY017950.

REFERENCES

1. Risau, W. (1997) Mechanisms of angiogenesis. *Nature* **386,** 671–674
2. Chang, J. H., Gabison, E. E., Kato, T., and Azar, D. T. (2001) Corneal neovascularization. *Curr. Opin. Ophthalmol.* **12,** 242–249
3. Fowler, M. J. (2008) Microvascular and macrovascular complications of diabetes. *Clin. Diabetes* **26,** 77–82
4. Ng, E. W., and Adamis, A. P. (2005) Targeting angiogenesis, the underlying disorder in neovascular age-related macular degeneration. *Can. J. Ophthalmol.* **40,** 352–368
5. Raza, A., Franklin, M. J., and Dudek, A. Z. (2010) Pericytes and vessel maturation during tumor angiogenesis and metastasis. *Am. J. Hematol.* **85,** 593–598
6. Weis, S., Cui, J., Barnes, L., and Cheresh, D. (2004) Endothelial barrier disruption by VEGF-mediated Src activity potentiates tumor cell extravasation and metastasis. *J. Cell Biol.* **167,** 223–229
7. Shibuya, M. (2006) Differential roles of vascular endothelial growth factor receptor-1 and receptor-2 in angiogenesis. *J. Biochem. Mol. Biol.* **39,** 469–478
8. Shibuya, M. (2008) Vascular endothelial growth factor-dependent and -independent regulation of angiogenesis. *BMB Rep.* **41,** 278–286
9. Albuquerque, R. J., Hayashi, T., Cho, W. G., Kleinman, M. E., Dridi, S., Takeda, A., Baffi, J. Z., Yamada, K., Kaneko, H., Green, M. G., Chappell, J., Wilting, J., Weich, H. A., Yamagami, S., Amano, S., Mizuki, N., Alexander, J. S., Peterson, M. L., Brekken, R. A., Hirashima, M., Capoor, S., Usui, T., Ambati, B. K., and Ambati, J. (2009) Alternatively spliced vascular endothelial growth factor receptor-2 is an essential endogenous inhibitor of lymphatic vessel growth. *Nat. Med.* **15,** 1023–1030
10. Ebos, J. M., Bocci, G., Man, S., Thorpe, P. E., Hicklin, D. J., Zhou, D., Jia, X., and Kerbel, R. S. (2004) A naturally occurring soluble form of vascular endothelial growth factor receptor 2 detected in mouse and human plasma. *Mol. Cancer Res.* **2,** 315–326
11. Uehara, H., Luo, L., Simonis, J., Singh, N., Taylor, E. W., and Ambati, B. K. (2010) Anti-SPARC oligopeptide inhibits laser-induced CNV in mice. *Vision Res.* **50,** 674–679
12. Anderson, J. R., Jones, B. W., Yang, J. H., Shaw, M. V., Watt, C. B., Koshevoy, P., Spaltenstein, J., Jurrus, E., U, V. K., Whitaker, R. T., Mastronarde, D., Tasdizen, T., and Marc, R. E. (2009) A computational framework for ultrastructural mapping of neural circuitry. *PLoS Biol.* **7,** e1000074

13. Marc, R. E., and Liu, W. (2000) Fundamental GABAergic amacrine cell circuitries in the retina: nested feedback, concatenated inhibition, and axosomatic synapses. *J. Comp. Neurol.* **425,** 560–582
14. Hayashi, T., Yamagami, S., Tanaka, K., Yokoo, S., Usui, T., Amano, S., and Mizuki, N. (2008) A mouse model of allogeneic corneal endothelial cell transplantation. *Cornea* **27,** 699–705
15. Sonoda, Y., and Streilein, J. W. (1992) Orthotopic corneal transplantation in mice—evidence that the immunogenetic rules of rejection do not apply. *Transplantation* **54,** 694–704
16. Jearawiriyapaisarn, N., Moulton, H. M., Buckley, B., Roberts, J., Sazani, P., Fucharoen, S., Iversen, P. L., and Kole, R. (2008) Sustained dystrophin expression induced by peptide-conjugated morpholino oligomers in the muscles of mdx mice. *Mol. Ther.* **16,** 1624–1629
17. Summerton, J. E. (2007) Morpholino, siRNA, and S-DNA compared: impact of structure and mechanism of action on off-target effects and sequence specificity. *Curr. Top. Med. Chem.* **7,** 651–660
18. Takahashi, T., and Shibuya, M. (1997) The 230 kDa mature form of KDR/Flk-1 (VEGF receptor-2) activates the PLC-gamma pathway and partially induces mitotic signals in NIH3T3 fibroblasts. *Oncogene* **14,** 2079–2089
19. Morcos, P. A., Li, Y., and Jiang, S. (2008) Vivo-morpholinos: a non-peptide transporter delivers morpholinos into a wide array of mouse tissues. *BioTechniques* **45,** 613–623
20. Ferrara, N. (2010) Binding to the extracellular matrix and proteolytic processing: two key mechanisms regulating vascular endothelial growth factor action. *Mol. Biol. Cell.* **21,** 687–690
21. Houck, K. A., Leung, D. W., Rowland, A. M., Winer, J., and Ferrara, N. (1992) Dual regulation of vascular endothelial growth factor bioavailability by genetic and proteolytic mechanisms. *J. Biol. Chem.* **267,** 26031–26037
22. Park, J. E., Keller, G. A., and Ferrara, N. (1993) The vascular endothelial growth factor (VEGF) isoforms: differential deposition into the subepithelial extracellular matrix and bioactivity of extracellular matrix-bound VEGF. *Mol. Biol. Cell.* **4,** 1317–1326
23. Muro, E. M., Herrington, R., Janmohamed, S., Frelin, C., Andrade-Navarro, M. A., and Iscove, N. N. (2008) Identification of gene 3′ ends by automated EST cluster analysis. *Proc. Natl. Acad. Sci. U. S. A.* **105,** 20286–20290
24. An, J. J., Gharami, K., Liao, G. Y., Woo, N. H., Lau, A. G., Vanevski, F., Torre, E. R., Jones, K. R., Feng, Y., Lu, B., and Xu, B. (2008) Distinct role of long 3′ UTR BDNF mRNA in spine morphology and synaptic plasticity in hippocampal neurons. *Cell* **134,** 175–187
25. Andreassi, C., and Riccio, A. (2009) To localize or not to localize: mRNA fate is in 3′UTR ends. *Trends Cell Biol.* **19,** 465–474
26. Yudin, D., Hanz, S., Yoo, S., Iavnilovitch, E., Willis, D., Gradus, T., Vuppalanchi, D., Segal-Ruder, Y., Ben-Yaakov, K., Hieda, M., Yoneda, Y., Twiss, J. L., and Fainzilber, M. (2008) Localized regulation of axonal RanGTPase controls retrograde injury signaling in peripheral nerve. *Neuron* **59,** 241–252
27. Peterson, M. L. (2007) Mechanisms controlling production of membrane and secreted immunoglobulin during B cell development. *Immunol. Res.* **37,** 33–46
28. Peterson, M. L., and Perry, R. P. (1989) The regulated production of mu m and mu s mRNA is dependent on the relative efficiencies of mu s poly(A) site usage and the c mu 4-to-M1 splice. *Mol. Cell. Biol.* **9,** 726–738
29. Lutz, C. S. (2008) Alternative polyadenylation: a twist on mRNA 3′ end formation. *ACS Chem. Biol.* **3,** 609–617
30. Abad, X., Vera, M., Jung, S. P., Oswald, E., Romero, I., Amin, V., Fortes, P., and Gunderson, S. I. (2008) Requirements for gene silencing mediated by U1 snRNA binding to a target sequence. *Nucleic Acids Res.* **36,** 2338–2352
31. Fukumura, K., and Inoue, K. (2009) Role and mechanism of U1-independent pre-mRNA splicing in the regulation of alternative splicing. *RNA Biol.* **6,** 395–398
32. Gunderson, S. I., Polycarpou-Schwarz, M., and Mattaj, I. W. (1998) U1 snRNP inhibits pre-mRNA polyadenylation through a direct interaction between U1 70K and poly(A) polymerase. *Mol. Cell* **1,** 255–264
33. Tian, B., Hu, J., Zhang, H., and Lutz, C. S. (2005) A large-scale analysis of mRNA polyadenylation of human and mouse genes. *Nucleic Acids Res.* **33,** 201–212
34. Jain, K., Kesharwani, P., Gupta, U., and Jain, N. K. (2010) Dendrimer toxicity: Let's meet the challenge. *Int. J. Pharm.* **394,** 122–142
35. Vorlova, S., Rocco, G., Lefave, C. V., Jodelka, F. M., Hess, K., Hastings, M. L., Henke, E., and Cartegni, L. (2011) Induction of antagonistic soluble decoy receptor tyrosine kinases by intronic polyA activation. *Mol. Cell* **43,** 927–939

Received for publication June 8, 2012.
Accepted for publication September 4, 2012.

CHAPTER 5

MORPHOLINO-MEDIATED INCREASE IN SOLUBLE FLT-1 EXPRESSION RESULTS IN DECREASED OCULAR AND TUMOR NEOVASCULARIZATION*

Leah Owen and Hironori Uehara were co-first authors of this manuscript and designed the study. My role in this manuscript was performing ELISA for sFLT (Figure 1D) and real-time PCR for cell cultures (Figure 1B&C and Figure 2).

*Reprinted with permission from PLoS One and Elsevier Publishing. Owen, LA. *et al. Morpholino-mediated increase in soluble Flt-1 expression results in decreased ocular and tumor neovascularization.* PLoS One 2012;7(3):e33576

OPEN ACCESS Freely available online

PLoS one

Morpholino-Mediated Increase in Soluble Flt-1 Expression Results in Decreased Ocular and Tumor Neovascularization

Leah A. Owen[◔], Hironori Uehara[◔], Judd Cahoon, Wei Huang, Jacquelyn Simonis, Balamurali K. Ambati*

Department Of Ophthalmology, Moran Eye Center, University of Utah, Salt Lake City, Utah, United States of America

Abstract

Background: Angiogenesis is a key process in several ocular disorders and cancers. Soluble Flt-1 is an alternatively spliced form of the *Flt-1* gene that retains the ligand-binding domain, but lacks the membrane-spanning and intracellular kinase domains of the full-length membrane bound Flt-1 (mbFlt-1) protein. Thus, sFlt-1 is an endogenous inhibitor of VEGF-A mediated angiogenesis. Synthetic mopholino oligomers directed against splice site targets can modulate splice variant expression. We hypothesize that morpholino-induced upregulation of sFlt-1 will suppress angiogenesis in clinically relevant models of macular degeneration and breast cancer.

Methods and Findings: *In vivo* morpholino constructs were designed to target murine exon/intron 13 junction of the Flt-1 transcript denoted VEGFR1_MOe13; standard nonspecific morpholino was used as control. After nucleofection of endothelial and breast adenocarcinoma cell lines, total RNA was extracted and real-time RT-PCR performed for sFlt-1 and mbFlt-1. Intravitreal injections of VEGFR1_MOe13 or control were done in a model of laser-induced choroidal neovascularization and intratumoral injections were performed in MBA-MD-231 xenografts in nude mice. VEGFR1_MOe13 elevated sFlt-1 mRNA expression and suppressed mbFlt-1 mRNA expression *in vitro* in multiple cellular backgrounds ($p<0.001$). VEGFR1_MOe13 also elevated sFlt/mbFlt-1 ratio *in vivo* after laser choroidal injury 5.5 fold ($p<0.001$) and suppressed laser-induced CNV by 50% ($p = 0.0179$). This latter effect was reversed by RNAi of sFlt-1, confirming specificity of morpholino activity through up-regulation of sFlt-1. In the xenograft model, VEGFR1_MOe13 regressed tumor volume by 88.9%, increased sFlt-1 mRNA expression, and reduced vascular density by 50% relative to control morpholino treatment ($p<0.05$).

Conclusions: Morpholino oligomers targeting the VEGFR1 mRNA exon/intron 13 junction promote production of soluble FLT-1 over membrane bound FLT-1, resulting in suppression of lesional volume in laser induced CNV and breast adenocarcinoma. Thus, morpholino manipulation of alternative splicing offers translational potential for therapy of angiogenic disorders.

Citation: Owen LA, Uehara H, Cahoon J, Huang W, Simonis J, et al. (2012) Morpholino-Mediated Increase in Soluble Flt-1 Expression Results in Decreased Ocular and Tumor Neovascularization. PLoS ONE 7(3): e33576. doi:10.1371/journal.pone.0033576

Editor: Wooin Lee, University of Kentucky, United States of America

Received September 3, 2011; **Accepted** February 16, 2012; **Published** March 15, 2012

Funding: This work was funded by a Research to Prevent Blindness Physician-Scientist Award, National Eye Institute 5R01EY017950, and a Veterans Affairs Merit Award. The funders had no role in study design, data collection and analysis, decision to publish, or preparation of the manuscript.

Competing Interests: The authors have declared that no competing interests exist.

* E-mail: bala.ambati@utah.edu

◔ These authors contributed equally to this work.

Introduction

Angiogenesis, though a fundamental physiologic process, is a key pathogenetic feature of numerous disease states. At present, therapeutic strategies have limited potential largely due to the fact that the underlying mechanisms of angiogenesis are incompletely understood. Work to elucidate the full complement of mediators and mechanisms important for angiogeneis, and further apply this knowledge in such a way to alter disease progression continues to be the foremost goal within the field.

Identification of VEGF as a critical mediator of vessel growth has been an important step to understanding the human condition in terms of the underlying molecular events. VEGF has been shown to be necessary and sufficient for ocular neovascularization [1–4]. In fact, transgenic mice which over-express human VEGF show widespread ocular neovascularization [5–6]. Additionally, pioneering work by Judah Folkman in the early 1970's demonstrated that solid tumor growth required VEGF expression [7]. However, it is not fully known what specific molecular mediators regulate VEGF expression. Soluble Flt-1, first described by Kendall and Thomas in 1993, is an alternatively spliced form of the *Flt-1* gene, also referred to as VEGF-receptor 1 [8]. This alternative splicing event occurs within intron 13 such that sFlt-1 contains the ligand-binding domain, but lacks the membrane-spanning and intracellular kinase domains of the full-length membrane bound Flt-1 (mbFlt-1) protein [9]. As suggested by its structure, sFlt-1 is a potent endogenous inhibitor of VEGF A-induced angiogenesis [9]. While the full complement of sFlt-1 expression and function has not been described, it has been shown to be both necessary and sufficient for maintenance of the

avascular cornea [10]. In addition, recent work has demonstrated a role for modulation of sFlt-1 in the development and treatment of a form of pathologic ocular neovascularization termed choroidal neovasculization (CNV), via modulation of VEGF ([11–12], unpublished data). Choroidal neovascularization is characterized by choroidal capillary growth through Bruch's membrane beneath the retinal pigmented epithelial (RPE) cell layer. This vascular pathology is most classically seen in exudative or "wet" age-related macular degeneration, the leading cause of vision loss in the western world [13–14]. Furthermore, sFLT-1 has also been shown to reduce VEGF expression and tumor vascularity in breast adenocarcinoma xenografts [15]. Thus, sFlt-1 represents a potential therapeutic target to reduce aberrant blood vessel growth over a spectrum of disease.

Current therapies targeting both CNV and tumor vasculature are focused on inhibiting the new vessel growth, and include such modalities as photocoagulation, photodynamic therapy, anti-VEGF intraocular injections, as well as systemic administration of anti-VEGF monoclonal antibody. These approaches have shown promise; however, they induce retinal damage, require repeated intraocular administration, or have recently been contraindicated for use in the case of systemic anti-VEGF therapy for breast adencarcinoma [4,13,16–17]. Additionally though certainly progress has been made, incomplete efficacy and recurrence is commonly seen with all modalities. Development of novel therapeutic techniques to either augment or circumvent our current treatments is necessary to improve both efficacy and the risk profile.

In this work, we describe the use of morpholino oligomers promoting the expression of soluble Flt-1 as a means to determine its potential for therapeutic use in disorders characterized by aberrant neovascularization. This technology has human precedent in Duchene Muscular Dystrophy, where morpholino technology targeting the dystrophin gene has shown efficacy in splice site alteration and disease modification in both animal and human trials [18–20]. Our work demonstrates the use of morpholino oligomers alters the splicing of VEGFR1 such that production of soluble Flt-1 is favored both *in vitro* and *in vivo*. Furthermore, we demonstrate the efficacy of increased sFlt-1 expression in treatment of aberrant blood vessel growth in ocular and cancer disease models. Thus, morpholino technology holds promise for use in the context of human disease.

Results

VEGFR1_MOe13 promotes a shift from membrane VEGFR1 to soluble VEGFR1 *in vitro*

In order to demonstrate the utility of morpholino constructs for modulating sFLT-1 expression, morpholino oligomers were designed targeting the FLT-1 mRNA exon13-intron13 junction (VEGFR1_MOe13) or intron13_exon14 junction (VEGFR1_MOi13). The canonical Flt-1 gene consists of thirty exons in human and mouse. Full-length mRNA from all exons produces mbFLT-1. By contrast, sFLT-1 utilizes a polyadenylation site within intron13. Therefore, interaction between the morpholino constructs and VegfR1 pre-mRNA is predicted to influence the alternative splicing event such that production of soluble FLT-1 is favored. To directly measure the relationship between membrane bound and soluble FLT-1 in the presence of VEGFR1_MOe13 and VEGFR1_MOi13, human umbilical vein endothelial cells (HUVEC) were electroporated with targeting or standard morpholino oligomers designed against human VEGFR1. Using this technique MO constructs were found to sufficiently access the nuclear compartment (Fig. 1a). Forty-eight hours after electroporation, total RNA was harvested and soluble VEGFR1 and membrane VEGFR1 mRNA expression was assessed using real-time PCR. We found that VEGFR1_MOe13, VEGFR1_MOi13, and a combination of a combination of one-half dose of both VEGFR1_MOe13 and VEGFR1_MOi13 significantly decreased membrane VEGFR1 mRNA and increased soluble VEGFR1 mRNA (Fig. 1b–c; Figure S1). To determine if the VEGFR1 morpholino constructs also affected soluble FLT-1 expression at the protein level, soluble VEGFR1 protein in HUVEC culture medium was measured by ELISA in the presence or absence of the VEGFR1 morpholino constructs or control mopholino. VEGFR1_MOe13 increased soluble VEGFR1 protein production as compared with standard morpholino or control PBS conditions (Fig. 1d). In contrast, VEGFR1_MOi13 were less effective, whereas combined delivery of both VEGFR1_MOi13 and VEGFR1_MOe13 showed intermediate response, possibly due to competitive interference or reduced efficacy of one morpholino as compared with the other. Thus, morpholino targeting of the FLT-1 mRNA exon13-intron13 junction using VEGFR1_MOe13 is most efficacious for increasing sFLT-1 and decreasing mbFLT-1 expression *in vitro*.

To ensure that this effect was not cell line specific, we sought to validate our findings in other cellular backgrounds. Although soluble FLT-1 is predominantly a product of endothelial cells per its role in angiogenesis, it is also expressed by a number of other cell types including tumor cells [15,21–24]. Thus, we sought to determine whether expression of the VEGFR1_MOe13 in MCF7 and MBA-MD-231 breast adenocarcinoma cells would increase soluble FLT-1 levels. As demonstrated in figure 2, electroporation of VEGFR1_MOe13 directed against the human FLT-1 transcript increases soluble FLT-1 RNA and decreases membrane FLT-1 RNA in both adenocarcinoma lines (Fig. 2a–d).

VEGFR1_MOe13 increases sFlt/mFlt mRNA ratio in the mouse retina and suppresses laser-induced choroidal neovascularization volume *in vivo*

In order to directly test the efficacy of the VEGFR1_MOe13 for both *in vivo* activity as well as predicted effect on the process of angiogenesis we adopted the well established murine model of laser-induced choroidal neovascularization which induces significant CNV lesions 1 week after laser injury [25–26]. We hypothesized that expression of VEGFR1_MOe13 *in vivo* would both increase soluble Flt-1 levels and lead to suppression of laser-induced CNV. To first evaluate the effectiveness of VEGFR1_MOe13 to modulate sFlt-1 levels *in vivo*, we examined the sFlt/mFlt mRNA ratio in the mouse retina 24 hours after injection with PBS, vivo-standard_MO, or vivo-VEGFR1_MOe13 designed to target murine sFlt-1 (the "vivo" denotes modification allowing MO construct to enter cells in vivo as demonstrated [27]). We found that intra-vitreol injection of vivo-VEGFR1_MOe13 leads to a significant increase of sFlt/mFlt mRNA ratio as compared with PBS or vivo-standard_MO injection (Fig. 3a). Thus, VEGFR1_MOe13 expression is sufficient to increase soluble Flt-1 expression *in vivo*.

To determine whether VEGFR1_MOe13 expression *in vivo* could suppress development of CNV in the setting of laser insult, vivo-VEGFR1_MOe13, vivo-standard_MO or PBS were injected intra-vitreously on day 1 and day 4 after laser photocoagulation. One week after laser photocoagulation, eyes were enucleated and the degree of CNV volume was measured by confocal microscope after isolectin GS-IB_4 vasculature staining. CNV volumes were quantified using confocal microscopy. Murine eyes treated with intra-vitreal vivo-VEGFR1_MOe13 displayed a statistically significant decrease in CNV volume as compared with eyes treated with either vivo-standard morpholino or PBS controls (Fig. 3b–d).

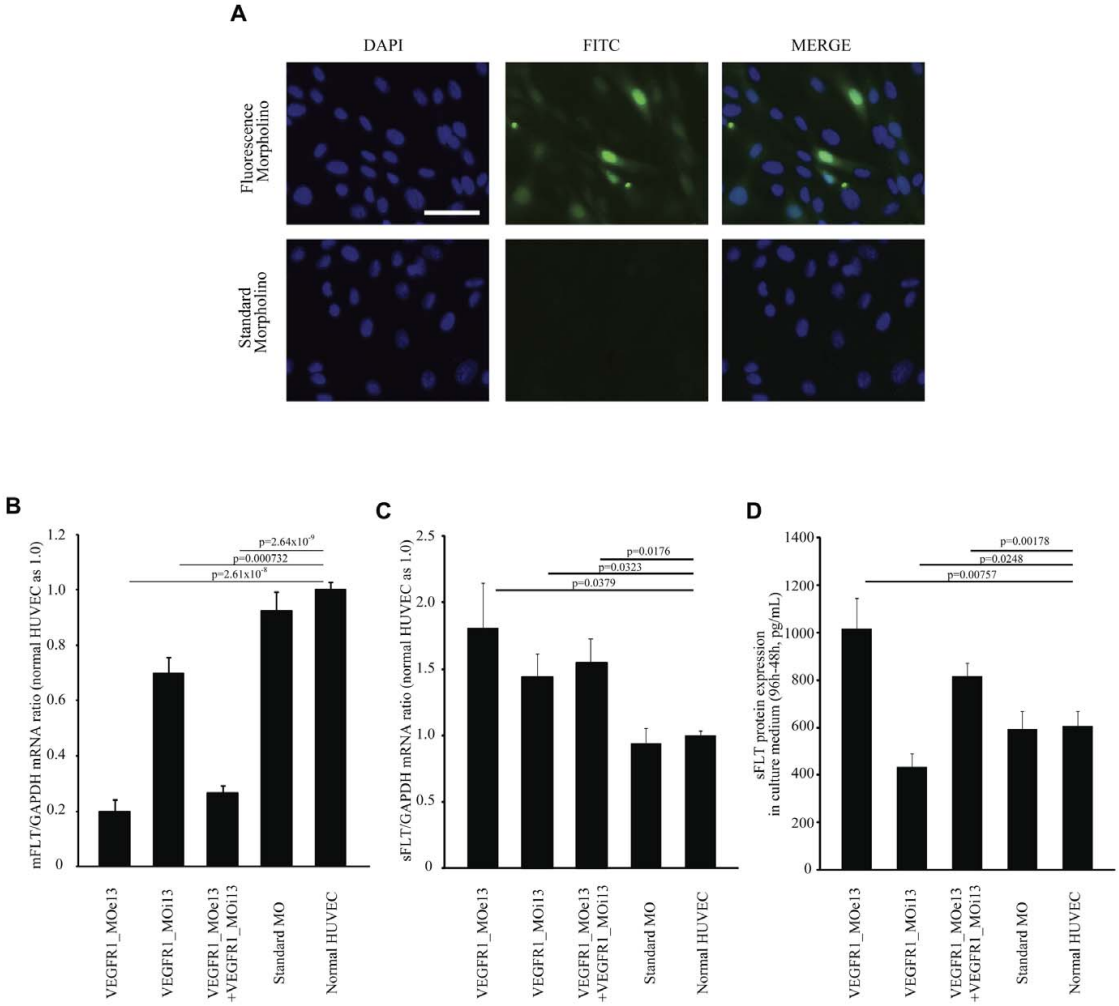

Figure 1. VEGFR1_MOe13 localizes to the nucleus and increases sFLT-1 expression in human endothelial vein cells (HUVEC). (a) Fluorescently tagged VEGFR1_MOe13 (F-MO) or standard morpholino (std-MO) were electroporated into HUVECs. After 48 hours fluorescence was assessed using light microscopy. Colocalization with DAPI staining represents nuclear localization of morpholino constructs. HUVECs were electroporated with VEGFR1_MOe13, VEGFR1_MOi13, a combination of VEGFR1_MOe13 and VEGFR1_MOi13, Standard_MO. All morpholino sequences were designed to target the human VEGFR1 transcript. (b) mbFLT-1 mRNA (n = 6) or (c) sFLT-1 mRNA expression (n = 6) were assessed using real time PCR. Values were normalized to GAPDH mRNA and normal HUVEC was used as 1.0. (d) sFLT protein expression in culture medium was determined by ELISA (n = 3). Data shows sFLT protein at 96 h – 48 h. Error bar is S.E.M. Each p-value was calculated by two-tail student's t-test against normal HUVEC.
doi:10.1371/journal.pone.0033576.g001

Thus, intra-vitreol injection of vivo-VEGFR1_MOe13 leads to increased levels of sFlt-1 and suppression of laser-induced CNV.

Short hairpin RNA-mediated sFlt-1 knock-down "rescues" the CNV phenotype *in vivo*

In order to demonstrate that the measured effect of reduced CNV following intra-vitreol injection of VEGFR1_MOe13 was specific for an increase in sFlt-1 expression, we knocked-down sFlt-1 expression AAV2_shsFlt encoding short hairpin RNA(shRNA) targeting sFlt-1 mRNA (unpublished data; [10]). Intra-vitreol injections were performed using PBS, AAV2_shNEG (non specific shRNA) or AAV2_shsFlt (shRNA targeting sFlt-1) and laser photocoagulation performed 2 weeks later. In a consistent fashion with prior studies, on day 1 and 4 following photocoagulation PBS, vivo-standard_MO or vivo-VEGFR1_MOe13 constructs were injected into pretreated eyes. We hypothesized that if increased sFlt-1 was sufficient for suppression of the laser-induced CNV phenotype, co-expression of AAV2_shRNA_sFlt would reverse this effect. In agreement with this hypothesis, we observed that pre-treatment with AAV2_shsFlt results in reversal of VEGFR1_MOe13-mediated CNV suppression (Fig. 4). Thus, increased soluble Flt-1 expression is sufficient to at least partially mediate CNV suppression in the setting of laser-induced injury.

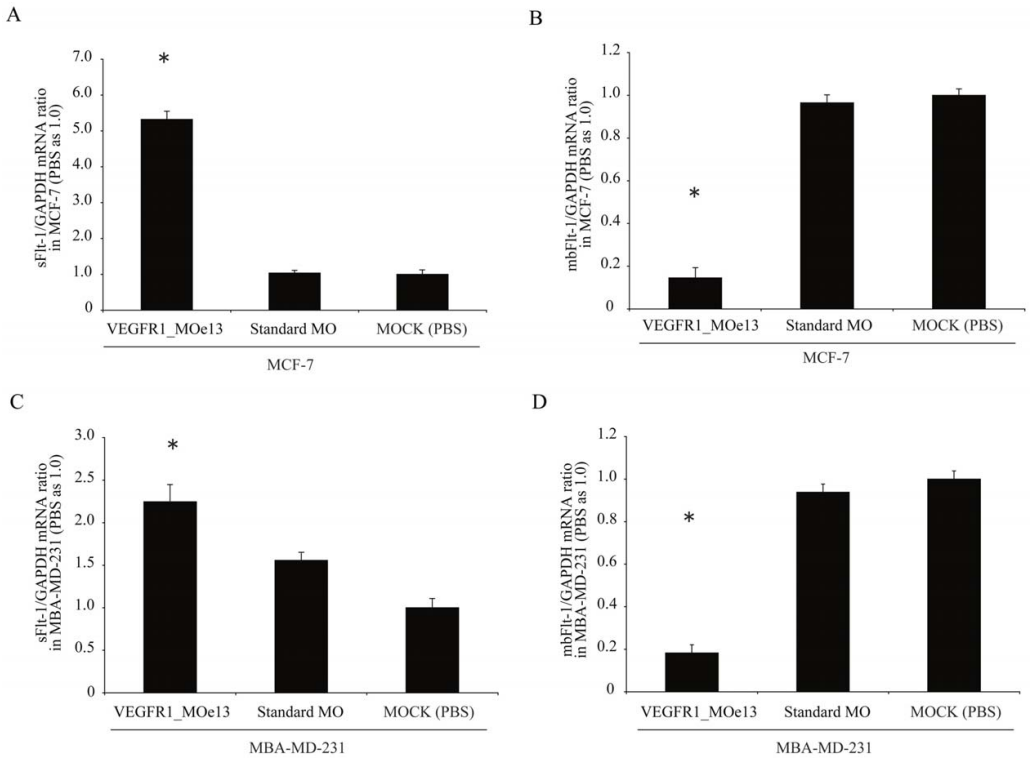

Figure 2. VEGFR1_MOe13 increases sFLT-1 and decreases mbFLT-1 mRNA in MCF-7 and MBA-MD-231 breast adenocarcinoma cell lines. MCF7 or MBA-MD-231 human breast adenocarcinoma cells were electroporated with VEGFR1_MOe13 and (a; c) sFLT-1 and (b; d) mbFLT-1 mRNA levels assessed at 72 hours using real time PCR (n = 3). Data were normalized to GAPDH mRNA levels and normal MCF7 or MBA-MD-231 cells were used a 1.0. *$p<0.01$.
doi:10.1371/journal.pone.0033576.g002

Treatment of established MBA-MD-231 human breast adenocarcinoma xenograft tumors with VEGFR1_MOe13 results in tumor regression

In order to demonstrate that anti-angiogenic activity of the VEGFR1_MOe13 construct is not limited to the ocular compartment, we sought to measure its efficacy in the setting of malignancy-associated neovascularization. Tumor vasculature is a rapidly emerging therapeutic target. As such, this model represents an attractive context in which to apply technologies designed to inhibit neovascularization. Within the context of malignancy, breast adenocarcinoma is known to demonstrate marked dependence on VEGF signaling for sustained neovascularization and growth [28–29]. In fact, VEGF inhibition has been shown to reduce tumor growth in both the experimental as well as the clinical setting [17,30]. We hypothesized that treatment of MBA-MD-231 human breast adenocarcinoma xenograft tumors with vivo-VEGFR1_MOe13 would result in increased levels of soluble Flt-1 and a subsequent decrease in neovascularization and tumor regression. To directly test this hypothesis, female nude mice were inoculated as described. Xenografts were permitted to grow for 14 days. Tumors were then directly injected with either murine vivo-VEGFR1_MOe13 or vivo-standard morpholino. Injections and tumor volume assessments were performed bi-weekly for a duration of 4 weeks. We found that treatment of xenograft tumors with vivo-VEGFR1_MOe13 led to tumor regression when compared with standard morpholino treatment ($p = 0.04$) (Fig. 5a). Furthermore, murine sFlt-1 mRNA transcript levels were increased and mbFlt-1 mRNA levels decreased in treatment tumors at the conclusion of the 4 week treatment period as compared with control tumors when assessed using real-time PCR (Fig. 5b–c). Finally, to determine whether vascular density was decreased in tumors treated with viv-VEGFR1_MOe13 injection, tumor vasculature was stained with GS-IB_4 and vessel density quantified using fluorescence microscopy following the 4 week treatment period. Tumors treated with the vivo-VEGFR1_MOe13 construct demonstrated a statistically significant decrease in vascular density (Fig. 5d). Interestingly, these results were achieved using VEGFR1_MOe13 targeting the murine Flt-1 transcript, while treatment with a VEGFR1_MOe13 construct targeting human FLT-1 did not demonstrate tumor regression *in vivo* (Figure S2). This may indicate that host vasculature is important for tumor growth,, suggesting that human sFLT-1 produced by tumor cells does not effectively inhibit murine VEGF signaling. However, analysis of the human and murine morpholino sequences demonstrates significant overlap between the murine morpholino construct with the human VEGFR1 sequence. The same is not true for the human morpholino with respect to the murine VEGFR1 mRNA sequence. Therefore, this cross-reactivity could account for our findings as could overall decreased efficacy of the human morpholino construct. The latter is unclear given the fact that *in vitro* this sequence increases soluble FLT-1 very effectively. Further studies are needed to fully understand this.

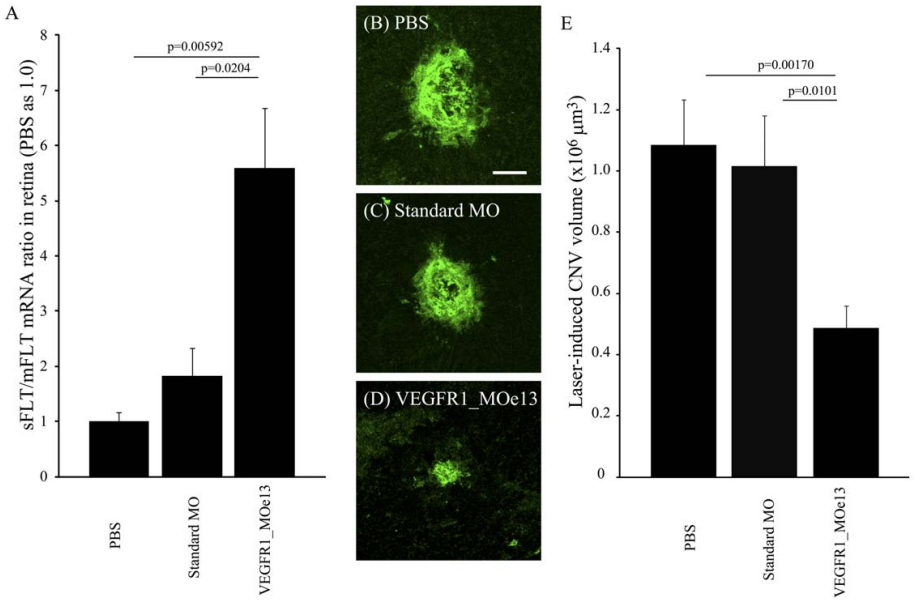

Figure 3. VEGFR1_MOe13 inhibits laser-induced CNV in vivo. a. sFlt/mFlt mRNA ratio in the retina treated with PBS, Standard_MO and VEGFR1_MOe13 (n = 4). Representative images of laser CNV injected with b PBS, c Standard_MO and d VEGFR1_MOe13 designed to target the murine VEGFR1 transcript. e The averages of laser CNV volumes (n = 11–14). Error bar is S.E.M. p-values were calculated by two-tail student's t test.
doi:10.1371/journal.pone.0033576.g003

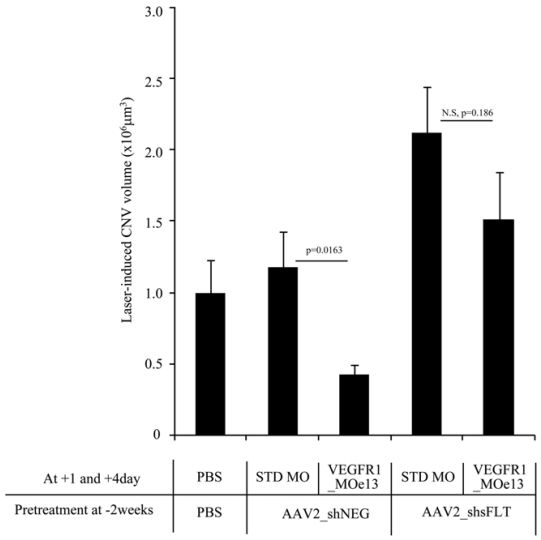

Figure 4. RNAi targeting sFlt-1 rescues the neovascular phenotype response to laser injury. Murine eyes were treated with PBS, AAV2_shNEG or AAV2_shsFLT. After 2 weeks, laser photocoagulation was performed. On 1 day and 4 day after photocoagulation, PBS Standard_MO or VEGFR1_MOe13 were injected. Error bar is S.E.M. N = 9–15.
doi:10.1371/journal.pone.0033576.g004

Discussion

Neovascularization is a common pathological process underpinning numerous disease states. Elucidation of key molecular mediators has allowed for the development of therapeutic strategies targeting the underlying molecular processes. Soluble Flt-1 first described in 1993, is an alternatively spliced form of the *Flt-1* gene [4–5]. The morpholino oligomer VEGFR1_MOe13 is designed to target the Flt-1 mRNA exon13-intron13; therefore, interaction between VEGFR1_MOe13 and VegfR1 pre-mRNA is predicted to influence the alternative splicing event such that production of soluble Flt-1 is promoted.

Herein we demonstrate that expression of VEGFR1_MOe13 both *in vitro* and *in vivo* results in elevated levels of soluble Flt-1 and decreased membrane bound Flt-1. Furthermore, these data show that VEGFR1_MOe13-mediated increase in soluble Flt-1 within the retina can prevent choroidal neovascularization following laser photocoagulation. Finally, our data indicate that this phenotype is attributable to increased sFlt-1 expression as co-treatment with sFlt-1-RNAi negates this effect. Thus, soluble Flt-1 expression is both necessary and sufficient for suppression of laser-induced CNV. Taken together these data indicate that modulation of soluble Flt-1 expression in the clinical setting has potential therapeutic value. This represents great promise when considering the over 7 million patients in the US alone with non-exudative age related macular degeneration (ARMD) currently "at risk" for development of CNV.

Angiogenesis in the form of aberrant neovascularization is fundamental to the pathophysiology of other disease states as well. Notably, new blood vessel formation is absolutely required for sustained solid tumor growth [7]. As noted, breast adenocarcinoma is dependent on sustained neovascularization both in animal and human studies [28–29]. As a "proof of principle" for broad

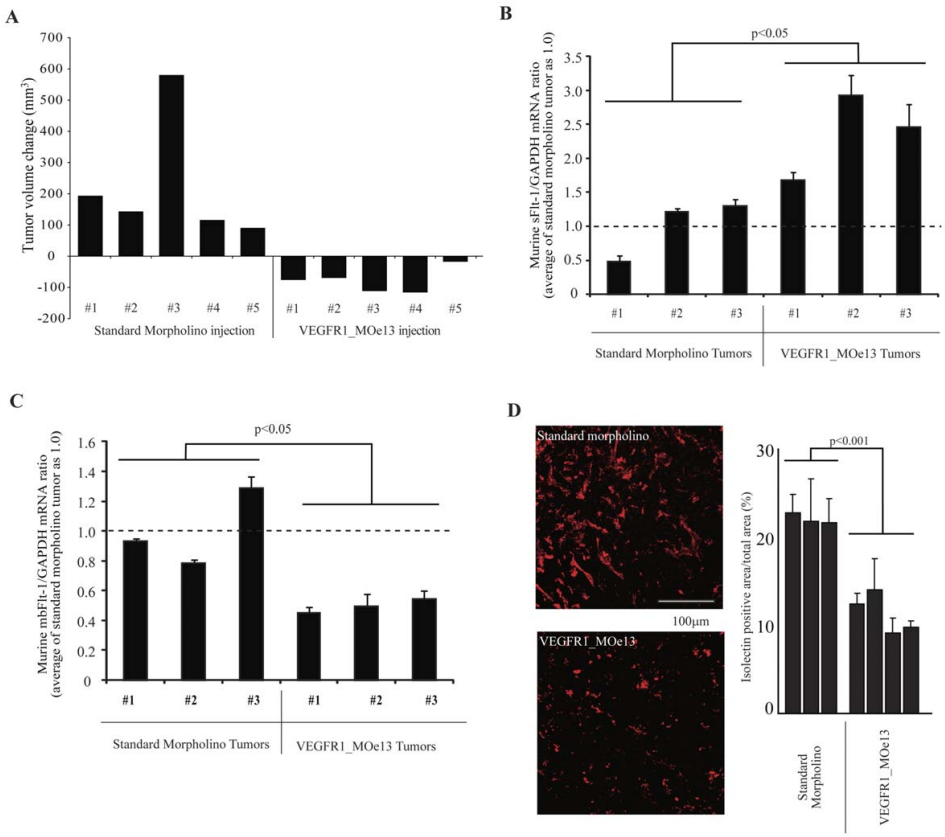

Figure 5. Intra-tumoral VEGFR1_MOe13 injection results in regression of established MBA-MD-231 human breast adenocarcinoma xenograft tumors and decreased tumor vascularity. a. MB-MDA-231 breast cancer cells were grown as xenografts in female nude mice for 2 weeks prior to beginning treatment with either a standard morpholino or VEGFR1_MOe13 designed to target the murine VEGFR1 transcript. Morpholino treated tumors demonstrate size regression after a 4 week treatment course as demonstrated by volume change analysis of 5 individual tumors within each treatment condition. p = 0.04 b–c. Following treatment course, RNA was extracted from xenograft tumors and soluble or membrane bound Flt1 levels were measured using real-time RT-PCR. Error bars indicate variation between individual PCR reactions per tumor sample. d. Following the treatment course, VEGFR1_MOe13 or standard morpholino xenograft tumors were sectioned and stained with isolectin as a measure of vascularity. Individual bars represent sections analyzed thoughout each tumor sample.
doi:10.1371/journal.pone.0033576.g005

applicability of morpholino-mediated Flt-1 modulation in the treatment of neovascular disease, we demonstrate that intra-tumoral injection of VEGFR1_MOe13 leads to increased intra-tumoral levels of sFlt-1 and decreased mbFlt-1.. Furthermore, breast adenocarcinoma xenografts expressing elevated levels of sFlt-1 demonstrate a blunted neovascular response and regress once established as compared with control tumors. Thus, modulation of soluble Flt-1 expression using morpholino technology represents a therapeutic tool with broad applicability across a spectrum of neovascular disease.

Taken together, these data indicate that morpholino expression is a viable tool for modulating the expression of FLT-1, i.e., the balance between membrane and soluble forms of this transcript. In our system, these data indicate that morpholino interference at the Flt-1 mRNA exon13-intron13 junction leads to the greatest amount of soluble FLT1 production. The VEGFR1_MOe13 construct is effective in two independent disease models, choroidal neovascularization and breast adenocarcinoma. In both, aberrant vasculature and disease burden are reduced. Given the highly divergent roles of FLT1 isoforms, morpholino oligos show promise in a variety of physiologic settings and disease states to act as an "exogenous switch" to modulate angiogenesis.

These data demonstrate the efficacy of morpholino technology to influence FLT-1 gene expression at the mRNA level both *in vitro* and *in vivo* setting. Recent application of splice-blocking morpholinos in the setting of DMD has demonstrated disease-modifying effects in both animal and human trials [18–20]. Therefore, these constructs hold promise as true "bench to bedside" tools. Within the setting of neovascularization, use of morpholino technology represents a shift from current therapies which are predominantly based on monoclonal antibody approaches. The evolving potential for morpholino technology to be targeted to areas of pathology following systemic administration may lend this technology to broader appeal and utility [31]. Additionally, combining morpholino-mediated sFLT-1 modulation with other known anti-angiogenic strategies is a promising area of investigation. For example,

morpholino-based inhibition of other angiogenic factors such as FGF and PDGF remains an interesting question, as these factors have been shown to promote intra-ocular neovascularization and inhibition shown to reduce neovascular pathology [32–34]. Furthermore, synergy between these pathways has been shown to promote tumor vascularity and metastasis in murine studies [35–36]. Therefore, steric inhibition of splice sites required for proper expression of these factors may represent yet another role for morpholino technology in the treatment of neovascular disease. Thus morpholino technology currently represents an effective mechanism for treatment of neovascular pathology across a spectrum of disease with high translational potential and exciting future applications.

Materials and Methods

Constructs and Reagents

In vivo morpholino constructs were designed to target murine intron/exon 13 junction of the FLT-1 transcript denoted VEGFR1_MOe13 and VEGFR1_MOi13. Constructs were chemically modified such that they would easily diffuse to access the intracellular compartment [27]. For use in xenograft assays, VEGFR1_MOe13 morpholino constructs were suspended in sterile PBS and used at a concentration of 400 ng/dose. Each dose is equal to 50 ul total volume. A standard morpholino targeting the murine beta-globin subunit2 was used as a control and prepared at the same concentration. Morpholino sequences are as follows.

Human VEGFR1_MOe13 GTTGCAGTGCTCACCTCT-GATTGTA

Human i13 GCTTCCTGATCTAGTGAAGAAAGAA

Mouse VEGFR1_MOe13 CTTTTTGCCGCAGTGCTCAC-CTCTA

STD MO CCTCTTACCTCAGTTACAATTTATA

AAV.shRNA.sFlt-1 was developed as previously described [11]. $2.5\times10^{\wedge}9$ GC of AAV.shRNA.sFlt-1 were injected per experimental condition.

Cell culture

Primary human umbilical vein endothelial cells (Lonza, Walkersville, MD, USA) were cultured in EBM with EGM SingleQuot Kit supplements and growth factors according to the manufacturer's instructions (Lonza, Walkersville, MD, USA). To prevent loss of endothelial cell properties, cell cultures were limited to passage number 4 to 7. MBA-MD-231 human breast adenocarcinoma cells were obtained from the laboratory of Dr. Bryan Welm MD at the Huntsman Cancer Institute, SLC, Utah and maintained in RPMI culture medium containing 10% FBS. MCF7 human breast adenocarcinoma cells were obtained for the laboratory of Dr. Alana Welm PhD at the Huntsman Cancer Institute, SLC, Utah and maintained per ATCC medium recommendations.

Morpholino delivery to cultured cells and total RNA extraction

10 ng of morpholinos were delivered to the nucleus by nucleofection (Amaxa, Gaithersburg, MD, USA) using a Basic Nucleofector Kit for Primary Mammalian Endothelial Cells (Amaxa, Gaithersburg, MD, USA), program A-034 for HUVEC. For one nucleofection, 1×106 cells were used and plated on a 6-well plate. After 2 days of culture, cells were trypsinized and total RNA was extracted using a RNeasy mini kit (Qiagen, Valencia, CA, USA)]. RNA concentrations were determined by 260 nm absorption measured with a spectrophotometer.

Complementary DNA synthesis and quantification with real-time PCR

Complementary DNA (cDNA) were synthesized from approximately 400 ng total RNA using an Omniscript RT kit (Qiagen, Valencia, CA, USA) and Oligo-dT primer (dT2) according to the manufacturer's instructions. Real-time PCR was performed using a QuantiTect SYBR Green PCR Kit (Qiagen, Valencia, CA, USA) and an aliquot 1:l of cDNA solution. The primer sequences used for human sequence real-time PCR were:

VEGFR1_F1: 5′-CTGCAAGATTCAGGCACCTA-3′

VEGFR1_R1: 5′- CCTTTTTGTTGCAGTGCTCA-3′

VEGFR1_F2: 5′-AACCAGAAGGGCTCTGTGGAAAGT-3′

VEGFR1_R2: 5′-CAAACTCCCACTTGCTGGCATCAT-3′

The combination of VEGFR1_F1 and R1 was designed to detect the soluble form of human VEGFR1. The combination of VEGFR1_F2 and R2 was designed to detect the membrane form of human VEGFR1 .

The primer sequences used for murine sequence real-time PCR were:

VEGFR1_F1: 5′ –AATGGCCACCACTCAAGATT

VEGFR1_R1: 5′ –TTGGAGATCCGAGAGAAAATG

VEGFR1 F2: 5′ –GATCAAGTTCCCCTGGATGA

VEGFR1_R2: 5′ –ATGCAGAGGCTTGAACGACT

Gapdh_F: 5′ –AACTTTGGCATTGTGGAAGGGCTC

Gapdh_R: 5′ -ACCAGTGGATGCAGGGATGATGTT

The combination of VEGFR1_F1 and R1 was designed to detect the soluble form of murine VEGFR1. The combination of VEGFR1_F2 and R2 was designed to detect the membrane form of murine VEGFR1 .

Real-time PCR conditions: 50°C for 2 minutes, 95°C for 10 minutes, followed by 40 cycles of 94°C for 15 seconds, 55°C for 30 seconds, and 72°C for 30 seconds.

Laser induced choroidal neovascularization

Laser photocoagulation (532 nm, 150 mV, 100 ms, 100 μm; NIDEK MC-4000) was performed on both eyes (2 to 5 spots per eye) as described [24–25]. After enucleating the eyes, sclera/choroid/RPE complex were fixed in 4% paraformaldehyde for 2 hours at 4°C. After blocking in 5% FBS/PBS with 0.02% tritonX-100 and 2 mM MgCl2, samples were stained with 5 μg/ml Alexa488 and Alexa546 conjugated isolectin GS-IB_4 (Invitrogen Corporation, Carlsbad, USA) overnight. After washing the samples were flat mounted on glass slides. CNV volume was measured by scanning laser confocal microscopy (Olympus America Inc., Center Valley, USA). These animal studies were performed under IACUC protocol approval number 09-03005 approved by the Committee on the Ethics of Animal Experiments at the University of Utah. All interventions were performed either under sodium pentobarbital anesthesia or after animals were humanely euthanized.

Xenograft analysis

3×10^6 MBA-MD-231 human breast adenocarcinoma cells were injected subcutaneously into the flanks of female nude mice. Following a standardized 2 week inoculation period, xenograft tumors were injected biweekly for a total duration of 4 weeks with VEGFR1_MOe13 or standard morpholino control. These constructs were prepared as detailed above. Tumor growth was assessed using digital calipers with bi-weekly measurements correlating with injection period. (Volume $mm^3 = width^2 \times length/2$. These animal studies were performed under IACUC protocol approval number 09-03005 approved by the Committee on the Ethics of Animal Experiments at the University of Utah. All

interventions were performed either under sodium pentobarbital anesthesia or after animals were humanely euthanized.

Immunohistochemical anlaysis

Tumors were fixed in 4% paraformaldehyde for 2 h at 4 C, cryoprotected in 15% sucrose and 30% sucrose, and then embedded in OCT (Tissue-Tek, USA). Sections (12 um) were cut and were incubated with isolectin (Griffonia simplicifolia, Alexa Fluo568 conjugate 1:1000, Invitrogen Corporation, Carlsbad, CA) overnight. Immunohistochemistry results were examined using scanning laser confocal microscopy (Olympus, FLUOVIEW, FV1000, 20×). These images were scored by Image-J morphometry system using biometry scoring (Wayne Rasband).

After electroporation of F-MO(10 ul of 1 mM) or STD MO into HUVECs, the cells were plated to 8 well glass slide (nunc, Rochester, NY) coated with collagen. 24 hours later, the cells were fixed with 4% parafolmaldehyde/PBS, stained with DAPI, and observed with the Zeiss Axiovert 200 inverted fluorescence microscope.

Statistical analysis

Data are presented as mean +/−SEM. Statistical analysis was performed using student T test. A p-value 0.05 was considered significant.

Supporting Information

Figure S1 The Soluble/Membrane FLT-1 ratio increases following electroporation of VEGFR1_MOe13 into HUVEC. HUVECs were electroporated with VEGFR1_MOe13, VEGFR1_MOi13, a combination of VEGFR1_MOe13 and VEGFR1_MOi13, Standard_MO. All morpholino sequences were designed to target the human VEGFR1 transcript. mbFLT-1 mRNA and sFLT-1 mRNA expression were assessed using real time PCR. Values were normalized to GAPDH mRNA and normal HUVEC was used as 1.0.
(TIF)

Figure S2 Intra-tumoral injection of VEGFR1_MOe13 targeting human FLT-1 does not induce xenograft tumor regression. MB-MDA-231 breast cancer cells were grown as xenografts in female nude mice for 2 weeks prior to beginning intra-tumoral injection treatment with either a standard morpholino or VEGFR1_MOe13 morpholino targeting the human FLT-1 transcript. Change in tumor volume was assessed following a 4 week treatment course. $p = 0.3$
(TIF)

Acknowledgments

We would like to thank Dr. A. Welm and Dr. B. Welm for their generous supply of the MCF7 and MBA-MD-231 human breast adenocarcinoma cell lines.

Author Contributions

Conceived and designed the experiments: LAO HU BKA. Performed the experiments: LAO HU WH JC JS. Analyzed the data: LAO HU BKA. Contributed reagents/materials/analysis tools: LAO HU BKA. Wrote the paper: LAO BKA.

References

1. Rosenfeld PJ, Brown DM, Heier JS, Boyer DS, Kaiser PK, et al. (2006) Ranibizumab for neovascular age-related macular degeneration. N Engl J Med 355: 1419–1431.
2. Green WR, Wilson DJ (1986) Choroidal neovascularization. Ophthalmology 93: 1169–1176.
3. Penfold PL, Madigan MC, Gillies MC, Provis JM (2001) Immunological and aetiological aspects of macular degeneration. Prog Retin Eye Res 20: 385–414.
4. Bressler NM (2004) Age-related macular degeneration is the leading cause of blindness… J Am Med Assoc 291: 1900–1901.
5. Aiello LP, Pierce EA, Foley ED, Takagi H, Chen H, et al. (1995) Suppression of retinal neovascularization in vivo by inhibition of vascular endothelial growth factor (VEGF) using soluble VEGF-receptor chimeric proteins. Proc Natl Acad Sci U S A 92: 10457–10461.
6. Ozaki H, Hayashi H, Vinores SA, Moromizato Y, Campochiaro PA, Oshima K (1997) Intraviteral sustained release of VEGF causes retinal neovascularizaiton in rabbits and breakdown of the blood retinal barrier in rabbits and primates. Exp Eye Res 64: 505–517.
7. Folkman J (1972) Anti-angiogenesis: new concept for therapy of solid tumors. Ann Surg 175(3): 409–416.
8. Kendall RL, Thomas KA (1993) Inhibition of vascular endothelial cell growth factor activity by an endogenously encoded soluble receptor. Proc Natl Acad Sci USA 90(10): 705–10.
9. Tolentino MJ, McLeod DS, Taomoto M, Otsuji T, Adamis AP, Lutty GA (2002) Pathologic features of vascular endothelial growth factor induced retinopathy in the nonhuman primate. Am J Ophthalmol 133: 373–385.
10. Ambati BK, Nozaki M, Singh N, Takeda A, Jani PD, et al. (2006) Corneal avascularity is due to soluble VEGF receptor-1. Nature 443: 993–997.
11. Lukason M, DuFresne E, Rubin H, Pechan P, Li Q, et al. (2011) Inhibition of choroidal neovascularization in a nonhuman primate model by intravitreal administration of an AAV2 vector expression a novel anti-VEGF molecule. Mol Ther 19(2): 260–5.
12. Lai CM, Shen WY, Brankov M, Lai YK, Barnett NL, et al. (2005) Long-Term Evaluation of AAV-Mediated sFlt-1 Gene Therapy for Ocular Neovascularization in Mice and Monkeys. Mol Ther 12(4): 659–668.
13. Macular Photocoagulation Study Group (1991) Argon laser photocoagulation for neovascular maculopathy Five year results from randomized clinical trials. Arch Ophthalmol 109: 1109–1114.
14. La Cour M, Kiilgaard JF, Nissen MH (2002) Age-related macular degeneration: epidemiology and optimal treatment. Drugs Aging 19: 101–133.
15. Elkin M, Orgel A, Kleinman HK (2004) An angiogenic switch in breast cancer involves estrogen and soluble vascular endothelial growth factor receptor 1. J Natl Cancer Inst 96(11): 875–8.
16. Brown DM, Kaiser PK, Michels M, Soubrane G, Heier JS, et al. (2006) Ranibizumab versus verteporfin for neovascular ae-related macular degeneration. N Engl J Med 355: 1432–1444.
17. Miles DW, Chan A, Dirix LY, Cortés J, Pivot X, et al. (2010) Phase III study of bevacizumab plus docetaxel compared with placebo plus docetaxel for the first-line treatment of human epidermal growth factor receptor 2-negative metastatic breast cancer. J Clin Oncol 28(20): 3239–47.
18. Sazani P, Weller DL, Shrewsbury SB (2010) Safety pharmacology and genotoxicity evaluation of AVI-4658. Int J Toxicol 29(2): 143–56.
19. Kinali M, Arechavala-Gomeza V, Feng L, Cirak S, Hunt D, et al. (2009) Local restoration of dystropin expression with the morpholino oligomer AVI-4658 in Duchenne muscular dystrophy: a single blind, placebo-controlled, dose escalation, proof-of-concept study. Lancet Neurol 8(10): 918–928.
20. Yin H, Moulton HM, Betts C, Merritt T, Seow Y, et al. (2010) Functional rescue of dystrophin-deficient mdx mice by a chimeric peptide-PMO. Mol Ther 18(10): 1822–1829.
21. Hasumi Y, Mizukami H, Urabe M, Kohno T, Takeuchi K, et al. (2002) Soluble FLT-1 expression suppresses carcinomatous ascites in nude mice bearing ovarian cancer. Cancer Res 62(7): 2019–23.
22. Ruffini F, Failla CM, Orecchia A, Bani MR, Dorio AS, et al. (2011) Expression of the soluble vascular endothelial growth factor receptor-1 in cutaneous melanoma: role in tumour progression. Br J Dermatol 164(5): 1061–70.
23. Bertin S, Mohsen-Kanson T, Baqué P, Gavelli A, Momier D, et al. (2010) Tumor microenvironment modifications induced by soluble VEGF receptor expression in a rat liver metastasis model. Cancer Lett 298(2): 264–72.
24. Kishuku M, Nishioka Y, Abe S, Kishi J, Ogino H, et al. (2009) Expression of soluble vascular endothelial growth factor receptor-1 in human monocyte-derived mature dendritic cells contributes to their antiangiogenic property. J Immunol 183(12): 8176–85.
25. Miller H, Miller B, Ishibashi T, Ryan SJ (1990) Pathogenesis of laser-induced choroidal subretinal neovascularization. Invest Ophthalmol Vis Sci 31(5): 899–908.
26. Krzystolik MG, Afshari MA, Adamis AP, Gaudreault J, Gragoudas ES (2002) Prevention of experimental choroidal neovascularization with intravitreal anti-vascular endothelial growth factor antibody fragment. Arch Ophthalmol 120(3): 338–46.
27. Morcos PA, Li Y, Jiang S (2008) Vivo-Morpholinos: A non-peptide transporter delivers morpholinos into a wide array of mouse tissues. Bio Techniques 45: 613–623.
28. Nieto Y, Woods J, Nawaz F, Baron A, Jones RB, et al. (2007) Prognostic analysis of tumour angiogenesis, determined by microvessel density and expression of vascular endothelial growth factor, in high-risk primary breast cancer patients treated with high-dose chemotherapy. Br J Cancer 97: 391–397.

29. Gasparini G (2000) Prognostic Value of Vascular Endothelial Growth Factor in Breast Cancer. Oncologist 5: 37–44.
30. Giovannini M, Aldrighetti D, Zucchinelli P, Belli C, Villa E (2010) Antiangiogenic strategies in breast cancer management. Crit Rev Oncol Hematol 76(1): 13–35.
31. Alter J, Lou F, Rabinowitz A, Yin H, Rosenfeld J, et al. (2006) Systemic delivery of morpholino oligonucleotide restores dystrophin expression bodywide and improves dystrophic pathology. Nature Medicine 12(2): 175–7.
32. Wong CG, Rich KA, Liaw LH, Hsu HT, Berns MW (2001) Intravitreal VEGF and bFGF produce florid retinal neovascularization and hemorrhage in the rabbit. Curr Eye Res 22(2): 140–147.
33. Abdel-Rahman MH, Yang Y, Salem MM, Meadows S, Massengill JB, et al. (2010) Investigation of the potential utility of a linomide analogue of treatment of choroidal neovascularization. Exp Eye Res 91(6): 837–843.
34. Hou X, Kumar A, Lee C, Wang B, Arjunan P, et al. (2010) PDGF-CC blockade inhibits pathological angiogenesis by acting on multiple cellular and molecular targets. Proc Natl Acad Sci U S A107(27): 12216–12221.
35. Cao Y, Cao R, Hedlund EM (2008) Regulation of tumor angiogenesis and metastasis by FGF and PDGF signaling pathways. J Mol Med Jul86(7): 785–89.
36. Nissen LJ, Cao R, Hedlund EM, Wang Z, Zhao X, et al. (2007) Angiogenic factors FGF2 and PDGFBB synergistically promote murine tumor neovascularization and metastasis. J Clin Invest 117(10): 2766–77.

CHAPTER 6

CONCLUDING REMARKS AND FUTURE DIRECTIONS

Diabetic retinopathy poses a significant challenge as the world experiences greater rates of diabetes. Current treatment options are helpful at slowing down the progression of retinopathy but do not stop or reverse its course (Campochiaro, Wykoff, Shapiro, Rubio, & Ehrlich, 2014). It is imperative that future therapeutics take advantage of the learned pathophysiology to harness parallel pathways and remedy this disease. The angiopoietin-Tie2 pathway is ripe for utilization and COMP-Ang1 is placed in the envious position of restoring homeostatic signaling DR (Lee et al., 2013).

One of the first attempts at understanding DR was conducted by Cunha-Vaz four decades ago by focusing on whether the retina also enjoys the same privilege of a blood-brain-barrier afforded to the brain and whether retinal diseases altered barrier function (Cunha-Vaz, 1966). Blood retinal barrier dysfunction was found to be a root cause of DR, which helped lead to the search for vascular permeability factors. Judah Folkman and Napoleon Ferrara helped usher in the modern era of anti-angiogenesis by discovering the hypothesized master angiogenic switch VEGF, also described as vascular permeability factor (Adamis et al., 1994; Leung, Cachianes, Kuang, Goeddel, & Ferrara, 1989). While their goal may have been directed at cancer therapy, anti-VEGF agents have played perhaps their most successful role in eye diseases including diabetic retinopathy.

Tony Adamis helped push the newly discovered anti-VEGF therapies toward treating vascular diseases of the eye. Realizing that increased VEGF was merely a downstream effect due to vascular dysfunction, Adamis and colleagues tested the idea restoration of deficient Ang1 signaling could ameliorate some of the effects of DR (Joussen et al., 2002). However, progress was stalled as utilization of Ang1 proved to be too difficult for therapeutic use. Importantly, the critical role of leukocyte-mediated

damage in the diabetic retina was discovered and recognized as an important therapeutic target in DR (Adamis et al., 2001; Joussen et al., 2004).

Despite the development of treatments for DR, revitalizing the dying retinal vasculature has remained an unrealized goal. Endothelial progenitor cell (EPC) therapy represents an exciting avenue to replenish damaged capillaries in diabetic retinopathy. However, circulating endothelial progenitor cells are damaged in diabetic patients, requiring either a treatment that can restore endogenous EPC function or transplantation of nondiabetic EPCs into patients with retinopathy (Afzal et al., 2007; Bhatwadekar, Shaw, & Grant, 2010). Alan Stitt's group has developed a reliable way to harvest true EPCs called endothelial colony-forming cells (ECFCs), which have very low MHC expression, resulting in low immunogenicity that could work to its advantage in treating patients with DR (Medina, O'Neill, Humphreys, Gardiner, & Stitt, 2010a; Medina et al., 2010b; Stitt et al., 2011).

Additionally, gene therapy continues to gain traction in treating retinal disease (Al-Saikhan, 2013). The eye is uniquely situated among organs to be amenable to gene therapy in so much as it is relatively isolated from the rest of the body. Jean Bennett has been at the forefront in advancing gene therapy, and in particular AAV-mediated therapy of inherited retinal diseases (Bennett et al., 2012). Thanks to the pioneering work with congenital retinal degeneration, AAV is gaining acceptance as a safe and effective therapy (Maclachlan et al., 2011). We have been able to harness this knowledge and apply it to a chronic, noninherited disease. Combining gene therapy with therapeutics for chronic diseases, like diabetic retinopathy, will ease future burdens for both patients and providers by decreasing the amount of office visits and intraocular injections.

This project was a synthesis of the previous attempts to restore homeostasis in the diabetic retina. By utilizing COMP-Ang1, we have built on the work done by Adamis, which stalled due to inability of Ang1 to be used in therapeutic doses. We have treated a chronic disease whose pathology is influenced by deficient Ang1 signaling with a viral vector usually reserved for inherited genetic disorders. Lastly, we have shown that COMP-Ang1 enhances the abilities of ECFCs to incorporate into the diabetic retina, getting closer to the elusive goal of capillary revitalization.

Improvements in this study, like every study, are needed to take this therapy to the clinic. Currently, we rely on mouse models of diabetes, which are limited in their ability to recapitulate advanced forms of the disease. While they do a remarkable job of imitating the early forms of diabetic retinopathy (as demonstrated in our data), they leave much to be desired in a model of proliferative retinopathy (Barber et al., 2005). This could be attributed to the duration required by diabetes to lead to severe pathology and that current animal models simply do not live long enough to develop the neovascular forms of the disease. Additionally, perhaps an as yet undiscovered physiological pathway is activated in humans as opposed to animals with diabetes. We have yet to address the important issue of turning off AAV2 gene therapy. While constitutive COMP-Ang1 is important for normal retinal homeostasis, we would ultimately like to have control of the AAV-product should the need arise to decrease the dose. These barriers will have to be addressed before this therapy is moved to the clinic.

This project represents a translatable therapeutic approach restoring a lost trophic factor, preserving remaining endothelial cells, and preventing neuronal dysfunction. Most excitingly, reversal of endothelial damage could be possible with a combination of

COMP-Ang1 and ECFCs. Future directions could look towards the effectiveness of COMP-Ang1 combined with current therapies (anti-VEGF, laser photocoagulation, and steroids) and experimental therapies (anti-Ang2, VE-PTP inhibitors) (Quaggin, 2012). Furthermore, future directions could help clarify the mechanisms by which COMP-Ang1 exerts its effects in the retina (lowering oxidative stress, mechanisms of decreasing VEGF).

6.1 References

Adamis, A. P., Joussen, A. M., Murata, T., Tsujikawa, A., Kirchhof, B., & Bursell, S. E. (2001). Leukocyte-mediated endothelial cell injury and death in the diabetic retina. *The American Journal of Pathology*, *158*(1), 147–152. doi:10.1016/S0002-9440(10)63952-1

Adamis, A. P., Miller, J. W., Bernal, M. T., D'Amico, D. J., Folkman, J., Yeo, T. K., & Yeo, K. T. (1994). Increased vascular endothelial growth factor levels in the vitreous of eyes with proliferative diabetic retinopathy. *American Journal of Ophthalmology*, *118*(4), 445–450.

Afzal, A., Caballero, S., Sengupta, N., Chang, K.-H., Li Calzi, S., Guberski, D. L., et al. (2007). Ischemic vascular damage can be repaired by healthy, but not diabetic, endothelial progenitor cells. *Diabetes*, *56*(4), 960–967. doi:10.2337/db06-1254

Al-Saikhan, F. I. (2013). The gene therapy revolution in ophthalmology. *Saudi Journal of Ophthalmology: Official Journal of the Saudi Ophthalmological Society*, *27*(2), 107–111. doi:10.1016/j.sjopt.2013.02.001

Barber, A. J., Antonetti, D. A., Kern, T. S., Reiter, C. E. N., Soans, R. S., Krady, J. K., et al. (2005). The Ins2Akita mouse as a model of early retinal complications in diabetes. *Investigative Ophthalmology & Visual Science*, *46*(6), 2210–2218. doi:10.1167/iovs.04-1340

Bennett, J., Ashtari, M., Wellman, J., Marshall, K. A., Cyckowski, L. L., Chung, D. C., et al. (2012). AAV2 gene therapy readministration in three adults with congenital blindness. *Science Translational Medicine*, *4*(120), 120ra15–120ra15. doi:10.1126/scitranslmed.3002865

Bhatwadekar, A. D., Shaw, L. C., & Grant, M. B. (2010). Promise of endothelial progenitor cell for treatment of diabetic retinopathy. *Expert Review of Endocrinology*

& Metabolism, *5*(1), 29–37. doi:10.1586/eem.09.75

Campochiaro, P. A., Wykoff, C. C., Shapiro, H., Rubio, R. G., & Ehrlich, J. S. (2014). Neutralization of vascular endothelial growth factor slows progression of retinal nonperfusion in patients with diabetic macular edema. *Ophthalmology*. doi:10.1016/j.ophtha.2014.03.021

Cunha-Vaz, J. G. (1966). Studies on the permeability of the blood-retinal barrier. II. Breakdown of the blood-retinal barrier by injury. *The British Journal of Ophthalmology*, *50*(8), 454–462.

Joussen, A. M., Poulaki, V., Le, M. L., Koizumi, K., Esser, C., Janicki, H., et al. (2004). A central role for inflammation in the pathogenesis of diabetic retinopathy. *The FASEB Journal*, *18*(12), 1450–1452. doi:10.1096/fj.03-1476fje

Joussen, A. M., Poulaki, V., Tsujikawa, A., Qin, W., Qaum, T., Xu, Q., et al. (2002). Suppression of diabetic retinopathy with angiopoietin-1. *The American Journal of Pathology*, *160*(5), 1683–1693. doi:10.1016/S0002-9440(10)61115-7

Lee, J., Kim, K. E., Choi, D.-K., Jang, J. Y., Jung, J.-J., Kiyonari, H., et al. (2013). Angiopoietin-1 guides directional angiogenesis through integrin αvβ5 signaling for recovery of ischemic retinopathy. *Science Translational Medicine*, *5*(203), 203ra127–203ra127. doi:10.1126/scitranslmed.3006666

Leung, D. W., Cachianes, G., Kuang, W. J., Goeddel, D. V., & Ferrara, N. (1989). Vascular endothelial growth factor is a secreted angiogenic mitogen. *Science (New York, N.Y.)*, *246*(4935), 1306–1309.

Maclachlan, T. K., Lukason, M., Collins, M., Munger, R., Isenberger, E., Rogers, C., et al. (2011). Preclinical safety evaluation of AAV2-sFLT01- a gene therapy for age-related macular degeneration. *Molecular Therapy: The Journal of the American Society of Gene Therapy*, *19*(2), 326–334. doi:10.1038/mt.2010.258

Medina, R. J., O'Neill, C. L., Humphreys, M. W., Gardiner, T. A., & Stitt, A. W. (2010a). Outgrowth endothelial cells: Characterization and their potential for reversing ischemic retinopathy. *Investigative Ophthalmology & Visual Science*, *51*(11), 5906–5913. doi:10.1167/iovs.09-4951

Medina, R. J., O'Neill, C. L., Sweeney, M., Guduric-Fuchs, J., Gardiner, T. A., Simpson, D. A., & Stitt, A. W. (2010b). Molecular analysis of endothelial progenitor cell (EPC) subtypes reveals two distinct cell populations with different identities. *BMC Medical Genomics*, *3*, 18. doi:10.1186/1755-8794-3-18

Quaggin, S. E. (2012). Turning a blind eye to anti-VEGF toxicities. *The Journal of Clinical Investigation*, *122*(11), 3849–3851. doi:10.1172/JCI65509

Stitt, A. W., O'Neill, C. L., O'Doherty, M. T., Archer, D. B., Gardiner, T. A., & Medina, R. J. (2011). Vascular stem cells and ischaemic retinopathies. *Progress in Retinal and Eye Research*, *30*(3), 149–166. doi:10.1016/j.preteyeres.2011.02.001

APPENDIX

COMP-ANG1 IN THE PROTECTION AGAINST CENTRAL RETINAL ARTERY OCCLUSION

The following material represents preliminary data collected and presented as a grant. The data gathered show the effectiveness of COMP-Ang1 treating a chronic retinal ischemia (diabetic retinopathy) and invited us to attempt to treat a currently untreatable form of acute retinal ischemia, central retinal artery occlusion. While development of these studies is still ongoing, I have laid important groundwork and proof-of-concept studies for the next graduate student to take on.

A.1 General background

Central retinal artery occlusion (CRAO) is the ocular correlate of stroke and heart attack (Suri, Nasar, Hussein, Divani, & Qureshi, 2007); however, no therapy has proven beneficial and improvement is extremely rare (Atebara, Brown, & Cater, 1995). Hence, potential neuroprotective or neuroregenerative therapies an unmet medical need.

The nervous and vascular systems develop in synchrony and share many receptors and signaling cascades in common, e.g., VEGF/VEGFR2 (Chen, Fu, Tung, & Ward, 2009; Jones & Li, 2007). Angiopoietins represent another family of growth factors that may mediate effects in both vascular and nervous systems (Zacchigna, Ruiz de Almodovar, & Carmeliet, 2008). Angiopoietin 1 (Ang1) is a pericyte-derived growth factor that increases blood vessel stabilization and survival via the Tie2 receptor (Ward & Lamanna, 2004). Moreover, Ang1 has neuroprotective effects (Papapetropoulos et al., 1999), and can act on neuronal cells independent of Tie2, primarily via β-1 integrin (Dallabrida, Ismail, Oberle, Himes, & Rupnick, 2005; Valable et al., 2003). COMP-Ang1 (a more soluble and potent recombinant form of Ang1) was shown to improve neurological deficits and increase number of endogenous neuronal progenitor cells (NPCs) in a rat model of cerebral stroke (Shin et al., 2010).

The neuroregenerative potential of the retina may lie with the Muller glia, whose position spanning all retinal layers has posited them as a target for healing potential within the retina. Certain subsets of Muller glia have been shown to undergo neurogenic changes when the retina is damaged (Chen et al., 2009). Muller glia in mice can even respond to damage by re-entering the cell cycle, expressing key neural progenitor markers, and producing new neurons (Karl et al., 2008).

Our central hypothesis is that COMP-Ang1 promotes neuronal survival in CRAO by 1) neuroprotection, or 2) neuroregeneration**.** This proposal will determine whether COMP-Ang1 promotes retinal ganglion cell survival through β-1 integrin and/or has the capacity to induce Muller glial neurogenesis. Our preliminary data demonstrate a role for COMP-Ang1 in neuroprotection via increasing neuroglobin in a β-1 integrin dependent manner and neuroregeneration by increasing neural progenitor markers in Muller glia after CRAO.

This project explores the potential mechanisms of adult retinal neuroprotection, neurogenesis, and the interplay between vascular signaling molecules and neurogenesis. This project will open a new avenue into retinal preserving-therapies.

While CRAO affects only a small population, exploring the field of retinal neurogenesis has the potential to reverse millions of cases of blindness including glaucoma, diabetic retinopathy, retinitis pigmentosa, with further implication in the CNS.

A.2 Preliminary data

C57/Bl6 mice were pretreated with intravitreal injection of adeno-associated virus serotype 2 (AAV2) that expressed either COMP-Ang1 or control (GFP). Three weeks after initial pretreatment CRAO was induced in after Rose Bengal tail vein injection and excitation with laser. Confirmation of occlusion was done with fluorescein angiography (Figure A.1a). Inner retinal cell layer loss was found three weeks after CRAO, but was prevented with COMP-Ang1 (Figure A.1b). In the COMP-Ang1 pretreated retinas, not only was histology preserved, but ganglion cell marker TuJ1 and progenitor marker Sox2 was increased (Figure A.2a,b). In addition to structural preservation, mice pretreated with

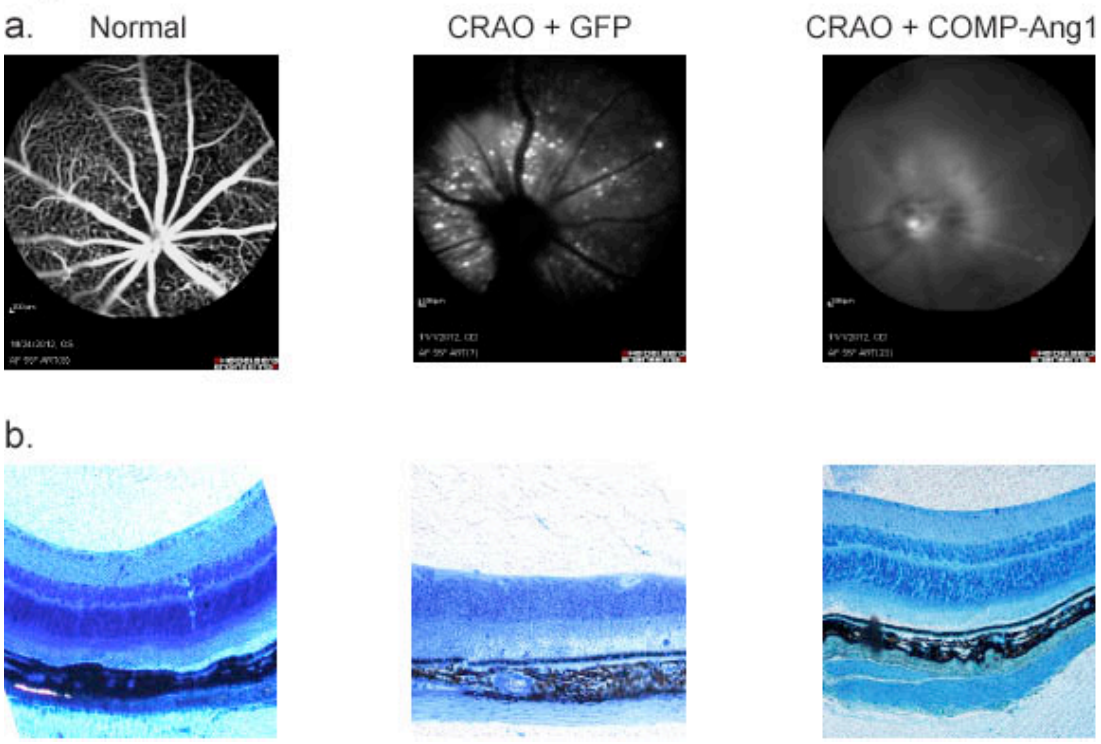

Figure A.1. Fluorescein angiography confirms presence of CRAO two hours after laser treatment (**a**). Histology confirms loss of inner retinal layers in the AAV2.GFP pretreated mice, which was prevented with AAV2.COMP-Ang1 (**b**).

COMP-Ang1 recovered visual acuity and electrical responsiveness better than control treated mice (Figure A.3a,b).

To determine whether COMP-Ang1 could serve a protective role *after* CRAO, mice expressing TdTomato in the muller glia were given CRAO followed by intravitreal injection of COMP-Ang1 protein (as opposed to pretreatment with AAV2.COMP-Ang1 before CRAO). These mice experienced increased neural progenitor markers (MCM6), markers colabeled with Muller glia, expressing TdTomato and increased proliferative markers (PCNA) in cells co-labeled with Sox2 compared to PBS treatment (Figure A.4). These preliminary data invite further investigation into the role of COMP-Ang1 after

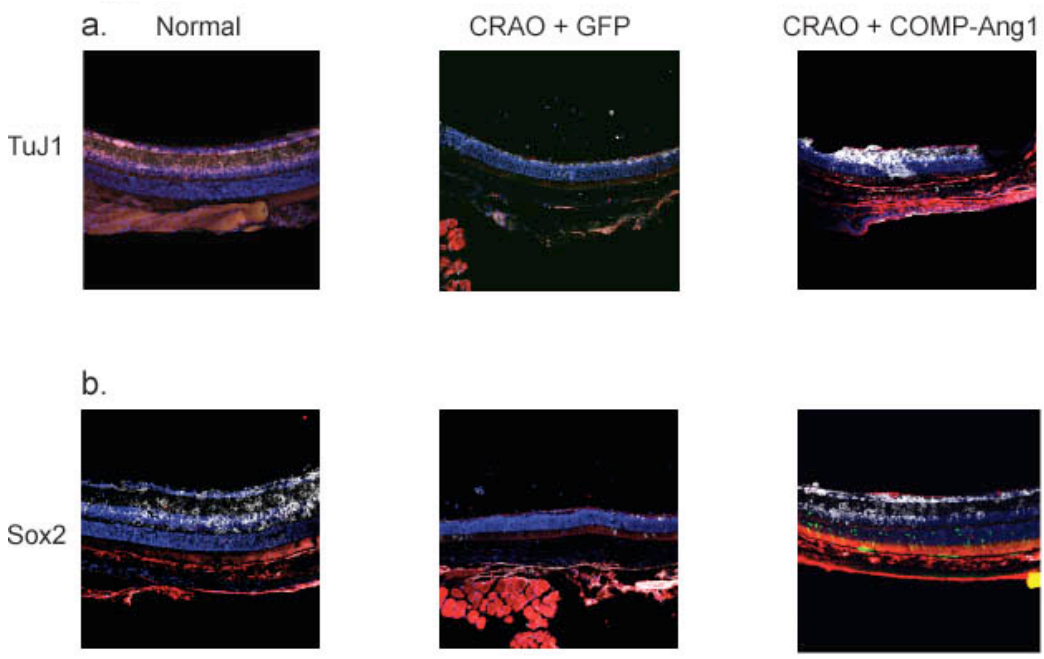

Figure A.2 Retinal cross sections taken three weeks after CRAO show COMP-Ang1 preserved the ganglion cell marker TuJ1, white (a) and neural progenitor marker Sox2, white (b).

CRAO. COMP-Ang1 increases neuroglobin in cell culture and mouse retina (Figure A.5a). The protective effects of COMP-Ang1 on a neuronal cell culture were dependent on beta-1 integrin (Figure A.5b).

A.3 Experimental design

Our preliminary experiments show that retinal neuronal structure and visual function are preserved by COMP-Ang1 therapy for CRAO. Retinal ganglion cells do not express Tie2 but do express beta-1 integrin, a pathway for direct neuroprotective effects.

We treated W3 and BD-RGC mice, which express YFP in distinct subsets of retinal ganglion cells, with an intravitreal injections of COMP-Ang1 protein (angiopoietin-1 and PBS will serve as controls) two hours and one week after CRAO and

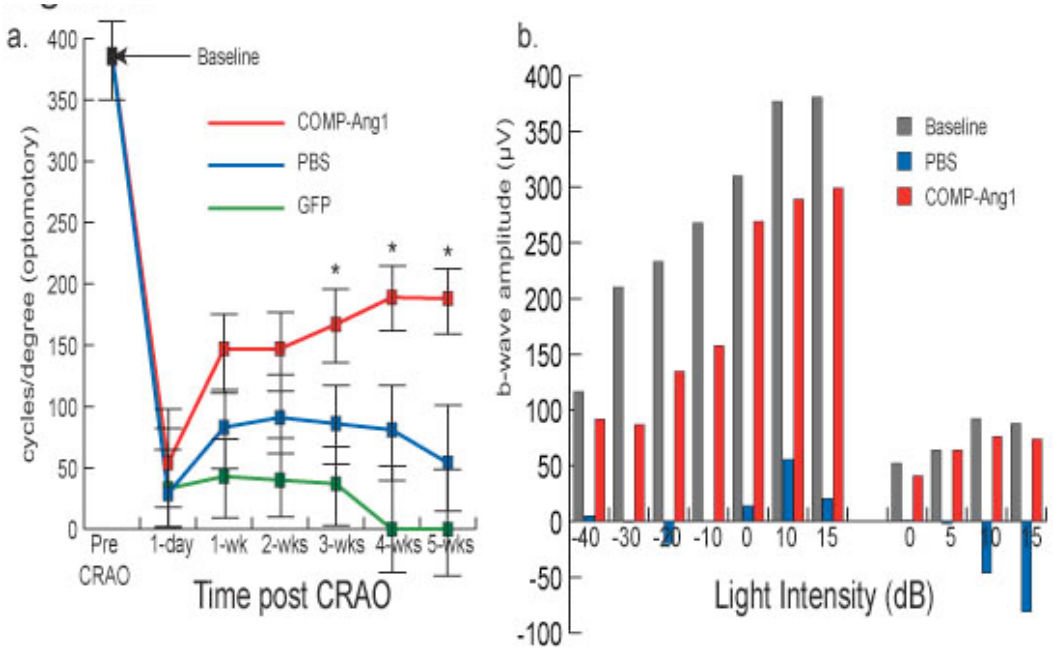

Figure A.3 Functional data showing COMP-Ang1 protects against prolonged visual tracking impairment (a) and ERG (b).

tracked mice over three weeks. We measured the following indices relative to control:

1. *Retinal ganglion cell survival*: We tracked YFP signal from RGCs before, and at day 0, 1, 3, 7, and 21 after CRAO using confocal scanning laser ophthalmoscopy (Spectralis, which can visualize YFP signal in the retina).
2. *Apoptosis*: TUNEL, Fluorescent-annexin V (FLIVO, for *in vivo* tracking on Spectralis).
3. *Neuroglobin*: assayed with Western blot and real-time qPCR.

To determine if effects are due to the Tie2 pathway or β-1 integrin, we performed the same experiments in subgroups of mice treated with anti-Tie2 neutralizing antibody (blocking Ang1 signaling through Tie2) or anti-β-1 integrin antibody (which would block COMP signaling through β-1 integrin); controls included AAV2.GFP, PBS, or IgG control.

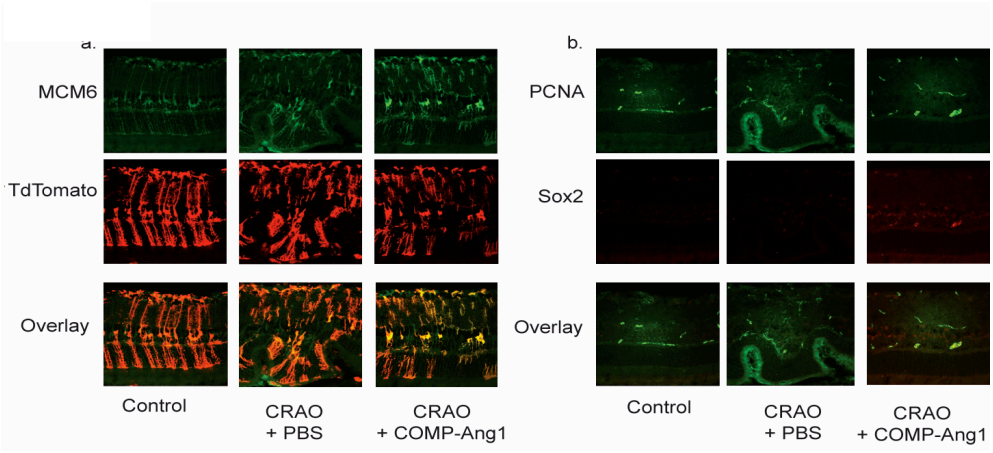

Figure A.4 Mice were treated after CRAO with COMP-Ang1 protein or PBS. COMP-Ang1 increased expression of MCM6 in muller glia (a) and Sox2 and PCNA colocalization (b).

We expected that COMP-Ang1 increases retinal ganglion cell survival in a β-1 integrin dependent manner. This would be manifest as persistence of YFP signal in mice and decreased apoptotic staining with a concomitant increase in neuroglobin.

W3 and BD-RGC mice were selected as they are mouse strains with highest and least sensitivity to ischemic insult (personal communication from Dr. Ning Tian). If they were found not suitable for any reason, four other mouse strains exist with YFP expression expressed selectively on other RGC subsets.

Our preliminary data demonstrated exciting findings that COMP-Ang1 protein given as an intravitreal injection immediately after CRAO induced Muller cells to express markers of neural progenitor cell transformation (MCM6) and other retinal cells to express both proliferative (PCNA) and progenitor (Sox2) markers. Defining whether this is true entailed elucidation of several transcriptional and protein expression events,

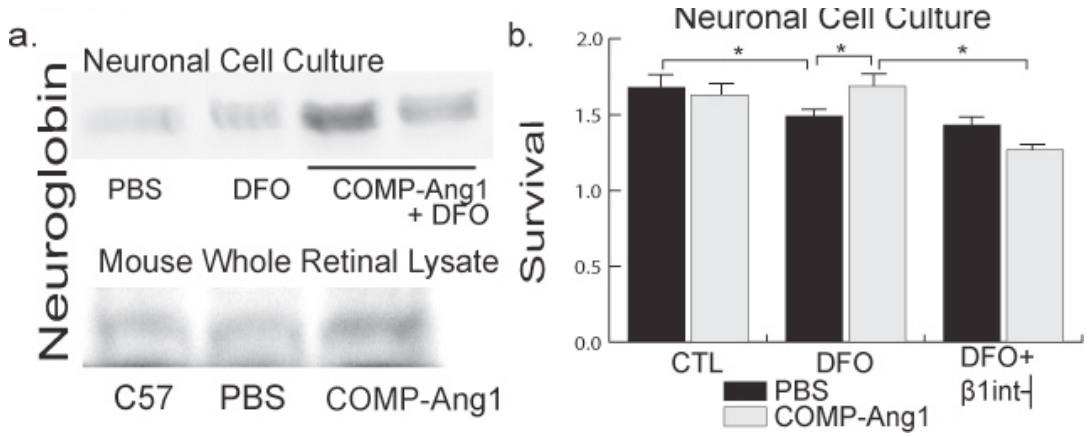

Figure A.5 COMP-Ang1 protein increased neuroglobin in cell culture and mouse retina (a). COMP-Ang1 promotes neuronal survival in a β-1 integrin dependent manner (b).

specifically for markers of transformation into neural progenitor phenotype, proliferation, cell type differentiation, and connectivity.

In vitro, MIO-M1 cells (the only established line of Muller cells) were exposed to acute hypoxia (using the EVOS cell culture incubator), and then treated with COMP-Ang1, COMP-Ang1+sTie2r, COMP-Ang1+anti- β-1 integrin antibody (or IgG control), or PBS. We then assessed RNA expression of neural progenitor markers (Sox2, Shh, Notch, Wnt, Hes1) by RT-PCR, and protein markers of phenotypic status (MCM6, TuJ1, Sox9) by immunocytochemistry. Other controls included COMP-Ang1 without hypoxia and hypoxic muller glia without COMP-Ang1.

In vivo, mice were treated with intravitreal injections of COMP-Ang1 two hours after and one week after CRAO; recombinant angiopoietin-1 and PBS injections served as controls. We then assessed the following indices relative to control:

1. Retinal neurogenesis. Retinas taken from mice underwent:
    a. Cryosection: *in situ* hybridization to examine expression of neural progenitor markers (Sox2, Shh, Notch, Wnt, Hes1) and immunofluorescence

for markers of proliferation (PCNA), neural progenitor status (MCM6), ganglion cells (TuJ1), Muller cells (Sox9), and synapses (bassoon).

b. Plastic embedding: for histologic staining (H&E, and Toluidine-Blue) as well as computational molecular phenotyping (CMP).

We predicted that COMP-Ang1 would induce Shh, Wnt, Notch, Sox2, and increase synapse formation compared to PBS. We predicted that COMP-Ang1 would promote neurogenesis from Muller glia resulting in increased number of ganglion cells (CMP).

Rose Bengal-induced central retinal artery occlusion can be altered to provide varying degrees of severity of occlusion. We have previously determined settings, which allow for severe occlusion (described above). Alternatively, we could have produced a less severe occlusion (by decreasing the power and number of pulses given per eye), which may have allowed us to see better integration.

A.4 References

Atebara, N. H., Brown, G. C., & Cater, J. (1995). Efficacy of anterior chamber paracentesis and carbogen in treating acute nonarteritic central retinal artery occlusion. *Ophthalmology*, *102*(12), 2029–34– discussion 2034–5.

Carlson, T. R., Feng, Y., Maisonpierre, P. C., Mrksich, M., & Morla, A. O. (2001). Direct cell adhesion to the angiopoietins mediated by integrins. *The Journal of Biological Chemistry*, *276*(28), 26516–26525. http://doi.org/10.1074/jbc.M100282200

Chen, X., Fu, W., Tung, C. E., & Ward, N. L. (2009). Angiopoietin-1 induces neurite outgrowth of PC12 cells in a Tie2-independent, beta1-integrin-dependent manner. *Neuroscience Research*, *64*(4), 348–354. http://doi.org/10.1016/j.neures.2009.04.007

Dallabrida, S. M., Ismail, N., Oberle, J. R., Himes, B. E., & Rupnick, M. A. (2005). Angiopoietin-1 promotes cardiac and skeletal myocyte survival through integrins. *Circulation Research*, *96*(4), e8–24. http://doi.org/10.1161/01.RES.0000158285.5719

Jones, C. A., & Li, D. Y. (2007). Common cues regulate neural and vascular patterning. *Current Opinion in Genetics & Development*, *17*(4), 332–336.

http://doi.org/10.1016/j.gde.2007.07.004

Karl, M. O., Hayes, S., Nelson, B. R., Tan, K., Buckingham, B., & Reh, T. A. (2008). Stimulation of neural regeneration in the mouse retina. *Proceedings of the National Academy of Sciences of the United States of America*, *105*(49), 19508–19513. http://doi.org/10.1073/pnas.0807453105

Papapetropoulos, A., García-Cardeña, G., Dengler, T. J., Maisonpierre, P. C., Yancopoulos, G. D., & Sessa, W. C. (1999). Direct actions of angiopoietin-1 on human endothelium: Evidence for network stabilization, cell survival, and interaction with other angiogenic growth factors. *Laboratory Investigation; a Journal of Technical Methods and Pathology*, *79*(2), 213–223.

Shin, H. Y., Lee, Y. J., Kim, H. J., Park, C.-K., Kim, J. H., Wang, K. C., et al. (2010). Protective role of COMP-Ang1 in ischemic rat brain. *Journal of Neuroscience Research*, *88*(5), 1052–1063. http://doi.org/10.1002/jnr.22274

Suri, M. F. K., Nasar, A., Hussein, H. M., Divani, A. A., & Qureshi, A. I. (2007). Intra-arterial thrombolysis for central retinal artery occlusion in United States: Nationwide In-patient Survey 2001-2003. *Journal of Neuroimaging: Official Journal of the American Society of Neuroimaging*, *17*(4), 339–343. http://doi.org/10.1111/j.1552-6569.2007.00121.x

Valable, S., Bellail, A., Lesné, S., Liot, G., Mackenzie, E. T., Vivien, D., et al. (2003). Angiopoietin-1-induced PI3-kinase activation prevents neuronal apoptosis. *FASEB Journal: Official Publication of the Federation of American Societies for Experimental Biology*, *17*(3), 443–445. http://doi.org/10.1096/fj.02-0372fje

Ward, N. L., & Lamanna, J. C. (2004). The neurovascular unit and its growth factors: Coordinated response in the vascular and nervous systems. *Neurological Research*, *26*(8), 870–883. http://doi.org/10.1179/016164104X3798

Zacchigna, S., Ruiz de Almodovar, C., & Carmeliet, P. (2008). Similarities between angiogenesis and neural development: What small animal models can tell us. *Current Topics in Developmental Biology*, *80*, 1–55. http://doi.org/10.1016/S0070-2153(07)80001-9